KfK 5250
Dezember 1993

NACOWA Experiments on LMFBR Cover Gas Aerosols, Heat Transfer, and Fission Product Enrichment

J. Minges, W. Schütz
Laboratorium für Aerosolphysik und Filtertechnik
Projekt Nukleare Sicherheitsforschung

Kernforschungszentrum Karlsruhe

KERNFORSCHUNGSZENTRUM KARLSRUHE
Laboratorium für Aerosolphysik und Filtertechnik
Projekt Nukleare Sicherheitsforschung

KfK 5250

NACOWA EXPERIMENTS ON LMFBR COVER GAS AEROSOLS, HEAT TRANSFER, AND FISSION PRODUCT ENRICHMENT

J. Minges, W. Schütz

Kernforschungszentrum Karlsruhe GmbH, Karlsruhe

Kernforschungszentrum Karlsruhe GmbH
Postfach 3640, 76021 Karlsruhe

ISSN 0303-4003

ABSTRACT

NACOWA EXPERIMENTS ON LMFBR COVER GAS AEROSOLS, HEAT TRANSFER, AND FISSION PRODUCT ENRICHMENT

NACOWA is an experimental KfK research program to study important parameters of the primary cover gas system of a pool-type sodium-cooled reactor. The primary cover gas space is an inert gas blanket lying between a hot pool of liquid sodium and a relatively cold roof structure. Due to the temperature gradients across the cover gas, sodium evaporates into the cavity where it may condense and form an aerosol. After transport by convective gas flow to the roof area, vapour will condense and aerosol will deposit which needs attention in safety considerations.

Heat transfer across the cover gas occurs by radiation, convection, and condensation, and determines the thermal load of the roof. The aerosols will interact, especially with radiation.

In case of pool contaminations from failed fuel elements, fission products like cesium and iodine will be released from the pool, and contaminate the aerosol and the deposits. For source term considerations, it is important to study the enrichment factors. It is also possible that zinc levels in the pool increase the level of radioactivity.

Fifteen different NACOWA test series were carried out. In the frame of these tests, the following items were investigated: sodium mass concentration in the cover gas, sodium aerosol particle size, radiative heat transfer across the cover gas, total heat transfer across the cover gas, sodium deposition on the cover plate, temperature profiles across the cover gas, phenomena if the argon cover gas is replaced by helium, enrichment of cesium, iodine, and zinc in the aerosol and in the deposits.

The conditions were mainly related to the design parameters of the European Fast Reactor EFR. According to the first consistent design, a pool temperature of 545°C and a roof temperature of only 120°C were foreseen at a cover gas height of 85 cm.

The experiments were carried out in a stainless steel test vessel of 0.6 m diameter and 1.14 m height. Pool temperature (up to 545°C), cover gas height (12.5 cm, 33 cm, and others), and roof temperature (from 100°C to 450°C) were the main parameters.

ZUSAMMENFASSUNG

NACOWA - EXPERIMENTE ZUM AEROSOL, ZUM WÄRMEÜBERGANG UND ZUR SPALTPRODUKTANREICHERUNG IM PRIMÄRSCHUTZGAS EINES SNR

NACOWA ist ein experimentelles KfK-Forschungsprogramm zur Untersuchung wichtiger Parameter des primären Schutzgassystems eines natriumgekühlten Reaktors vom Pool-Typ. Die primäre Schutzgaszone ist ein Inertgasraum zwischen einem heißen Natriumpool und einem relativ kalten oberen Abschluß ("Dach"). Infolge der über diese Zone verlaufenden Temperaturgradienten kommt es zur Natriumverdunstung in das Schutzgas mit anschließender Kondensation und Aerosolbildung. Nach dem Transport in der konvektiven Gasströmung kann der Natriumdampf an den Dachstrukturen kondensieren und das Aerosol sich ablagern; dies ist bei Sicherheitsüberlegungen zu berücksichtigen.

Der Wärmeübergang durch das Schutzgas setzt sich aus den Anteilen der Wärmestrahlung, der Konvektion und der Kondensation zusammen. Er bestimmt die thermische Belastung des Daches. Zwischen Aerosol und Wärmeübergang findet eine Wechselwirkung statt, insbesondere mit der Wärmestrahlung.

Im Falle einer radioaktiven Kontamination des Pools infolge schadhafter Brennelemente werden Spaltprodukte wie Cäsium und Jod aus dem Pool in das Schutzgas freigesetzt. Dies führt zu einer Kontamination des Aerosols und der Ablagerungen. Für Quelltermuntersuchungen ist es wichtig, die entsprechenden Anreicherungsfaktoren zu untersuchen. Es ist auch möglich, daß Zinkanteile im Pool zu einer Erhöhung der Radioaktivität des Aerosols und der Ablagerungen führen.

Es wurden fünfzehn verschiedene NACOWA-Versuchsreihen durchgeführt. Im Rahmen dieser Versuchsreihen wurden die folgenden Themen behandelt: Natrium-Massenkonzentration im Schutzgas, Natriumaerosol-Partikelgröße, Strahlungswärmeübergang durch das Schutzgas, Gesamtwärmeübergang durch das Schutzgas, Natriumablagerung am Deckel, Temperaturprofile im Schutzgas, Phänomene beim Übergang von Argon-Schutzgas auf Helium-Schutzgas, Anreicherung von Cäsium, Jod und Zink im Aerosol und in den Ablagerungen.

Die Versuchsbedingungen wurden hauptsächlich durch die Auslegungsparameter des European Fast Reactor EFR bestimmt. Beim "first consistent design" war eine Pooltemperatur von 545°C und eine Dachtemperatur von nur 120°C bei 85 cm Argon-Schutzgashöhe vorgesehen.

Die Experimente wurden in einem Edelstahlbehälter von 0,6 m Durchmesser und 1,14 m Höhe durchgeführt. Pooltemperatur (bis 545°C), Schutzgashöhe (12,5 cm, 33 cm und andere) sowie Deckeltemperatur (von 100°C bis 450°C) waren die wichtigsten experimentellen Parameter.

KfK 5250

NACOWA EXPERIMENTS ON LMFBR COVER GAS AEROSOLS, HEAT TRANSFER, AND FISSION PRODUCT ENRICHMENT

J. Minges, W. Schütz

CONTENTS

1. INTRODUCTION

The primary cover gas space of a pool-type liquid-metal cooled fast breeder reactor (LMFBR, see ref. [1.1]) is an inert gas blanket lying between a hot pool of liquid sodium coolant and a relatively cold roof structure. Due to the temperature gradients across the cover gas, sodium evaporates into the cavity where it may condense and form an aerosol. The gradients are sufficient to drive a turbulent convective gas flow which transports aerosol and vapour to the roof area. The possibility of vapour condensation and aerosol deposition onto roof structures needs attention in safety considerations, such as for control rod penetrations which must be kept free of solid sodium deposits. The operating conditions of the reactor are influenced by the heat transfer across the cover gas. Heat transfer occurs by radiation, convection and condensation, and determines the thermal load of the roof. The aerosol system will interact with the heat transfer mechanisms, especially with the radiative part. In Fig. 1.1, the typical geometry of the cover gas space is shown, including the relevant phenomena.

In case of pool contaminations from failed fuel elements, not only sodium but also fission products will evaporate or escape from the pool and contaminate the aerosols and the deposits. For source term considerations in case of a leak in the roof area, it is important to know the possible enrichment of the aerosol and of the deposits with fission products such as cesium and iodine. It is also possible that zinc levels in the pool sodium increase the level of radioactivity.

The European collaboration in the field of fast breeder reactors is at present mainly related to the design of the European Fast Reactor EFR. According to the first consistent design [1.2], it will be a pool-type reactor of 1500 MW_{el} with a primary sodium pool of 17 m diameter and a temperature of 545°C under normal operating conditions, covered by an argon gas layer of 0.85 m height, and an air-cooled upper closure (roof) which originally had a temperature of only 120°C. Meanwhile, however, a solid steel roof with thermal shields has been adopted in place of the previous welded-box construction. Thus, the lower side roof temperature will be, according to the latest design, significantly above 300°C.

NACOWA (German acronym for sodium - cover gas - heat transfer) is a KfK research programme to study parameters of the pool-type LMFBR primary cover gas system under the conditions of normal operation and of design basis accidents. The programme is mainly related to EFR. The aim is to provide input data for the design of the EFR cover gas system and for the upper closure of the primary vessel, and to provide enrichment factors for the assessment of source terms in case of a cover gas leak. A sketch to characterize the NACOWA conditions is given in Fig. 1.2.

In the frame of the NACOWA experiments, mainly the following items are investigated:

- Sodium mass concentration in the cover gas.
- Sodium aerosol particle size.
- Radiative heat transfer across the cover gas.
- Total heat transfer across the cover gas.
- Sodium deposition on the cover plate.
- Temperature profiles across the cover gas.
- Phenomena if the argon cover gas is replaced by helium.
- Enrichment of cesium in the aerosol and in the deposits.
- Enrichment of iodine in the aerosol and in the deposits.
- Enrichment of zinc in the aerosol and in the deposits.

Pool temperature and cover gas height are the main experimental parameters. Other parameters which are varied within certain limits are the roof temperature, the amount of admixtures to the pool sodium, and the type of gas (argon or helium).

Investigations on selected cover gas phenomena, especially heat and mass transfer, have been performed by several countries in recent years and are still going on to extend this understanding. The reader will refer to ref. [1.3] for a summary of these activities (status 1985). At that time, most national activities were directed towards the individual national LMFBR projects.

When the NACOWA programme was initiated, the main target was to provide verification data for the German GASMO code [1.4] which had been written for the SNR-2 project. Later on, however, the European national activities merged into the EFR project, and a new intent of our tests was, among others, to provide data for EFR cover gas codes like CGAS [1.5].

In the frame of the European collaboration, mainly within France, UK and Germany, NACOWA results had been reported to common working groups, namely to AGT 4 (Safety) and AGT 6 (Reactor Vessel Handling and Auxiliaries) as tasks of two 'Work Packages'. Our work is mainly of experimental nature. Important theoretical and analytical work on cover gas phenomena, especially aerosol formation and behaviour as well as interaction with thermal radiation, has been performed in the UK [1.6, 1.7, 1.8], and also in Japan [1.9]. Important French experiments and results from facilities up to ten times larger in pool diameter than ours are reported in ref. [1.10] and [1.11]. The British cover gas experiments have not been reported in the open literature but internal reports exist from Harwell Laboratory [1.12] and Manchester University [1.13].

The first NACOWA test series was carried out in 1987. Since then, 15 test series were performed. Due to the decision of the German Ministry of Research and Technology to cease breeder funding by the end of 1993, a continuation of the programme seams unlikely although several questions remain open.

2. DESCRIPTION OF THE TEST FACILITY

The NACOWA test stand is a modification of the FAUST facility [2.1, 2.2] which has originally been built to study source terms from severe accidents. The modification was mainly achieved by exchanging the cover plate and the related instrumentation. So, in some sense, the test stand has to be regarded as a compromise. For example, it has no sodium loop but is operated under stationary conditions. A diagram of the entire NACOWA facility, including sodium storage and handling, is shown in Fig. 2.1. A diagram of the test vessel is given in Fig. 2.2.

The test vessel (diameter 60 cm, full height 114 cm, gross volume 322 liters) is fabricated from stainless steel and designed for a maximum pressure of 1.6 MPa and a maximum temperature of 600°C. It is electrically heated on the outer cylindrical walls and on the bottom. For thermal insulation, an asbestos-type ring of 4 cm height is installed between the upper rim of the cylindrical part and the cover plate. The main part of the temperature drop between vessel walls and cover plate occurs across this ring. Thermal insulation is provided on the outer side of the cylindrical walls, on the bottom, and - optionally - on top of the cover plate.

The test vessel has an air-cooled cover plate which is shown in Figs. 2.3 and 2.4. The cooling is achieved by forced air convection within two parallel spiral ducts which are normally operated in the counterflow mode. The air flow, achieved by blowers, is of the order of 10 m^3 / h. The entrance and exit temperatures are monitored (e.g. 20°C / 119°C). The air flow can be varied in order to vary the plate temperature. For low-temperature tests (plate temperature below 200°C), the plate has no outer thermal insulation. For higher temperatures, an additional insulation is applied.

A radiometer to measure the radiative heat flux is installed in the center of the plate. It is a thermo-electronical radiometer (TER) which has been developed and fabricated by INTERATOM, well-suited to operate in a high-temperature environment with sodium aerosols. A sketch of the device and the principle of operation are illustrated in Fig. 2.5. It is a windowless device for absolute measurement of electromagnetic radiation from infrared to ultraviolet with high sensitivity, wide scale and short response time. The working principle is based on two black-body, conically-shaped cavities which absorb the incoming thermal radiation. One cavity is used as absorber, the other as reference absorber. The circular opening of each cavity, defined by a shutter system, is 0.5 cm^2. Three positions are possible, namely both openings closed (0), one open (1), or two open (2). Position 0 is normal to avoid sodium ingress, and 2 is for test purposes. Position 1 is used to generate data: the radiative heat flux causes a temperature rise of the open cavity, and an equilibrium with the closed reference cavity is achieved by electrical resistance heating of this cavity. From the equilibrium current, the radiative heat flux can be determined. A more detailed description is presented in ref. [2.3].

Furthermore, the plate has four penetrations (2 x 23 mm ID, 2 x 10 mm ID) for thermocouples, sampling devices like wash-bubblers or impactors, and inert gas supply. The sampling devices will be described in more detail in chapters 4 and 5. To determine temperature profiles across the cover gas and the plate, twelve thermocouples are mounted on a vertical 'ladder', covering the space between plate and pool, and five horizontally touching selected spots of the lower side of the plate (see Figs. 2.3 and 2.6).

For visual inspection, the plate has two viewports (50 mm ID). It is necessary to have a visual control of the pool surface quality (impurities will enhance the emissivity), and it is helpful to have a control of the aerosol conditions. The viewports are mounted under a vertical angle of 45° towards the plate surface. Normally, one viewport is used for illumination (2000 watt lamp), the other for inspection.

A cesium source is installed inside the vessel to be operated under sodium by the following principle: A sealed bellow pipe with a steel spike at its front may be pressurized with argon gas up to 0.6 MPa. The spike will hit and destroy a glass capsule which is filled with cesium. By this method, the liquid cesium (typically 1 g or 5 g) is introduced into the sodium pool at a well-defined time. In a similar way, other materials like iodine can be introduced into the pool.

Using the original FAUST setup [2.1, 2.2]), data on sodium mass concentrations in the cover gas at high plate temperature (above 400°C) were gained. These tests are summarized under the title 'NACOWA - 15', and the main principles of the setup are shown in Fig. 2.7.

Fig. 2.8 is a photograph of the NACOWA facility. Fig. 2.9 is a photograph of the cover plate with its installations.

3. DESCRIPTION OF NACOWA TESTS N-1 TO N-15

Test NACOWA - 1

The main purpose was to check the performance of the components and to gain experience with the instrumentation. Two runs were performed under the following conditions: pool temperature 408°C, plate temperature at TER position 130.6°C / 126.6°C, pool height 76 cm. The radiometer readings were 274 mW / 259 mW corresponding to 5.48 kW/m^2 and 5.18 kW/m^2. The pool surface was covered with an oxide layer. This fact caused the relatively high radiative heat transfer rates (since oxide has a much higher emissivity than pure sodium), and was not acceptable for future tests.

Test NACOWA - 2

Before performing this test series, the sodium was treated as follows: the lower, clean portion was pumped back from the test vessel into the dump tank. The upper portion which had the oxide layer was removed. The test vessel was thoroughly cleaned and flooded with argon for several days. After sodium refilling, the surface appeared clean and shiny. However, when increasing the pool temperature, a slight surface oxidation effect was observed.

Above 400°C, the surface condition could no longer be judged visually because of aerosol formation. The test series compraised eleven runs with pool temperatures from 410°C to 500°C, plate temperatures from 123°C to 141°C, and pool heights from 73 to 83 cm. The TER data were around 1 kW / m^2, significantly below the N-1 data.

Test NACOWA - 3

The sodium supply was completely exchanged. However, this measure was still insufficient. After refilling the test vessel, about 30% of the surface appeared to be shiny, the other 70% were covered with floating oxide islands. When turning on the plate cooling, a slow circular motion of the impurities around the central vessel axis was realized. Only one run was performed at 405°C pool temperature, 158°C plate temperature, and 99 cm pool height. The TER reading was 204 mW corresponding to 4.08 kW/m^2, which is again a relatively high value, and most likely caused by the impurities. After the problems with oxide layers during the tests N-1 to N-3, an "overflow ring" was constructed and installed to achieve a clean pool surface.

Test NACOWA - 4

To achieve a clean pool surface, two additional components were installed: The first one is an "overflow ring" (as shown in Fig. 2.2) to direct the sodium from the contaminated surface layer into a dump tank during the filling process. The second one is a double steel-mesh filter (40 µm and 1 µm) between storage vessel and test vessel to retain solid particles during the filling process. Both installations, especially the first one, turned

out to be very efficient, and N-4 was the first test series with an absolutely clean and shiny pool surface. Furthermore, it was the first test series where the wash-bubbler and impactor methods were used to determine sodium mass concentrations in the cover gas and aerosol particle size spectra. It compraised twelve runs with pool temperatures from 260°C to 500°C, plate temperatures from 115°C to 150°C, and cover gas heights of 12.5 cm and 33 cm. The first height is defined by the level of the overflow ring, the second by the drain pipe. Radiative heat transfer rates were determined in all cases.

Test NACOWA - 5

It was similar to N-4 with some improvements concerning the cover gas sampling methods. It compraised nine runs with pool temperatures from 273°C to 512°C, plate temperatures from 100°C to 147°C, and cover gas heights from 12 cm to 82 cm. Radiative heat transfer rates were determined in all cases.

Test NACOWA - 6

N-6 was an empty-vessel test to understand the "frame" without sodium and aerosols, and to study thermal radiation off the walls. Radiative heat transfer was measured from 160°C to 470°C side wall and bottom temperature. Due to the relatively large heat transfer rates, the roof temperature increased from 72°C to 200°C in spite of forced air cooling (in the future, two separate air blowers are used in such a case). The data from N-6 are an upper limit. Even with a small sodium supply in the vessel, the heat transfer rate will decrease significantly.

Test NACOWA - 7

After the empty-vessel test, we wanted to study the decrease of radiative heat transfer compared to N-6 if the vessel bottom is just covered with sodium. At this test, the TER will recognize the full side wall effect plus effects from sodium aerosol and sodium deposition at the side walls. The effect of the pool itself is expected to be relatively small. Sodium aerosol deposition at the side walls will cause a decrease of radiative heat transfer. Possibly, the effect of deposited sodium is more important than the aerosol effect.

N-7 was a test which lasted ten days. The pool temperature was slowly raised from 210°C to 400°C, with a plateau at 350°C and 400°C over several days. Visually, aerosol production was observed at 350°C and above. Aerosol samples were taken at 400°C by the wash-bubbler method. A very pronounced time-dependent deviation from the empty-vessel case was observed. After several days, the radiative heat transfer rate decreased to almost one half of its original value. However, ten days were not enough to reach a lower plateau. This plateau may, in an extreme case, be fully governed by the emissivity of sodium if the steel surfaces are fully wetted.

Test NACOWA - 8

This test was the beginning of a new series on design basis accidents, concerning the enrichment of cesium in the cover gas aerosol after a simulated fuel pin failure. The main purpose of this test was to determine cesium enrichment factors for cover gas aerosol and cover plate deposits, and to practice the handling of the cesium source. Since the released amount had to be determined by chemical analysis (no radioactive material is used), we introduced the relatively large amount of 5 g in order to stay above the detection limit. Similar to our earlier tests, we also determined aerosol mass concentrations, radiative heat transfer rates and temperature profiles across the cover gas. We had a cover gas height of 33 cm, corresponding to 229 liters of sodium in the vessel. The pool temperatures were mainly in the vicinity of 500°C. The plate temperature was between 120°C and 155°C.

Visually, through the view ports, we observed a very dense aerosol, so that the pool surface was barely visible. However, we can clearly state that the pool surface showed a slow circular motion with a wave-like structure, possibly driven by the convective cover gas flow.

Unfortunately, it turned out that the cesium source broke unintentionally during the early heating phase, but already inside the sodium pool. So, we could not open the source at a well-defined time but had a mixture Cs / Na right from the beginning. This experimental fault was repaired for test N-10.

In the course of the test, we took eight cover gas samples and made five measurements of the radiative heat transfer. After disassembling and removal of the cover plate, we took four samples of deposits at the lower side of the plate.

Test NACOWA - 9

In all our previous tests, we had a thermal insulation only at the side walls and at the bottom of the test vessel. The cover plate had no insulation. N-9 was our first test to determine the total heat transfer in relation to the radiative transfer. The cover plate area, and thus the whole test vessel, was thermally insulated. So, the total heat flux into the plate could be determined from flow rate and temperature difference of the cooling air.

We had no cesium source installed but used the same sodium as in the previous test N-8. Cover gas aerosol samples and samples from deposits in the plate area were analysed on their cesium content.

It turned out that the air-cooling system was not sufficient to maintain the 'low' plate temperature of 120 °C in case of a full insulation, even at maximum air flow. At 500°C pool temperature, the plate temperature was around 200°C.

The main experimental parameters were: Pool temperatures from 372°C to 503°C and argon cover gas height 12.5 and 33 cm. We had fourteen different parameter combinations where we took cover gas aerosol samples and made measurements of radiative and total heat transfer. After disassembling and removal of the cover plate, we took five samples of sodium deposits in the plate area.

Test NACOWA - 10

This test was a combination of the features of N-8 (cesium source) and N-9 (total thermal insulation). In addition, it was our first test with helium cover gas instead of argon.

N-10 was the first test with successful break of the cesium source at a well-defined time. The cesium run was performed under the following conditions: Pool temperature 508°C, plate temperature up to 210°C (because of insulation), argon cover gas height 33 cm (corresponding to 229 liters of sodium), 5 g cesium source in addition to the background from former tests.

Concerning the total heat transfer measurements, we had a setup similar to N-9 with additional features, e.g. pressure measurement of the cooling air at entrance and exit of the plate, and a regulation of the volume flow. Since 120°C plate temperature could not be achieved, the new approach was to use the air volume flow as a parameter and extrapolate to the low temperature.

Similar to the previous tests, we determined aerosol mass concentrations, radiative heat transfer and temperature profiles. We also took samples from the sodium pool to get experimental numbers for the cesium concentration in the pool sodium. Pool temperatures varied from 373°C to 508°C, and the cover gas height remained constant at 33 cm. We had eleven runs with different parameter combinations throughout the test. Argon was used from N-10 / 1 to N-10 / 7, and helium from N-10 / 8 to N-10 / 11. The cesium capsule was broken between N-10 / 3 and N-10 / 4. Most of the heat transfer data with air flow variation were gained from N-10 / 1 to N-10 / 3.

Test NACOWA - 11

In all our previous tests, we had not yet achieved the high pool temperature of 545°C corresponding to EFR conditions. The maximum temperatures had been around 510°C. The reason is of technical nature: with the installed electrical heating capacity, it was difficult to reach higher temperatures during a normal working day. However, since the aerosol concentration rises strongly with pool temperature, it is necessary to have this information at 545°C and even above.

The main purpose of the test was to determine mass concentrations with wash-bubblers, particle size spectra with impactors, and radiative heat transfer at high pool temperatures. We used argon cover gas in all cases. We had five runs with different parameter combinations, with pool temperatures from 369°C to 545°C and 12.5 or 33 cm cover gas

height. The cover plate temperature was near 150°C, and the plate had no thermal insulation. Since the radiometer was out-of-order, we could not gain data on heat transfer.

Test NACOWA - 12

The main purpose of this test was to perform cesium measurements with a lower amount of cesium in the source (1 g instead of 5 g) to study dependencies on pool concentration. Another issue was the repetition of impactor measurements at a lower flow rate compared to N-11 where most of the sodium was found on the pre-impactor stage. To interprete the impactor data and create particle size spectra, especially the 50% mass median diameter, it is necessary to have the sodium well-distributed over all the stages. The third issue was like N-11, namely high pool temperatures around 545°C. Unfortunately, two electric heaters of the test vessel failed during the test, and the maximum pool temperature which could be reached was only 518°C.

We used argon cover gas in all cases. We had nine runs with different parameter combinations, with pool temperatures from 375°C to 518°C and mainly a 33 cm cover gas height (12.5 cm only at N-12 / 9). The 1 g cesium source was opened between runs N-12 / 4 and N-12 / 5. Besides impactor measurements, we took cover gas samples as usual with wash bubblers and determined temperature profiles across the cover gas.

Test NACOWA - 13

This test had two main topics, namely to study the enrichment of zinc in the aerosol and to study the cover gas phenomena if argon is replaced by helium. Other topics were to investigate the enrichment of cesium (no new source but cesium from test N-12 still in the sodium pool) and to achieve high pool temperatures.

Zinc is not a fission product but it may get entrained into the pool sodium by contact with structures and activated to Zn-65 by neutron capture (see chapter 13). We had 50 g of zinc powder with a grain size of about 1.5 mm distributed on the bottom of the test vessel before we filled in the liquid sodium. Its melting point is 419.4°C, and so we can assume that we have a mixture of two liquids at our experimental conditions. The fairly large amount of zinc has been chosen because of the chemical detection limit.

Helium had already been used in test N-10. It turned out that we observed a dense aerosol in argon cover gas but almost no aerosol in helium cover gas. It was necessary to study this phenomenon in more detail.

We had 21 runs during test N-13 with different parameter combinations. The main zinc test in argon cover gas atmosphere was performed by runs N-13 / 1 to N-13 / 4 at pool temperatures from 512°C to 538°C and cover gas heights of 12.5 and 33 cm. We took samples using wash-bubblers and impactors, and also took pool samples. Runs N-13 / 5 to N-13 / 21 were performed with helium cover gas at pool temperatures from 481°C to 546°C and cover gas heights of 12.5 cm / 33 cm / 53 cm, taking samples as above.

The cover plate temperatures had values from 138°C to 192°C. Like N-12, we did not gain any data on heat transfer during test N-13.

Test NACOWA - 14

The main topic of this test series was to study the enrichment of iodine in the aerosol and in the deposits. Similar to the cesium tests, a quartz glass capsule with 0.59 g of elemental iodine was placed onto the source device and prepared to be crushed under sodium.

We had eight runs with pool temperatures from 426°C to 539°C, plate temperatures from 108°C to 159°C, cover gas heights of 12.5 cm / 33 cm, and argon or helium as cover gas. A special feature of N-14 was that two additional air blowers were installed on top of the plate to achieve low temperatures. We took wash-bubbler and impactor samples as usual.

It turned out that the iodine source opened unintentionally before taking the first sample. So, there is no background measurement. However, we may assume that the background can be neglected due to the high volatility of iodine.

Test NACOWA - 15

This test is related to sodium mass concentrations at high plate temperatures. The data which are summarized under the title N-15 are byproducts from a series of FAUST tests on radiological source terms. These tests have already been mentioned in chapter 1 and are described in detail in ref. [2.1]. Compared to N-1 to N-14, the same test vessel has been used but a different cover plate which was designed for high pressure and high mechanical load. The tests were performed with a completely isolated vessel and without any plate cooling. The plate temperatures were above 400°C. The technique to take cover gas samples was different to the previous one: the plate was connected to four stainless-steel pots of 7.5 liters volume each which could be evacuated and were kept at room temperature. The connection was made by steel pipes with 4 cm inner diameter and pneumatically driven valves. Sampling was performed by connecting the evacuated pots to the cover gas volume until pressure equilibrium was achieved. Afterwards, the sodium mass concentration was determined from the amount of sodium which had been trapped on the cold walls of the pots. As expected, the mass concentrations were much smaller compared to the data which were gained under low plate temperature conditions. A simplified diagram of the experimental setup is shown in Fig. 2.7.

4. SODIUM MASS CONCENTRATION IN THE ARGON COVER GAS

Because of the high pool temperature, the low cover plate temperature and the large temperature gradient across the cover gas, we have a convective argon gas flow. Sodium evaporates from the hot pool surface, and sodium vapour is carried into cooler regions by argon convection. Due to supersaturation in these cooler regions, the vapour will form an aerosol which consists of metallic sodium droplets with an average size of several micrometers. It is evident that the amount of generated aerosol depends on pool temperature (evaporation rate) and plate temperature (supersaturation). It will be shown later (helium, see chapter 10) that it may also depend on the type of cover gas. In general, the cover gas system is a mixture of inert gas, sodium aerosol, and sodium vapour.

Two methods are applied to determine mass concentrations, namely wash-bubblers and impactors. Both methods have in common that samples must be extracted from the cover gas volume. The wash-bubbler method is illustrated in Fig. 4.1. We insert a steel pipe of 16 mm inner diameter into the cover gas volume. The pipe is connected to four glass bottles, two of which are filled with water, and to a steel receptacle of 7.5 liters volume. The position of the pipe entrance may be varied from cover plate down to sodium level. The steel receptacle is evacuated before the sampling process and completely filled during sampling. So, we have a well-defined sampling volume, but no constant gas flux. The sampling system is at room temperature except the steel rod which indirectly takes up some heat from the test vessel. Normally, the cover gas is adjusted to a slight overpressure (e.g. 0.105 MPa total pressure). The pressure drop during the sampling process may be neglected since there is a permanent connection between cover gas volume and 300-liter dump tank via the overflow ring. The sampling procedure may be repeated in case of very low concentrations. After sampling, we remove the full system and determine the amount of sodium which has been trapped in the pipes, the bottles and the receptacle (normally, the last item is negligible) by chemical analysis (titration). The sodium mass concentration is determined by the relation

$$\rho_{NA} = m \cdot \frac{T_A}{V_A \cdot n} \cdot \frac{1}{T_G}$$

where

- m = amount of sodium trapped in the sampling system
- T_A = room temperature
- V_A = sampling volume (volume of receptacle)
- n = sampling steps (mostly 1, sometimes 2)
- T_G = cover gas temperature at location of sampling, to be determined from temperature profile measurements

This method has been applied in all NACOWA tests. It has to be pointed out that we trap aerosol particles as well as vapour which condenses during the sampling process.

So, ρ_{Na} is not an aerosol concentration but a concentration of sodium in the cover gas. An experimental error may occur by non-condensing vapour and small particles passing through the whole sampling system without getting trapped.

The impactor measurements are a second source of information on mass concentrations (see Fig. 4.2). Since impactor measurements are mainly done to determine particle size spectra, they will be described in detail in the next chapter. However, if we summarize the amount of sodium trapped on all stages and add the amount which is deposited in the ducts, we determine mass concentrations in a similar way as above. Unlike the wash-bubbler case, impactor measurements are carried out at a constant gas volume flux. The impactors are heated to the average cover gas temperature, and the flux is measured at room temperature. Under these conditions, the sodium mass concentration is determined by the relation

$$\rho_{Na} = m \cdot \frac{T_A}{T_G} \cdot \frac{1}{v \cdot \Delta t}$$

where

m = amount of sodium trapped in the system
T_G = cover gas temperature at location of sampling
T_A = room temperature
v = gas volume flux [liters per minute]
Δt = sampling time

Although the impactor is heated, we have the steel pipe duct which passes through the cover plate (120°C) as a 'cold spot', and we may have vapour condensation during the sampling process. So, ρ_{Na} is a number which may exceed the actual aerosol concentration and may again be interpreted as the sodium mass concentration in the cover gas. Impactor measurements were carried out throughout tests N-11, N-12 and N-13.

A general feature is that the amount of sodium in the cover gas below 300°C pool temperature is almost negligible. The onset of a steep rise is near 350°C pool temperature, and at 545°C concentrations between 20 and 40 g/m^3 are measured.

No concentration measurements were performed during N-1 to N-3 because of problems with oxide layers on the pool surface. First data were gained from N-4 and N-5. They are listet in Tab. 4.1 and shown in Fig. 4.3. We had pool temperatures from 320°C to 512°C, plate temperatures from 106°C to 152°C, and the two standard cover gas heights of 12.5 cm and 33 cm. Mass concentrations up to 17 g/m^3 were measured, showing an extremely steep increase, no onset of a plateau, and a slight indication that the increase starts for the 12.5 cm case at a lower temperature than for the 33 cm case. Strong aerosol formation was observed through the view ports.

N-6 was an empty-vessel test with no mass concentration measurements. N-7 was performed with a very shallow (2 cm) sodium layer on the bottom and, correspondingly, 112 cm cover gas height. A few concentration measurements were made at 400°C pool temperature. They were between 1 and 2 g/m^3 (see chapter 6 and Fig. 6).

During test N-8, we had pool temperatures from 445°C to 500°C, plate temperatures between 125°C and 155°C, and a constant cover gas height of 33 cm. By visual observation through the view ports, we saw a dense aerosol, with the pool surface at the limit of the visibility. Results from mass concentration measurements with wash-bubblers are shown in Fig. 4.3., and listed in Tab. 4.2. The average number is near 17 g of sodium per m^3 argon cover gas. Samples were taken from half-way position between pool surface and plate.

During test N-9, we had pool temperatures from 372°C to 503°C, and plate temperatures from 148°C up to 232°C because of the thermal insulation. Cover gas heights were 12.5 and 33 cm. Because of the higher plate temperatures compared to N8, the formation of aerosols was suppressed, and the visibility was much better. By observation through the view ports, we had a fairly undisturbed view on the pool surface. Nevertheless, we determined sodium mass concentrations up to 11 g/m^3 by the wash-bubbler method. We assume that a major part thereof has been sodium vapour and not an aerosol. The data are summarized in Tab. 4.3, and in Fig. 4.4.

In a similar way, we had an elevated plate temperature during test N-10 because of thermal insulation, and a very good visibility. We had pool temperatures from 373°C to 508°C, plate temperatures from 120°C to almost 300°C, and a constant cover gas height of 33 cm. By the wash-bubbler method, we found concentrations up to almost 20 g/m^3, as summarized in Tab. 4.4, and shown in Fig. 4.5. Again, a major part thereof may be sodium vapour.

During test N-11, we had no thermal cover plate insulation but pool temperatures up to 545°C. We took cover gas samples with wash-bubblers and eight-stage Andersen impactors. Cover gas heights were 12.5 and 33 cm. Unlike earlier tests, the sampling pipe was not inserted to a central position, but to a position close to the plate: 3 cm in the 12.5 cm case, and 6 cm in the 33 cm case. In this area, we probably have a strong convective flux and inhomogeneous mass concentrations since our data exhibit strong fluctuations. However, the average values are in good agreement with our scheme, namely around 35 g/m^3 in the first case, and around 23 g/m^3 in the second case, with fairly good agreement between wash-bubblers and impactors. These data are summarized in Tab. 4.5, and included in Fig. 4.6.

In the frame of test N-12, we gained new data with wash-bubblers and impactors in the pool temperature range from 376°C to 518°C, with plate temperatures from 123°C to 154°C, mainly at 33 cm cover gas height. Due to a failure of an electrical heater, we

could not achieve 545°C. Alltogether, nine wash-bubbler samples and nine impactor samples have been taken under conditions similar to N-11, but at a reduced gas volume flux through the impactors. The results are summarized in Tab. 4.6, and included in Fig. 4.6. Maximum concentrations from N-12 are near 25 g/m^3, and the impactor data are somewhat above the wash-bubbler data for reasons which are not yet clarified.

From test N-13, we gained additional data at high pool temperatures. With argon cover gas, we took three wash-bubbler samples and one impactor sample. The conditions were als follows: Cover gas height 12.5 cm, pool temperature 512°C, plate temperature 179°C; cover gas height 33 cm, pool temperature 538°C, plate temperature 160°C. We found mass concentrations from 16 to 31 g/m^3, as summarized in Tab. 4.7 and shown, together with our N-11 and N-12 data, in Fig. 4.6. Again, we measured higher concentrations with impactors than with wash-bubblers.

In the early phase of N-14, an unusually high aerosol development was observed which even caused plugging of the sampling ducts in some cases. This may be explained by the presence of iodine vapour in the cover gas. Data from N-14 will, due to this fact, not be reported in the present chapter.

N-15 is a summary of measurements from FAUST tests with plate temperatures above 400°C. The mass concentrations are significantly below the values from N-1 to N-14. A typical number is 5 g/m^3. The data are listed in Tab. 4.8, the experimental setup is shown in Fig. 2.7, and a diagram of mass concentrations versus plate temperature is given in Fig. 4.7.

5. PARTICLE SIZE MEASUREMENTS

Measurements of particle size spectra for cover gas aerosols were performed during several tests. Parameters and conditions were optimized in the frame of N-12. In the present report, we mainly restrict ourselves to the presentation of results from N-12. We used an eight-stage Andersen impactor (stack sampler) in an arrangement as shown in Fig. 4.2. The impactor was connected to the cover gas via a steel pipe of 0.9 m length and 1.6 cm diameter, and the pipe was inserted to the half-way distance between plate and pool in most cases. The impactor was heated to a temperature which was close to the gas temperature at the sampling location (typically 250°). We did not heat the pipe, however.

Two experimental difficulties arise in our case: Firstly, sampling should be performed under isokinetical conditions, i.e. the sampling volume flux should be adjusted to the flux in the cover gas system. This can not be achieved since we have no well-defined flux in the cover gas. Secondly, the presence of sodium vapour may lead to condensation effects during the sampling process, and the measured size spectra may thus be different from the true spectra.

Impactors separate particles by differences in inertia. Particles are classified aerodynamically into multiple size ranges. The results are plotted on logarithmic probability graph paper (log-normal plot) with the particle diameter as abscissa and the cumulative percent less than stated size by weight as the ordinate. The calibration of the impactor stages (air, room temperature, unit density particles), as given by the manufacturer, has to be corrected with respect to the argon viscosity and the elevated temperature, but not to sodium density since unit density is assumed by definition of the aerodynamic diameter. From the log-normal plots, we gain the aerodynamic mass median diameter d_{50} of the size distribution, and the standard deviation σ_g, defined as

$$\sigma_g = \left(\frac{84.13\,\%\,diameter}{15.87\,\%\,diameter} \right)^{1/2}$$

This is, however, only true if we have a "log-normal distribution", i.e. a straight line on the log-normal plot. It does not exactly apply to our case.

Impactors are well-suited for the size range from 0.1 to 10 µm. If larger particle sizes are expected, a pre-separator should be used. An optimum gas flow rate is around 15 liters per minute. We have used a pre-separator and took samples at flow rates from 8 to 20 liters per minute.

We took five impactor samples during test N-11, using a flow rate of approximately 20 liters per minute. Unfortunately, more than one half of the collected amount of sodium was found on the pre-separator in four cases (at high pool temperature and high concentration), which may be interpreted as an unexpectedly large amount of "coarse" parti-

cles with diameters above 10 µm. Evaluation of these data by extrapolation leads to d_{50} values from 12 to 14 µm. These numbers, however, are questionable.

During test N-12, we took six impactor samples at 33 cm cover gas height and pool temperatures from 410°C to 518°C, plus one sample at 12.5 cm / 375°C. The gas flow rate had been reduced to 12 liters per minute, and, consequently, much better spectra were gained since the amount of sodium deposited on the pre-separator was reduced to about 20%. Size spectra are shown in Fig. 5.1. It is obvious that a log-normal distribution is too simple to interprete the data. We need at least two straight lines, in most cases even three lines. This behaviour may be related to condensation processes but still needs further interpretation. The d_{50}-values as deduced from these spectra are shown in Fig. 5.2 as a function of the pool temperature. Extrapolation to reactor conditions leads to a value around 9 µm.

Only one impactor measurement with argon cover gas was performed during test N-13. The conditions were: 33 cm cover gas, 538°C pool temperature, 8.8 l/min gas flow rate. The pre-separator had 45% of the total amount of sodium collected. The d_{50}-value from the size spectrum was 9.0 µm.

It should be mentioned that we also performed several impactor measurements for the case of helium atmosphere. Although the cover gas visibility was very good in all cases, we found significant amounts of sodium in the impactor but most of it (up to 90%) on the pre-separator. Obviously, condensation and formation of a coarse aerosol occurred during the sampling process. It is not possible to generate reliable size distributions from these measurements.

6. RADIATIVE HEAT TRANSFER

6.1 Overview on radiative transfer

The radiative heat flux between two non-black, finite surfaces is proportional to the fourth power of temperature. The governing equation will be discussed in the next chapter.

In our case, the heat flux which is accepted by the radiometer may have three different origins:

- radiation off the pool surface
- radiation off the side walls
- reflected radiation which originates from pool or from side walls.

In addition, we have an aerosol effect. The aerosol may have a mitigating effect, similar to the effect of clouds between sun and earth. On the other side, the effect of sodium aerosol is mainly scattering with very small absorption. Thus, by multiple scattering of radiation off the walls, an overall increase to the roof may be possible as well. For an interpretation of the measured heat flux which is the sum of these different contributions, it is necessary to have a computer program which calculates the view factors and the different contributions. We have written such a program, assuming specular reflections. The aerosol effect is not yet considered. The emissivities of pool, side wall and cover plate are used as fit parameters. A detailed description of the program will be given in chapter 6.2, an of its verification in chapter 6.3

The radiometer has a double aperture which defines the solid angle. For our test vessel conditions, direct radiation from the side walls is not visible if the vertical distance of the radiating surface element from the cover plate is less than 17 cm (see Fig. 6.15). This is, for example, the case in our runs with 12.5 cm cover gas height. At 33 cm, the wall effects dominate since the wall emissivity is much higher than the emissivity of sodium. Reflections must be taken into account in any case and may play an important role, especially since the metallic pool surface acts like a mirror.

We had an extensive program on radiative heat transfer during tests N-4 to N-7. Additional data were gained during N-8, N-9, and N-10.

6.2 Description of the NACOWA computer program

We have written a computer program to calculate the radiative heat transfer from the sodium pool and from the vessel walls into the aperture of the TER, including reflections, but not considering aerosol effects. The double aperture of the TER which defines the solid angle is taken into account.

The radiative heat flux between two non-black, finite surfaces 1 and 2 at any defined spacial orientation is calculated by the following equation:

$$\dot{Q}_{12} = \sigma \cdot \varepsilon_1 \cdot \varepsilon_2 \cdot \phi_{12} \cdot A_1 \cdot (T_1^4 - T_2^4)$$

where

σ = 5.67 E-08 $W \cdot m^{-2} \cdot K^{-4}$
$\varepsilon_1, \varepsilon_2$ = emissivities of the surfaces
A_1 = surface area 1
T_1, T_2 = absolute temperatures

The geometrical configuration between the two surfaces is considered by the view factor ϕ_{12}. It has to be determined analytically from a double-integral expression over the two areas A_1 and A_2, considering the cos β-law of Lambert. However, for standard configurations, e.g. radiation from a rectangular surface element onto a circular area at parallel or perpendicular orientation, relations for ϕ_{12} may be taken from tables. In our case, the two important configurations are a rectangular area A_1 radiating onto a circular area A_2 which is parallel or perpendicular to A_1; this corresponds to a surface element on the sodium pool (parallel) or on the wall (perpendicular) radiating onto the circular TER aperture. Expressions for both cases were taken from the "VDI-Wärmeatlas" [6.1]. The situation is illustrated in Fig. 6.1. To perform the numerical computations, the pool surface is subdivided into concentrical rings and the wall into cylindrical rings.

As for the effect of the double aperture, we use the inner opening with radius RB as reference (see Fig. 6.2). The possible shadowing or cut-off effect from the outer opening with radius RA is considered by a correction factor FDOP; it is calculated from geometrical correlations which follow from the projection of the outer circular area onto the plane of the inner area as illustrated in Fig. 6.2.

In the above equation for $\dot{Q}_{12}$, the emissivities ε_1 correspond to pool (ε_p) or wall (ε_w), and ε_2 to the TER opening. The latter is assumed to be equal to one. T_1 is the temperature of the considered surface element on pool or wall. The temperature drop across the wall in the vicinity of the cover plate is considered by a relation deduced from experiments. The standard value of the cover plate temperature T_2 is 393 K.

The NACOWA program has five subroutines to calculate the total amount of radiation accepted by the TER (see, for illustration, Fig. 6.3):

A. Subroutine NAPO calculates the amount of direct radiation from the pool surface.

B. Subroutine WAND calculates the amount of direct radiation from the vessel walls.

C. Subroutine POREFL calculates multiple reflections from an element of the pool p via cover plate c, assuming specular reflections. The total contribution is the sum of the following terms:

p - c - p - TER (i = 1)
p - c - p - c - p - TER (i = 2) etc.
until infinity.

D. Subroutine WPREFL calculates multiple reflections from an element of the side wall w with first reflection on the pool surface:

w - p - TER (i = 1)
w - p - c - p - TER (i = 2) etc.
until infinity.

E. Subroutine WDREFL calculates multiple reflections from an element of the side wall with first reflection on the cover plate:

w - c - p - TER (i = 1)
w - c - p - c - p - TER (i = 2) etc.
until infinity.

In the numerical computation, we stop if reflection term i adds less than 1 percent of term 1.

The attenuation of a reflected ray after surface interaction, compared to a direct ray, is considered by a factor FREFL which is a combination of the emissivity and of the index i, and by replacing the real surface element by a virtual element at a location which follows from geometrical extrapolation as shown in Fig. 6.4. This is equivalent to introducing a virtual cover gas height.

Case C: $hc \rightarrow hc \cdot (1+2i)$
$FREFL = (1 - \varepsilon_D)^i \cdot (1 - \varepsilon_{Na})^i$

Case D: $hc \rightarrow hc \cdot (2i+1) + x$
$FREFL = (1 - \varepsilon_{Na})^i \cdot (1 - \varepsilon_D)^{i-1}$

Case E: $hc \rightarrow hc \cdot (2i + 1) - x$
$FREFL = (1 - \varepsilon_{Na})^i \cdot (1 - \varepsilon_D)^i$

In summary, the NACOWA program solves the following equations (see also Fig. 6.4 for symbols):

A. Direct radiation from pool

$$\Delta Q_{pool} = \sigma \cdot \varepsilon_{Na} \cdot \phi(r, O) \cdot \Delta A_P \cdot (T_{Na}^4 - T_c^4) \cdot FDOP(r, O)$$

$$Q_{pool} = \sum_{r=0}^{R} \Delta Q_{pool}; \quad \Delta A_P = \pi \cdot (r + \Delta r)^2 - \pi \cdot r^2$$

B. Direct radiation from walls

$$\Delta Q_{wand} = \sigma \cdot \varepsilon_W \cdot \phi(R,x) \cdot \Delta A_W \cdot (T_W^4(x) - T_c^4) \cdot FDOP(R,x)$$

$$Q_{wand} = \sum_{x=0}^{hc} \Delta Q_{wand}; \quad \Delta A_w = 2\pi R \cdot \Delta x$$

C. Reflection type POREFL

$$\Delta(\Delta Q)_{pr,i} = \sigma \cdot \varepsilon_{Na} \cdot \phi(r,x^*) \cdot \Delta A_P \cdot (T_{Na}^4 - T_c^4) \cdot FDOP(r,x^*) \cdot FREFL(i)$$

$$\Delta Q_{pr} = \sum_i \Delta(\Delta Q)_{pr,i}; \quad Q_{pr} = \sum_{r=0}^{R} \Delta Q_{pr}$$

D. Reflection type WPREFL

$$\Delta(\Delta Q)_{wpr,i} = \sigma \cdot \varepsilon_w \cdot \phi(R,x^*) \cdot \Delta A_w \cdot (T_w^4(x) - T_c^4) \cdot FDOP(R,x^*) \cdot FREFL(i)$$

$$\Delta Q_{wpr} = \sum_i \Delta(\Delta Q)_{wpr,i}; \quad Q_{wpr} = \sum_{x=0}^{hc} \Delta Q_{wpr}$$

E. Reflection type WDREFL

$$\Delta(\Delta Q)_{wdr,i} = \sigma \cdot \varepsilon_w \cdot \phi(R,x^*) \cdot \Delta A_w \cdot (T_w^4(x) - T_c^4) \cdot FDOP(R,x^*) \cdot FREFL(i)$$

$$\Delta Q_{wdr} = \sum_i \Delta(\Delta Q)_{wdr,i}; \quad Q_{wdr} = \sum_{x=0}^{hc} \Delta \cdot Q_{wdr}$$

The total radiative heat flux (in units of Watt) accepted by the TER is the sum of five terms:

$$\dot{Q} = \dot{Q}_{pool} + \dot{Q}_{wand} + \dot{Q}_{pr} + \dot{Q}_{wpr} + \dot{Q}_{wdr}$$

It should be pointed out again that aerosol effects are not considered. The specific heat flux (in units of Watt $\cdot$ m^{-2}) is determined from

$\dot{Q}_S = \dot{Q} / (\pi \cdot R_B^2)$
with $R_B = 0.4$ cm
or $F_B = 0.5$ cm^2, TER acceptance area.

$\dot{Q}$ or $\dot{Q}_S$ have to be compared with the experimental numbers. Experimental input parameters are the cover gas height h_c and the temperatures of pool and cover plate. We assume that pool and wall temperatures are the same if h_c exceeds 11 cm. The program calculates automatically the heat transfer from 160 °C to 640 °C in steps of 10 °C. Fit parameters are the emissivities of pool, wall, and cover plate. A full documentation of the NACOWA code (status March 1989) is available as an internal report (ref. [6.2]). Meanwhile, a few alterations were introduced, e.g. double-precision calculation.

Small-scale verification tests will be described in chapter 6.3, and calculations for the conditions of NACOWA tests in chapter 6.4

6.3 Small-scale tests with heated metal plates and a black body (Cavity radiator)

To check the performance of the TER and to verify the computer program, we have performed small-scale tests with hot metal plates and a cavity radiator as black body in an arrangement which is shown in Fig. 6.5. We used four different circular plates (stainless steel polished, steel grey, copper, and steel black-finished) for variation of the emissivities over a wide range. The plates were placed on a circular copper block to achieve a homogenized temperature, and the block itself was placed on an electric heater. Experimental parameters were the plate temperature (max. 500 °C) and the distance between plate and TER (from 3 cm to 39 cm). The cavity radiator was a stainless-steel pot with a circular opening on top. The inner walls were blackened by soot. The pot was heated electrically. Again, different distances and temperatures were used as experimental parameters.

We have scaled-down the NACOWA computer program to the conditions of these small-scale tests. The method of code verification was as follows:

- Run the code for each metal plate with the emissivity as free parameter
- Run the code for the cavity radiator with an emissivity of almost one (no free parameter).

A selection of results is shown in Figs. 6.6 to 6.8. We have very good agreement in all cases if we use the following emissivities:

ε = 0.155 (polished plate)
0.265 (grey plate)
0.580 (black-finished plate)
0.790 (copper plate)
0.99 (cavity radiator)

The copper plate was optically black after the first heating test due to oxidation. Its emissivity is above the black-finished steel plate. The most valuable result is the good agreement in case of the cavity radiator since we have no free parameter in that case. It needs to be pointed out, however, that we could not verify the reflection terms since the experimental setup had no side walls.

A full documentation of the small-scale tests and their comparison with the code is available as an internal report [6.3].

6.4 Experimental results and calculations

Data on radiative heat transfer were gained during tests N-4 to N-10. These data cover a wide range of pool temperatures and cover gas heights. Most tests were carried out under the conditions of standard cover gas heights. Parameters and results of these tests are listed in Tab. 6.1 for N-4, 6.2 for N-5, 6.3 for N-8, and 6.4 for N-9. These data cover the range of pool temperatures from 273°C to 512°C, and roof temperatures from 109°C to 171°C. A correction factor is applied to unify the data to 120°C plate temperature. Heat transfer rates vary from 0.38 kW/m^2 to 2.2 kW/m^2.

In addition, we have the empty-vessel test N-6, and the test with a shallow sodium layer N-7. During the empty-vessel test (N-6, Tab. 6.5), the wall temperature increased from 160°C to 470°C, the plate temperature from 72°C to 200°C, and, correspondingly, the heat transfer rate from 0.31 kW/m^2 to 6.78 kW/m^2. In the frame of N-7, the pool temperature was raised in steps from 210°C to 400°C over several days, and decreasing heat transfer rates compared to N-6 were observed due to sodium deposition at the walls (see Tab. 6.6).

Shown in Fig. 6.9 are our data on the 12.5 cm case. These data are plotted together with calculated results from the computer program which has been described above. A reasonable fit is achieved, although not considering the aerosol effect, with a sodium emissivity of 0.05, a wall emissivity of 0.4, and a roof emissivity of 0.25. At 500°C, the relative contributions to the calculated values are:

- pool directly 35.1 %
- walls directly 0 %
- reflected radiation, originating from the pool 6.4 %
- reflected radiation, originating from the walls 58.5 %

There is, however, an experimental tendency towards lower sodium emissivity values with increasing temperature. In fact, 0.03 appears to be superior for temperatures above 450°C. In that case, the relative contribution from the pool directly is only 24.5%.

It is evident from these calculations that reflected radiation plays a dominant part. Although the radiation which is emitted from the walls is not directly seen by the radiometer (outside of solid angle acceptance), reflected radiation originating from the walls

adds a higher contribution to the total amount than the direct radiation from the pool. In connection to this, another important effect comes into play: the wall emissivity may change significantly during a test due to sodium aerosol and vapour deposition, depending on sodium temperature, wall temperature, and time. Because of this, our experimental data exhibit fluctuations far above statistical variations. The effect of a lower wall emissivity (0.3 instead of 0.4) is demonstrated in Fig. 6.10.

Shown in Fig. 6.11 are our data on the 33 cm case. Again, they are shown together with calculations. Since we have now a direct wall contribution, the values are higher than in case of 12.5 cm, and the fluctuations are even stronger. A reasonable fit is achieved, again without considering an aerosol effect, with a sodium emissivity of 0.05, a wall emissivity of 0.14, and a roof emissivity of 0.25. The 'low' wall emissivity reflects the effect of sodium deposition on the visible part of the wall. At 500°C, the relative contributions to the calculated values are:

- pool directly 21.2 %
- walls directly 37.6 %
- reflected radiation, originating from the pool 2.7 %
- reflected radiation, originating from the walls 38.5 %

Obviously, radiation off the walls is dominant, and 'walls directly' is almost twice the amount of 'pool directly'. Besides the fluctuations, our data show the tendency to lie above the calculations at low temperatures, and below the calculations at high temperatures. This may be due to the wall deposition effect which increases with temperature. In fact, we should use a larger wall emissivity at low temperatures (e.g. 0.4), and a lower one at high temperatures. But our data are not from a straight-forward test, but from many separate tests, with no well-defined history of wall deposition, which makes an accurate interpretation difficult.

Of course, there is an additional aerosol effect. But metallic sodium aerosol particles are small spheres which mainly reflect and randomize radiation from pool and walls. This may even lead to an overall increase. An estimate of the aerosol effect for our case has been made by Clement and Ford in ref. [6.4]. The result was that the radiative transfer to the roof is increased by some 20%. It should be mentioned that our data do not indicate a strong aerosol effect since they show the same trend in the region below 400°C (few aerosol), and above 400°C (dense aerosol).

Concerning the empty-vessel test (N-6, Tab. 6.5, Fig. 6.12), we have a very good agreement if we use a wall emissivity of 0.4. From the calculations, the relative contributions to the total radiative heat transfer are: Walls directly 92%, bottom directly 5%, reflections 3%. It should be mentioned that the vessel is fabricated from 316 stainless steel (German notation 1.4948). The state of the surface may be described as 'unwetted' or

'dried-out', i.e. it has previously been wetted but no longer has liquid sodium on it, and visually exhibits a dark grey-brown colour.

Parameters and results from test N-7 with a shallow layer of sodium are shown in Tab. 6.6 and Figs. 6.13 and 6.14. We have a very pronounced, time-dependent deviation from the empty-vessel case. After several days, the radiation decreased to almost one half of its original value. Unfortunately, we have not reached the lower plateau at our conditions. As an extreme case, the wall emissivity may decrease from ~ 0.4 down to the sodium emissivity near 0.03. By visual inspection through the cover plate windows, we could clearly recognize a thin sodium layer on the wall surface.

It needs to be pointed out that we do not claim to have performed emissivity measurements, neither for sodium nor for steel in contact with sodium. The information currently available on the emissivity values of materials in the cover gas and the roof space, including the problems related to sodium deposition (wetting) on steel surfaces, is presented and discussed in an internal AEA-Harwell report (ref. [6.5]). Measurements of the emissivity of a liquid sodium surface are particularly difficult to make accurately and reproducibly. Effects of surface oxidation, of aerosols, and of reflections must be extremely minimized. In the open literature, such measurements are reported in ref. [6.6] from the UK, and in ref. [6.7] from Japan. Our best-fit-parameters (0.03 to 0.05) are well within the values which are quoted there.

7. TOTAL HEAT TRANSFER

Heat transfer across the cover gas occurs by radiation, convection, and condensation. It determines the thermal load of the roof. A background effect is heat conduction along the vessel walls to the roof. The total heat transfer may be significantly higher than the radiative part. In the frame of N-9 and N-10, an attempt was made to determine radiative and total heat transfer simultaneously at pool temperatures from 370°C to 500°C. As described earlier, the test vessel was fully insulated during these tests (see Fig. 7.1), and the heat flux to the cover plate was determined from the temperature difference of the cooling air. A background heat flux exists due to thermal conduction along the vessel walls into the plate, although an insulation ring is installed between walls and plate to reduce this term. Because of this background, we can not exactly determine the contribution of convection and condensation, but give only a conservative upper limit.

The cooling of the plate is achieved by air flow through two spiral ducts, as shown in Fig.2.4. The flow through channel 1 is clockwise, through channel 2 counter-clockwise.

The total heat transfer is determined from mass flow and temperature difference of the cooling air. This has been achieved by the two methods which are illustrated in Fig.7.2. The first measurements during N-9 were carried out with setup No. 1, i.e. the sequence flow meter - pump - cover plate, with thermocouples at positions 2 and 3 and (in some cases) a pressure gauge at position 2. The disadvantage of this setup is the fact that the pump causes a compression and a temperature rise of the cooling air at the entry of the cover plate; it adds additional heat to the amount of heat which has to be determined and, thus, causes undesirable corrections. By set-up No. 2, i.e. the sequence flow meter - cover plate - heat exchanger - pump, this effect does not exist, and we have well-defined initial conditions (room temperature, atmospheric pressure). The heat exchanger is necessary to protect the pump from damage due to the hot air. We used a copper pipe of about 10 m length. A negative consequence of the heat exchanger is that it adds an additional resistance to the air flow rate through the cooling duct and, thus, reduces the cooling capacity. Setup No. 2 has been used during the second part of N-9 and during N-10.

Two problems need to be reported: Due to the total thermal insulation, we could not achieve a cover plate temperature as low as 120°C, even with both cooling ducts operating under maximum air flow. The plate temperature was higher, sometimes exceeding 200°C, and it was not possible to keep the plate temperature constant when varying the pool temperature. Secondly, the temperature distribution across the cover plate was not very homogeneous, but exhibited variations up to ±45°C.

So, in order to produce a set of reasonable experimental data, we had to perform a sequence of measurements with the air flow rate as a parameter (which means different

plate temperatures), determine the average plate temperature, and extrapolate to 120°C later on. This was done in the frame of N-10.

The total heat flux Q_{tot} to the cover plate is calculated from the experimentally determined temperature difference $\Delta T = T_f - T_i$ between inlet ('initial') and outlet ('final') of the cooling air, the air mass flow rate v and the heat capacity of air at constant pressure c_p according to the equation

$$Q_{tot} = v \cdot c_p \cdot (T_f - T_i) \quad [Watt]$$

The specific heat flux is

$$q_{tot} = \frac{1}{F} \cdot Q_{tot} \quad [Watt/m^2]$$

with F = surface area of the cover plate,

F = 0.3318 m^2.

For air under normal pressure and at room temperature, we have

$$c_p = 1.007 \frac{kJ}{kg} \cdot K$$

It increases slightly with increasing temperature, e.g. to 1.012 at 100°C and 1.026 at 200°C. The dependence on pressure may be neglected at our conditions (a 2% increase from 0.1 to 1 MPa).

For our calculations, we used the c_p-value corresponding to the average between the inlet and outlet temperature. The air flow rate, measured by flow meters in liters per minute, is transformed into a mass flow rate using the air density which is typically 1.188 kg/m^3 at 20°C.

So, finally, the equation to be used is

$$q_{tot} = 3.056 \cdot v \cdot \Delta T \quad [Watt/m^2)$$

with v in kg/s. The equation has to be applied individually to flow channel 1 with v_1, ΔT_1, and flow channel 2 with v_2, ΔT_2.

The results from test N-10 are summarized in Fig. 7.3. We had pool temperatures of 370°C, 433°C and 508°C at 33 cm cover gas height and 430°C at 12.5 cm. The average plate temperatures are between 143°C and 276°C. They were achieved by air flux variation. The problem of extrapolation to 120°C is evident, especially in the case 508 / 33, where we could not gain values below 200°C, even at maximum air cooling. The extrapolation numbers vary from 2.2 to 5.1 kW / m^2, with some uncertainties in the upper case. Lowering the plate temperature from 200°C to 120°C leads to an increase of heat flux between a factor 2 and 4.

In Fig. 7.4, radiative and total heat transfer are shown for the 33 cm case. In this figure, the extrapolated numbers are linked by an eyeball-fit curve. This curve is almost constantly a factor of 2.8 above the calculated radiative transfer with sodium emissivity 0.05. At 12.5 cm, the equivalent factor is near 4. It is not shown in a figure, since we have only one measurement.

However, a very careful interpretation of this comparison is necessary. We did not measure the overall radiative heat load of the cover plate, but only the amount of oncoming thermal radiation which is accepted by the TER radiometer with emissivity 1 at the center of the plate. To estimate the overall radiative heat load of the plate, it is necessary to consider the emissivity (= absorptivity) of the cover plate material. So, in case of 0.25 instead of 1, the radiative heat load should be only 1/4 of the TER values, since only 1/4 is absorbed and 3/4 are reflected. The next step, however, is that the reflected part may be re-reflected from the pool surface and, after multiple reflections, be absorbed by the plate to a large extent, so that the overall radiative load, divided by the plate area, may be close to the specific TER values.

8. SODIUM DEPOSITION ON COVER PLATE

At the end of a test series, the sodium is drained from the test vessel into the dump tank by cover gas overpressure. The heaters are turned off, and the facility cools down to room temperature. The cover plate is removed when this state is achieved. This is usually the case after two days. Now, sodium deposits on cover plate and surroundings can be inspected and may be analysed.

Typically, we found a very thin, homogeneous layer of sodium on flat, horizontal areas. However, near penetration holes, we found larger droplets of 1 mm to 1 cm size, especially near the penetration to the view ports. Larger deposits were found on the windows. Droplets of about 0.5 cm size hung on the thermocouple wires underneath the plate. A lot of sodium, practically a continuous layer of about 0.5 cm height, was found on the horizontal step between vessel and insulation ring, as illustrated in Fig. 8.1. The vertical surface of the test vessel was continuously wetted by sodium in the cover gas area, but unwetted in the area which had been covered by the pool sodium.

In the frame of test NACOWA - 12, we took a well-defined sample of the sodium deposit from a rectangular area of 122.5 cm^2 of the plate which was horizontally flat and had no obstructions. This area was convered with a thin and almost homogeneous film of sodium. The amount of sodium was 131 mg or 6.19 g/m^2. This corresponds to a layer thickness of 6.4 µm. The total amount of sodium which had been washed off the plate was 9.80 g, corresponding to 29.5 g/m^2, since the plate area is 0.3318 m^2. The total deposit per m^2 is larger than the deposit on horizontally flat areas due to enhanced deposit on obstructions.

The total deposit has been measured after several tests. The numbers are listed in Tab. 8.1. It is interesting to note that the deposits at elevated plate temperatures (N-9, N-10 with insulation) are higher than at lower temperatures (N-8, N-12, N-13 without insulation). This may be explained by the fact that a larger amount of sodium vapour exists near the plate at increasing temperature as the main source of sodium deposits. The presence of iodine seems to enhance the deposits significantly, according to the result from N-14.

A rough average for total deposits in our case at 120°C plate temperature is 50 g/m^2, for deposits on horizontally flat areas 6 g/m^2.

A picture of sodium deposits on the plate is shown in Fig. 8.2.

9. TEMPERATURE PROFILES ACROSS THE COVER GAS

A large amount of temperature profiles across the cover gas has been determined during all of our tests, using an array of thermocouples. These twelve thermocouples were mounted along a vertical rod at a radial distance of 20 cm from the center of the plate. Their position was selected in such a way that the distance between 0 and 33 cm cover gas height was covered, with special attention to the region of strong temperature gradients in the neighbourhood of the plate.

Examples are shown in Figs. 9.1 to 9.4 for argon and helium cover gas at 12.5 and 33 cm height. A few characteristical features exist:

- In the 12.5 cm argon case, we have a fairly continuous temperature decrease from pool to plate, with no pronounced gas bulk temperature, and a 50% value at 6.25 cm which is significantly lower than the average between pool and plate. For example, an experimental sequence plate - middle - pool is 179°C - 289°C - 512°C, whereas the average would be 345°C.
- In the 33 cm argon case, we have a steep drop above the pool, a fairly pronounced gas bulk temperature, and again a steep drop underneath the plate, with some irregularities (back-bending) which are probably caused by convective hot gas from the side walls. Again, the 50% value is lower than the average between pool and roof, e.g. 311°C compared to 350°C.
- In the 12.5 cm helium case, we have a profile similar to argon but the 50% temperature is very close to the average between pool and plate.
- In the 33 cm helium case, we have a steep drop above the pool, a fairly constant bulk temperature up to about the position of 15 cm, a step downward of more than 50°C between 15 cm and 10 cm, and a smooth decrease to the plate temperature without irregularities. The bulk temperature is very close to the average between pool and plate.

The most likely reason for the different behaviour of argon and helium is: convection with argon, stable layers with helium (see also chapter 10).

10. PHENOMENA IF THE ARGON COVER GAS IS REPLACED BY HELIUM

It is well-known from experience with the French Rapsodie reactor that aerosol formation is suppressed if helium is used as cover gas instead of argon. In the frame of our tests, we tried to get the equivalent information on this phenomenon under EFR conditions. Although argon is presently well-established as cover gas, it is worth while to demonstrate the advantages of helium for future considerations.

Our main helium test was N-13. A few helium runs have also been performed throughout N-10.

After replacing argon by helium during N-10, we realized that we had a very clear view through the view ports onto the pool surface (the surface is almost invisible due to aerosols if argon is used), with a slightly yellow colouring. We took four cover gas samples (N10/8 to N10/11) at 433°C pool temperature and 150°C plate temperature. The sodium mass concentrations, in units of g/m^3, were 3.75 / 3.69 / 3.50 / 4.00. From the visual impression, we must assume that a major part thereof has been sodium vapour and not an aerosol.

During N-13, we had the similar impression from our view port observations that almost no aerosol was present in the cover gas. We had a very clear view onto the pool surface, this time with a slightly blue colouring. Even in the extreme case of 53 cm height, we only realized a very light fog. We took eleven wash-bubbler samples with helium and made six impactor measurements at pool temperatures from 481°C to 545°C. The amounts of sodium which were trapped by these measurements were larger than expected and can only be interpreted by assuming a large fraction of sodium vapour. In tables 10.1 and 10.2, mass concentrations and experimental conditions are listed for wash-bubbler and impactor measurements. Wash-bubbler data increase from 6 to 17 g/m^3, and impactor data from 10 to 19 g/m^3. In the latter case, typically 90% of the sodium was deposited on the pre-separator stage (which is installed to trap coarse particles!). A theoretical interpretation of this effect still needs to be done; it is certainly related to condensation during the sampling process.

The differences in aerosol formation in argon and helium may be explained as follows: Due to the temperature gradient above the pool, we have a natural convection of argon gas and transport of sodium vapour from the hot pool region to the cooler region near the cover plate where aerosol droplets will form due to supersaturation. A mixture of argon gas and sodium vapour (molecular weights 40 and 23) has a specific weight which is lower than argon alone (40 and 40). Thus, convection will be enhanced.

The opposite happens in the helium case. A mixture of helium and sodium vapour (4 and 23) is heavier than helium alone, and convection will be suppressed. Instead, we have stable layers in the cover gas, and not enough vapour in the cooler regions to form an aerosol.

This effect is illustrated by a calculation with the REVOLS code which has been developed at University of Bochum to calculate the evaporation of sodium and the release of volatile fission products from a hot sodium pool into an inert gas atmosphere (see refs. [10.1, 10.2]). The calculation demonstrates the density effect and is shown in Fig. 10.1.

11. ENRICHMENT OF CESIUM IN THE AEROSOL AND IN THE DEPOSITS

In the frame of the tests N-8, N-9, N-10, N-12, N-13, the enrichment of cesium in the cover gas aerosol and in the deposits has been investigated. The sodium samples were chemically analysed on their cesium content by atomic absorption, using the analytical facilities of the KfK-Institute of Material Research (IMF I).

We present our data in terms of enrichment factors, EF. These factors are related to the initial pool concentration, assuming homogeneous distribution (or, more exactly, to the amount of cesium in the source, divided by the initial amount of pool sodium):

$$EF \quad \frac{\left({}^{Cs}/_{Na} \right) \; sample}{\left({}^{Cs}/_{Na} \right) \quad pool}$$

Density, melting point and boiling point are listed in Tab.11.1. Cesium and sodium vapour pressure and the ratio thereof are shown in Fig. 11.1. Since cesium has a much higher vapour pressure than sodium, we expect EF values bigger than one in all cases. If we assume that the release rates of sodium and cesium from the pool are proportional to the individual vapour pressure, an enrichment factor of 21 is expected at 500°C, decreasing at higher temperatures and increasing at lower temperatures.

Tests NACOWA - 8 and - 9

Due to the unintentional early break of the cesium glass capsule, we cannot relate our data to a zero-time. Enrichment factors from cover gas samples are shown in Fig. 11.2 for N-8 and Fig. 11.3 for N-9. In all cases, we find values between 8 and 20, with no significant change, although the experimental parameters may have changed. This is in good agreement with the vapour pressure assumption. Cesium enrichment in the cover plate deposits are illustrated in Fig. 11.4 (N-8) and Fig. 11.5 (N-9). EF values exceeding 1000 have been measured, especially on cold spots. On the other side, EF of only 1.1 was found in the heavy sodium deposits (several grams) on the 'balcony' underneath the cover plate.

Test NACOWA - 10

The absolute amounts of Na and Cs in the cover gas samples taken during test N-10 are shown in Fig. 11.6. We have a fairly large background (first two samples) since the same sodium had been used as for N-8 and N-9, thus already containing several grams of Cs from the 5 g source of N-8. But the increase between samples two and three due to the additional release of 5 g Cs (increase more than factor of two) is clearly visible.

The time-dependent behaviour of the enrichment factor EF, deduced from these samples, is shown in Fig. 11.7. The average amount of cesium in the first two samples has been subtracted to correct for the background. It is very interesting to note that we already have maximum enrichment just a few minutes after the break of the glass capsule (EF = 13) and a decrease to EF = 7 within the following two hours. These numbers are fairly close to the expected value of 20 according to the vapour pressure.

It is necessary to relate the aerosol concentration to the pool concentration near the surface. We took one pool sample 1 hour before and one sample 1.5 hours after opening the source from a position a few centimeters below the pool surface, as shown in Fig.11.8. The difference of both numbers is $2.51 \cdot 10^{-5}$ and, thus, almost identical with the expected number $2.50 \cdot 10^{-5}$ for the homogeneous mixture of 5 g Cs and 200 kg Na.

Numbers for the enrichment factor in the deposits on the lower side of the cover plate are illustrated in Fig. 11.9. These are integral numbers, achieved from cleanup samples after dismantling. A certain problem is how to relate the cover plate samples to the pool concentration since the conditions had changed several times during the test. We had four days with the low concentration (~4 g Cs left from N-8) and only 1.5 days with the additional 5 g Cs. So, we used 5.4 g as an average normalization number, corresponding to an average pool concentration of $2.68 \cdot 10^{-5}$. With this number, we have an average enrichment factor of 13.3 for the flat areas of the cover plate and 36.9 for the viewports, i.e. the average number is close to the airborne concentration, and a significant increase is observed for the 'cold spots'. This is in a qualitative agreement with N-8 and N-9, although the absolute numbers exhibit strong fluctuations.

There seems to be an effect, however, which is related to the plate temperature. EF may be very high if the plate temperature is low (test N-8, and view ports in general), and decrease if the plate temperature increases (N-9, N-10 with full thermal insulation).

Test NACOWA - 12

Instead of a 5 g source as in the previous tests, we used a 1 g source to gain information on effects related to the pool concentration. This lower amount of Cs was not far away from the amount of background from the previous tests, although the sodium in the storage tank had been exchanged. Unlike N-10, we found no increased cover gas concentration after break of the capsule during our runs on Feb. 1. However, when the next series of runs was performed on Feb. 6 (after draining and refilling of the sodium), the cover gas concentration had increased as shown in Fig. 11.10. After background correction, we gained enrichment factors near 15, in good agreement with the earlier tests. Concerning the enrichment in the cover plate deposits, our results are shown in Fig. 11.11.

Test NACOWA - 13

With the background pool concentration from earlier tests, we determined enrichment factors as usual. The results are shown in Fig. 11.12. We have values of the order of 20, in good agreement with previous tests with a slight, but not significant increase from argon to helium cover gas. The sodium in the storage tank had been exchanged. Enrichment factors from cover plate deposits are shown in Fig. 11.11, together with N-12 values.

12. ENRICHMENT OF IODINE IN THE AEROSOL AND IN THE DEPOSITS

In the frame of test N14, the enrichment of iodine in the cover gas aerosol and in the deposits has been investigated. The sodium samples were chemically analysed on their iodine content by photometry, using the analytical facilities of the KfK Institute of Material Research (IMF I). As usual, the results are presented in terms of enrichment factors, EF, according to the definition

$$EF = \frac{\left(I/_{Na}\right)\ sample}{\left(I/_{Na}\right)\ pool}$$

Physical properties of iodine are listed in Tab. 11.1. Since the iodine release occurs far above its boiling point, we expect fairly large enrichment factors. However, some mitigation will become effective by the iodide reaction (NaI) during the rise of the iodine bubble through the liquid sodium pool. The melting point of NaI is 651°C, and it is much less volatile than iodine.

Similar to the cesium tests, a quartz glass capsule with 0.59 g of elemental iodine was placed onto the source device and prepared to be crushed under sodium. The amount of sodium was 245 kg. Unfortunately, it turned out that we had an early break of the capsule. So we could neither take background samples nor give an exact time-zero value. On the other side, background is expected to be negligible due to the high volatility of iodine.

The theoretical pool concentration is $2.41 \cdot 10^{-6}$. From pool samples near the surface region, we found values which were up to two orders of magnitude above this number. This may be explained by the fact that iodine rises as a vapour bubble (or several bubbles) with iodide reaction at the bubble surface and, thus, is preferably transported to the upper regions of the sodium pool. Nevertheless, we applied the theoretical pool concentration to the EF determination rather than the measured surface concentrations in order to be consistent with all the previous tests.

Cover gas samples were taken over a period of several days. The results are summarized in Fig. 12.1. We found a time-dependent behaviour (unlike the cesium and zinc case) with EF = 706 initially, 570 in the second sample and 101 in the third sample. The last number corresponds to 271.7 mg Na and 0.066 mg I in the sample, and is near detection limit. After replacement of the argon cover gas by helium later on, we found values below detection limit in all cases.

Concerning the cover plate deposits, our results are summarized in Fig. 12.2. We have 832 for the bulk deposit on flat horizontal areas, and 508/338 for the view port duct and

windows, respectively. It is interesting to note that 18.9% of the initial iodine inventory were found in the cover plate deposits at the end of the test.

Obviously, there is a need for further iodine tests. However, due to the decision of the German Ministry of Research and Technology to cease breeder research funding by the end of 1993, a continuation of these tests is unlikely.

13. ENRICHMENT OF ZINC IN THE AEROSOL AND IN THE DEPOSITS

Zinc is not a fission product. However, as stated earlier, zinc levels in the pool sodium can increase the levels of radioactivity since stable Zn-64 is transformed into radioactive Zn-65 (half-life 244 days) by neutron capture. Unlike cesium, the vapour pressure of zinc is far below sodium (see Fig. 11.1). However, a thermodynamic analysis of the Na-Zn system (see, e.g., ref. [13.1]) indicates that zinc concentrations in the gas space above the sodium pool are strongly enhanced. A factor of 100 is quoted in [13.1].

Our test N-13 was carried out with 50 g zinc powder introduced into 288 liters of sodium at 420°C, corresponding to a mass ratio of $2.04 \cdot 10^{-4}$. This fairly large amount of zinc was chosen with respect to the chemical detection limit. Samples from cover gas, pool and deposits were taken as usual and chemically analysed on their zinc content. The enrichment factor EF is defined as

$$EF = \frac{\left({}^{Zn}/_{Na} \right) sample}{\left({}^{Zn}/_{Na} \right) pool}$$

We took pool samples during the test at sodium temperatures between 500°C and 540°C from positions a few centimeters below the surface. Initially, we found a concentration of $2.28 \cdot 10^{-4}$, which is within 11% of the theoretical value. After draining and refilling, we had an average value of $1.23 \cdot 10^{-4}$.

Fourteen wash bubbler samples were taken during the test and analysed on their Zn content. In addition, seven impactor measurements were analysed (only the sodium on the preimpactor stage). Finally, we determined enrichment factors for the cover plate deposits. It has to be pointed out again that a major part of the measurements has been done in helium atmosphere.

The wash bubbler measurements are listed in Tab. 13.1. We have enrichment factors between 6 and 20 for argon, and between 10 and 38 for helium. The impactor measurements are listed in Tab. 13.2. We have 15.6 for the argon case, and values between 8 and 30 for helium. Similar numbers were found for the plate deposits: 9.1 for the total deposit, and 11.7 / 9.6 for the two view ports. A sample taken from the upper rim of the test vessel had 22.4 (see Fig. 13.1).

Concerning the background, e.g. zinc contamination of the samples during the handling procedure, several samples from the previous test N-12 were analysed. Transformed into enrichment factors, typical numbers would be below 0.5.

During N-14, we had no additional zinc source but still a sodium contamination from N-13. From pool samples, we found an average zinc concentration of $1.54 \cdot 10^{-7}$, i.e. three orders of magnitude less than at N-13. Several wash-bubbler samples as well as the plate deposits were analysed on their zinc content. The results are summarized in Tab. 13.3 (wash-bubbler samples), and in Fig. 13.2 (deposits). It is very interesting that the enrichment factors are similar to N-13, in spite of the large concentration difference: From wash-bubbler samples, we have EF values between 5 and 27, and for the deposits, the values are between 4 and 51.

14. SUMMARY AND DISCUSSION

We have performed fifteen different NACOWA test series on phenomena related to the primary cover gas system of a pool-type sodium-cooled reactor. The intent of the tests was mainly to provide data for the design and for source term assessments of the European Fast Reactor EFR. The primary cover gas system is an inert gas blanket lying between a hot sodium pool and a colder roof structure. In the first consistent design of EFR, a pool temperature of 545°C, a roof temperature of 120°C, and an argon cover gas of 0.85 m height were foreseen. Meanwhile, however, a higher roof temperature has been adopted.

The NACOWA tests were performed using a stainless steel vessel of 0.6 m diameter and 1.14 m height. The amount of sodium involved was up to 288 liters. The standard test conditions were: pool temperature near 500°C, plate temperature near 150°C, and argon cover gas heights 12.5 cm or 33 cm. However, the experimental parameters were varied as far as possible in order to achieve generic information. We had pool temperatures from 270°C to 545°C, plate temperatures from 100°C to 300°C (in one special test even above 400°C), and cover gas heights up to the case with empty vessel. Argon was replaced by helium in several cases, and several cesium, iodine, and zinc contamination levels were adjusted to gain a variety of enrichment factors. Alltogether, ten different topics were investigated in the frame of the programme:

Sodium mass concentration in the cover gas is the sum of sodium vapour and sodium aerosol. Aerosol is generated from vapour due to supersaturation in cooler regions. It depends strongly on the evaporation rate and on the gas bulk temperature (for experimental work on sodium evaporation see ref. [14.1], for theoretical work see ref. [10.2]). Calculations on aerosol formation, transport and removal in the cover gas space are reported in refs. [1.6 to 1.8], and computer codes to describe heat and mass transfer in the cover gas system of pool-type reactors including aerosols were developed in Britain (CGAS, ref. [1.5]), and Germany (GASMO, ref. [1.4]). Our experiments are suitable to verify these codes. A corresponding French code (TEMPGAZ) has not yet been presented in the open literature.

Our two methods of sampling (wash-bubblers, impactors) are based on extraction of the sample from the cover gas into external devices. In case of wash-bubblers at room temperature, sodium vapour will condense and be trapped in the water as well as the aerosol. So, the total amount of sodium in the cover gas is determined. By visual inspection of the cover gas system, the degree of aerosol formation may be judged. An analytical model to calculate the vapour and aerosol fraction has been developed in Japan [1.9] but not yet applied to our data.

At our standard conditions with low plate temperature, the onset of aerosol formation was near 350°C pool temperature. We found a steep increase of mass concentration with

temperature, and 36 g/m^3 were measured at 545°C (reactor operating conditions). A plateau has not yet been achieved. It may be, as French results indicate [1.10], near 50 g/m^3. The influence of the plate temperature on mass concentration has been demonstrated: At 420°C plate temperature and 500°C pool temperature, the concentration is only of the order of 5 g/m^3.

Particle size spectra of the sodium aerosol in argon cover gas were measured using eight-stage Andersen impactors. Our typical size spectra deviate from a simple log-normal distribution and may be approximated by three straight lines on a log-normal plot, with aerodynamic mass median diameters increasing with pool temperature (near 4 µm at 400°C, near 8 µm at 545°C, when plate temperatures are from 120°C to 150°C). Similar particle sizes, which are relatively large in terms of aerosol physics, have also been reported from Japanese work [1.9].

Radiative heat transfer across the cover gas consists of radiation off the pool surface, radiation off the side walls, and reflected radiation which originates from pool or from side walls. There is also an interfering effect with the sodium aerosol and the deposits. We measured the radiative heat transfer using a windowless thermo-electronical radiometer which was mounted in the center of the cover plate. To interprete the data with respect to their different contributions, a computer program was written, based on specular reflections, and neglecting the aerosol effect. Fit parameters for the calculations are the emissivities of pool, side wall, and cover plate.

Empty vessel measurements on the dried-out machined 316 stainless steel were very well interpreted with an emissivity of 0.4. The strong effect of sodium deposition on the side walls was demonstrated with a shallow layer of sodium on the bottom: Radiative heat transfer decreased to one half of its original value, with decreasing tendency still continuing after several days. Our tests at standard conditions indicate a sodium emissivity from 0.05 around 300°C to 0.03 around 500°C. However, a strong interrelation exists between wall emissivity and sodium emissivity. At the extreme case of 12.5 cm cover gas height (walls directly not visible), we measured values near 1.2 kW/m^2 with the radiometer at 500°C. According to the computer program, only 24.5% of this value are from the pool directly, and 75.5% from reflections, if we use a sodium emissivity of 0.03, a wall emissivity of 0.4, and a plate emissivity of 0.25. Extrapolation to 545°C yields 1.50 kW/m^2 alltogether, but only 0.37 kW/m^2 directly from the pool. Of course. there is an aerosol effect, and in the case of dense aerosol with almost invisible pool surface, the no-aerosol assumption of the computer program must be wrong. But nevertheless, the no-aerosol and the dense-aerosol region are well interpreted by the program with the same set of parameters. So, we may conclude that there is some randomizing effect caused by the aerosol (which mainly scatters and absorbs little), but no strong effect of mitigation or enhancement.

An estimate of the aerosol effect for our case has been made by Clement and Ford [6.4]. The result was that the radiative transfer is increased by some 20%. This may mainly be understood as a randomizing effect of reflections from radiation off the walls. Our best-fit emissivity values (0.03 to 0.05 for sodium, 0.14 for wetted side-walls, 0.4 for dried-out steel, 0.25 for cover plate) are suggestions but not results from real emissivity measurements. Such measurements are presented or discussed in refs. [6.5 to 6.7].

The total heat transfer was determined from the cooling air flow rate through the cover plate and from inlet and outlet temperature. It was up to a factor of 4 above the radiative transfer. Total heat transfer across the cover gas is the sum of radiation, convection and condensation, with a background effect due to conduction along the side walls. The contribution from condensation is estimated to be small. Convection and conduction are the main contributors but can not be separated by our measuring methods.

Sodium deposition on the cover plate was determined after several tests. Typically, we found a very thin, homogeneous layer of sodium on flat, horizontal areas. At 120°C, it was of the order of 6 g/m^2, corresponding to a layer thickness near 6 µm. However, near penetration holes and on obstructions, we found larger droplets of 1 mm to 1 cm size, and the overall deposits were near 50 g/m^2. A fairly large layer of about 0.5 cm height was found on the upper side of the step between vessel and insulation ring, most likely caused by turbulent aerosol deposition. Deposits at elevated plate temperatures are larger then at lower temperatures since more sodium vapour is present near the plate at higher temperature.

Temperature profiles across the cover gas were determined during all of our tests, using an array of thermocouples. Interesting differences exist between argon and helium. In the 12.5 cm argon case, we have a continuous temperature decrease from pool to plate, and a 50% value at 6.25 cm which is significantly lower than the average between pool and plate. In the 33 cm argon case, we have in addition some irregularities underneath the plate which are probably caused by convective hot gas from the side walls. In the 12.5 cm helium case, we have a profile similar to argon but a 50% temperature very close to the average between pool and plate. In the 33 cm helium case, we have no irregularities, a bulk temperature close to the average between pool and plate, and some evidence that stable layers exist instead of convection.

Phenomena if the argon cover gas is replaced by helium were studied in several tests. Aerosol formation is suppressed if helium is used instead of argon. This fact has clearly been demonstrated by visual inspection of the cover gas during our tests, even at very high temperatures. A mixture of argon gas and sodium vapour has a lower specific weight than argon alone. Thus, convection will be enhanced. The opposite happens in the helium case. A mixture of helium and sodium vapour is heavier than helium alone, and convection is suppressed. Instead, we have stable layers and not enough vapour in

the cooler regions below the plate to generate an aerosol. This effect is also demonstrated by REVOLS code [10.1] calculations.

Nevertheless, helium cover gas samples taken by wash-bubblers or impactors contain a fairly large amount of sodium. Since almost no aerosol is visible, it must have been vapour which condenses during the sampling process. We found, as a rough guideline, sodium mass concentrations which were one third to one half of the corresponding argon values.

The enrichment of cesium in the aerosol and in the deposits was investigated in the frame of several tests and under various conditions. Assuming that the release rates of sodium and cesium from the pool are proportional to the vapour pressure of each species, an enrichment factor of 21 is expected at 500°C, decreasing at higher temperature, and increasing at lower temperature. In fact, enrichment factors from 7 to 20 were measured in all our samples from the cover gas. This is in good agreement with the vapour pressure assumption. The deposits, however, behave differently. Typically, we find larger enrichment factors compared to the aerosol. In a few cases, we had values exceeding 1000, especially on cold spots. However, there may also exist values down to almost 1. For example, EF = 1.1 was found for the sodium deposits on the step between vessel and insulation ring after test N-9. At the same time, we had EF = 1532 at one of the windows. In general, deposit enrichment is very sensitive to the local temperature. The enrichment is low at locations with high temperatures, and high at low temperatures. This qualitative behaviour is clearly demonstrated by our tests N-9 and N-10, although the absolute numbers may vary over a wide range.

Investigation of the enrichment of iodine in the aerosol and in the deposits was the main subject of test N-14. Since iodine is highly volatile, large enrichment factors were expected. In fact, values exceeding 700 were found in cover gas samples, but decreasing with time. The deposits had enrichment factors exceeding 800, and almost 20% of the iodine inventory were found in the plate deposits after dismantling.

Zinc is not a fission product. However, the enrichment of zinc in the aerosol and in the deposits from zinc levels in the pool will increase the levels of radioactivity due to radioactive Zn-65 (after neutron capture of stable Zn-64). Investigations on zinc enrichment were carried out during tests N-13 and N-14. From thermodynamical considerations of the Na-Zn-system, enrichment factors far above the vapour pressure ratio (which is ~0.35 at 500°C) were predicted. In fact, we measured EF-values between 4 and 51, with no significant difference between samples from cover gas and deposits, argon or helium cover gas, and wash-bubbler or impactor sampling. Even at pool concentration difference of three orders of magnitude (N-13 versus N-14), very similar results were gained.

ACKNOWLEDGEMENT

We thank Prof. W. Schikarski for fruitful discussions and his permanent interest in this work.

We thank Mr. W. Seither for his contribution to design and construction of the experimental facility, and Dr. Ch. Adelhelm for her very helpful supervision of the chemical analysis.

We thank Mr. M. Vögtle for his contribution to the experiments, and Mr. M. Mackert for his contribution to the chemical analysis.

We also thank Mrs. K. Brecht, Mrs. P. Schmitt, and Mr. M. Koyro for their contributions to the development of the NACOWA heat transfer code and its verification.

And finally, we thank Mrs. E. Böhme for the preparation of the manuscript.

REFERENCES

[1.1] A.E. Waltar, A.B. Reynolds
Fast Breeder Reactors.
Pergamon Press, New York, 1981

[1.2] D. Coors, K. Ebinghaus
EFR Consistent Design - Justification of the main design features.
EFRA Report A 000 / 0 / 168 A (Dec. 1991), Ed. EFR Associates

[1.3] IAEA, Int. Working Group on Fast Reactors
Proc. of a Specialists' Meeting on Heat and Mass Transfer in the Reactor Cover Gas.
Harwell, England, 8 - 10 October 1985
IAEA - IWGFR - 57 (July 1986)

[1.4] K. Freudenstein
Simplified model for heat transfer in cover gas of SNR 2 (GASMO Code).
IAEA - IWGFR - 57 (1986), pp. 6/3-1 to 6/3-5 (see also ref. 1.3)

[1.5] Y.L. Sinai, I.J. Ford, J.C. Barrett, C.F. Clement
Prediction of coupled heat and mass transfer in the fast reactor cover gas: the CGAS code.
Nucl.Eng. Design 140 (1993) 159 - 192

[1.6] C.F. Clement, P. Hawtin
Transport of sodium through the cover gas of a sodium-cooled fast reactor.
Proc. Int. Conf. on Liquid Metal Technology in Energy Production, Seven Springs, Pennsylvania (1976), pp. 603 - 609

[1.7] C.F. Clement
Aerosol formation from heat and mass transfer in vapour-gas mixtures.
Proc. Roy. Soc. A398, (1985), pp. 307 - 339

[1.8] I.J. Ford
Sodium aerosol formation and removal mechanisms in the fast reactor cover gas space.
J. Aerosol Sci. Vol. 24, No. 2, pp. 237 - 253 (1993)

[1.9] H. Yamamoto, T. Sakai, N. Murakami
Analytical study on mass concentration and particle size distribution of sodium mist in cover gas phase of LMFBR reactor vessel.
J. Aerosol Sci. Vol. 22 Suppl. 1 (1991), pp. S713 - S716

[1.10] M. Julien-Dolias
Sodium aerosol development in an argon cover gas.
Proc. of the Fourth Int. Conf. on Liquid Metal Engineering and Technology, Avignon/France, Oct. 1988, pp. 113-1 to 113-11

[1.11] P. Pradel, S. Frachet, D. Petit
Radiation heat transfer through the gas of sodium-cooled fast breeder reactor.
Proc. of the Third Int. Conf. on Liquid Metal Engineering and Technology, Oxford, April 1984, Vol. 1, pp. 459 - 462

[1.12] G. Costigan
Private Communication

[1.13] J.D. Jackson
Private Communication.

[2.1] J. Minges, W. Schütz
SNR-Quelltermexperimente mit Berstscheibenentladungen unter Natrium.
KfK 5082, Mai 1993

[2.2] J. Minges, H. Sauter, W. Schütz
Retention factors for fission products from sodium tests to simulate a severe LMFBR accident.
Nucl. Eng. Design 137 (1992), 133-138

[2.3] L. Lange, J. Gilles, G. Ast
TER Thermo-Electronic Radiometer, a new fast-response non-intrusive device for radiation and temperature measurement.
6th European Symposium on Material Science under Microgravity Conditions, Bordeaux/France, Dec. 1986, European Space Agency, ESA SP-256 (Feb. 1987)

[6.1] **VDI-Wärmeatlas**
4. Auflage 1984
Abschnitt "Einstrahlzahlen KB 2"

[6.2] P. Schmitt
"Unpublished Results, March 1989"

[6.3] K. Brecht
"Unpublished Results, April 1989"

[6.4] I.J. Ford, C.F. Clement, W. Schütz
An analysis of the NACOWA cover gas aerosol experiments.
Harwell report AERE-R 13676, Nov. 1989

[6.5] G. Costigan
Private Communication.

[6.6] J.D. Jackson, D.K.W. Tong, P.G. Barnett, P. Gentry
Measurement of liquid sodium emissivity.
Nucl. Energy, 1987, 26 No. 6, pp. 387 - 392

[6.7] O. Furukawa, A. Furutani, N. Hattori, I. Iguchi
Experimental study of heat transfer through cover gas in the LMFBR
Proc. of the Third Int. Conf. on Liquid Metal Engineering and Technology, Oxford, April 1984, Vol. 1, pp. 451 - 458

[10.1] M. Koch, J. Starflinger, U. Brockmeier,H. Unger, W. Schütz
The release code package REVOLS / RENONS for fission product retention factor calculation.
Proc. of the 2nd ASME / JSME Nuclear Engineering Joint Conference, San Francisco/California, March 1993, pp. 457 - 462

[10.2] U. Brockmeier, M. Koch, H. Unger
A mechanistic model for the prediction of sodium release from a liquid pool into an inert gas atmosphere.
Proc. of the 1990 Int. Fast Reactor Safety Meeting, Snowbird/Utah, Aug. 1990, Vol 1., pp. 307 - 318

[13.1] A.W. Thorley, A. Blundell, R. Lloyd
Chemical behaviour of zinc in cover gas environment.
IAEA / IWGFR / 61, Specialists' Meeting on Fast Reactor Cover Gas Purification, Richland/Washington/USA, Sept. 1986

[14.1] W. Schütz, H. Sauter
Experimental determination of sodium evaporation rates.
Nucl. Science and Engineering 80, 667 - 672 (1982)

LIST OF TABLES

The table numbers are related to the chapter where the table is discussed.

Sample	h_c (cm)	T_{pool} (°C)	T_{plate} (°C)	ρ Na (g/m³)
4 / 8	12.5	450	128	6.60
4 / 10	12.5	477	135	14.75
4 / 9	33	460	141	5.13
4 / 11	33	500	152	8.68
5 / 2	12.5	320	106	0.40
5 / 4	12.5	410	120	12.50
5 / 6	12.5	505	134	16.14
5 / 1	33	300	114	0.19
5 / 5	33	412	124	0.34
5 / 7	33	512	147	12.07

Tab. 4.1: *Sodium mass concentration in cover gas from tests NACOWA-4 and -5, determined with wash-bubblers.*

Sample	h_c (cm)	T_{pool} (°C)	T_{plate} (°C)	ρ Na (g/m³)
8/1	33	475	140	18.03
8/2		485	141	14.52
8/3		495	148	10.46
8/4		500	153	14.66
8/5		500	160	17.60
8/6		500	150	17.64
8/7		500	135	15.27
8/8		500	128	17.92

Tab. 4.2: *Sodium mass concentration in cover gas from test NACOWA-8, determined with wash-bubblers.*

sample	h_c (cm)	T_{pool} (°C)	T_{plate} (°C)	ρ Na (g/m³)
9/ 1	12.5	372	148	1.04
9/ 2		419	148	3.27
9/ 3		452	189	5.81
9/ 4		468	193	11.21
9/12		491	214	9.63
9/ 8	33	374	151	1.68
9/ 9		374	151	1.53
9/ 6		425	183	3.08
9/10		467	184	7.06
9/11		467	177	6.60
9/13		497	236	8.57
9/14		503	232	8.23

Tab. 4.3: *Sodium mass concentration in cover gas from test NACOWA - 9, determined with wash-bubblers.*

sample	h_c (cm)	T_{pool} (°C)	T_{plate} (°C)	ρ Na (g/m³)
10/1	33	373	181	1.39
10/2		475	240	10.45
10/3		495	260	8.83
10/4		508	294	7.81
10/5		508	294	10.71
10/6		508	294	8.78
10/7		508	294	7.70

Tab. 4.4: *Sodium mass concentration in cover gas from test NACOWA - 10 (argon), determined with wash-bubblers.*

h_c (cm)	x (cm)	T_{pool} (°C)	T_{plate} (°C)	$\rho_{Na,I}$ (g/m³)	$\rho_{Na,W}$ (g/m³)
12.5	3	369	112	4.0	2.0
12.5	3	530	153	30.1	35.6
33	6	541	145	24.0	22.9

Tab. 4.5: *Sodium mass concentrations in cover gas from test NACOWA - 11, determined from impactor measurements (I) and wash-bubbler measurements (W). x = distance from plate to sampling point.*

sample	h_c (cm)	T_{pool} (°C)	T_{plate} (°C)	$\rho_{Na,I}$ (g/m³)	$\rho_{Na,W}$ (g/m³)
12/1	33	410	137	5.2	5.0
12/2		467	146	12.5	9.1
12/3		473	120	13.7	8.9
12/4		496	153	-	19.9
12/5		500	154	-	10.9
12/6		500	130	19.7	13.9
12/7		513	131	25.3	16.6
12/8		518	123	24.4	15.5
12/9	12.5	376	132	4.0	6.0

Tab. 4.6: *Sodium mass concentrations in cover gas from test NACOWA - 12.*
I = impactor, W = wash-bubblers

Sample	h_c (cm)	x (cm)	T_{pool} (°C)	T_{plate} (°C)	$\rho_{Na,I}$ (g/m³)	$\rho_{Na,W}$ (g/m³)
13 / 1	12.5	6	512	179	-	19.6
13 / 2	12.5	6	518	179	-	31.0
13 / 3	33	16	538	161	26.7	-
13 / 4	33	16	538	156	-	16.3

Tab. 4.7: *Sodium mass concentrations in cover gas from test NACOWA - 13, with argon. I = impactor, W = wash-bubblers, x = distance from plate to sampling point.*

Sample	h_c (cm)	T_{pool} (°C)	T_{plate} (°C)	ρ_{Na} (g/m³)	FAUST test No.
15 / 1	68	501	384	8.27	403
15 / 2	40	506	420	5.30	407
15 / 3	30	510	443	3.16	408
15 / 4	30	510	400	3.83	410

Tab. 4.8: *Sodium mass concentration in cover gas from test NACOWA - 15 at elevated plate temperature.*

Measurement No.	T_p [°C]	T_r [°C]	hc [cm]	N_{exp}		corr	N_{120} [kW/m²]
				[mW]	[kW/m²]		
4/1	360	115	12.5	27.7	0.554	0.991	0.549
4/2	366	113	12.5	26.8	0.536	0.989	0.530
4/3	382	116	12.5	30.6	0.612	0.994	0.608
4/4	412	133	12.5	45.1	0.902	1.017	0.917
4/5	412	134	12.5	38.7	0.774	1.018	0.787
4/6	412	135	12.5	40.8	0.816	1.020	0.831
4/7	412	139	33.0	69.3	1.386	1.026	1.422
4/8	450	128	12.5	42.8	0.856	1.008	0.863
4/9	460	141	33.0	64.3	1.286	1.021	1.313
4/10	477	135	12.5	46.5	0.930	1.013	0.942
4/11	500	152	33.0	69.0	1.380	1.027	1.417
4/12	500	150	33.0	68.5	1.370	1.025	1.404

Tab. 6.1: **Radiative heat transfer measurements from NACOWA - 4.**

T_p = pool temperature

T_r = cover plate temperature at position of radiometer

N_{exp} = radiometer reading (0.50 cm²) and specific radiative transfer (1 m²)

corr = correction factor for 120 °C cover plate temperature: $corr = (T_p^4 - 393^4) / (T_p^4 - T_r^4)$

N_{120} = specific radiative heat transfer for 120 °C cover plate temperature

Measurement No.	T_p [°C]	T_r [°C]	hc [cm]	N_{exp}		corr	N_{120} [kW/m²]
				[mW]	[kW/m²]		
5/1	310	114	82.0	90.0	1.800	0.985	1.772
5/2	320	106	12.5	24.8	0.496	0.969	0.480
5/3	320	100	27.0	40.8	0.816	0.957	0.781
5/3a	320	100	41.0	53.6	1.072	0.957	1.026
5/4	410	120	12.5	38.0	0.760	1.000	0.760
5/5	410	124	33.0	49.1	0.982	1.005	0.987
5/6	505	134	12.5	63.2	1.264	1.011	1.277
5/7	512	147	33.0	86.0	1.720	1.021	1.756
5/8	313	116	12.5	22.1	0.442	0.990	0.438
5/9	273	113	12.5	19.6	0.392	0.975	0.382

Tab. 6.2: **Radiative heat transfer measurements from NACOWA - 5.**

T_p = pool temperature
T_r = cover plate temperature at position of radiometer
N_{exp} = radiometer reading (0.50 cm^2) and specific radiative transfer (1 m^2)
corr = correction factor for 120 °C cover plate temperature: corr = $(T_p^4 - 393^4) / (T_p^4 - T_r^4)$
N_{120} = specific radiative heat transfer for 120 °C cover plate temperature

Measurement No.	T_p [°C]	T_r [°C]	N_{exp}		corr	N_{120} [kW/m²]
			[mW]	[kW/m²]		
8/1	475	122	79	1.58	1.002	1.58
8/2	485	127	68	1.36	1.006	1.37
8/3	495	132	75	1.50	1.010	1.51
8/4	500	142	76	1.52	1.018	1.55
8/5	500	126	82	1.64	1.004	1.65

Tab. 6.3: *Radiative heat transfer measurements from NACOWA - 8. Cover gas height 33 cm.*

Measurement No.	T_p [°C]	T_r [°C]	N_{exp}		corr	N_{120} [kW/m²]
			[mW]	[kW/m²]		
9/ 1	372	109	44.9	0.899	0.982	0.883
9/ 2	419	118	45.4	0.908	0.998	0.906
9/ 4 a	468	138	47.2	0.944	1.017	0.960
9/ 5	421	134	45.5	0.910	1.018	0.926
9/ 7	375	108	28.7	0.574	0.982	0.564
9/12	491	141	64.0	1.280	1.018	1.303

Tab. 6.4: *Radiative heat transfer measurements from NACOWA - 9. Cover gas height 12.5 cm*

T_p = *pool temperature*
T_r = *cover plate temperature at position of radiometer*
N_{exp} = *radiometer reading (0.5 cm²) and specific radiative transfer (1 m²)*
corr = *correction factor for 120°C cover plate temperature:* $corr = (T_p^4 - 393^4) / (T_p^4 - T_r^4)$
N_{120} = *specific radiative heat transfer for 120°C cover plate temperature*

Measurement No.	Tw [°C]	Tr [°C]	N		corr	N_{120} [kW / m^2]
			[mW]	[kW/m^2]		
6/1	160	72	28.7	0.574	0.540	0.310
6/2	190	80	45.4	0.908	0.727	0.789
6/3	230	85	65.6	1.312	0.843	1.106
6/4	290	118	117.9	2.358	0.993	2.343
6/5	340	150	168.3	3.366	1.075	3.618
6/6	370	158	210.9	4.218	1.08	4.547
6/7	430	176	280.0	5.600	1.08	6.062
6/8	470	200	307.5	6.150	1.10	6.780

Tab. 6.5 ***Radiative heat transfer measurements from NACOWA - 6 test with empty vessel***

T_w = wall temperature
T_r = cover plate temperature at position of radiometer
N = radiometer reading (0.5 cm^2) and specific radiative transfer
corr = correction factor for 120 °C cover plate temperature: $corr = (T_w^4 - 393^4) / (T_w^4 - T_r^4)$
N_{120} = specific radiative heat transfer for 120 °C cover plate temperature

Measurement	Date	Tw [°C]	Tr [°C]	N [kW/m2]	corr	N_{120} [kW / m2]
7/1	03.08.89	210	85	1.02	0.81	0.82
7/2	03.08.89	210	91	0.93	0.83	0.77
7/3	04.08.89	250	106	1.54	0.94	1.45
7/4	04.08.89	300	129	2.08	1.03	2.14
7/5	07.08.89	355	159	3.39	1.07	3.61
7/6	08.08.89	350	149	2.85	1.07	3.04
7/7	08.08.89	350	150	2.81	1.07	3.00
7/8	08.08.89	350	149	2.68	1.07	2.86
7/9	09.08.89	350	147	2.49	1.06	2.64
7/10	09.08.89	400	174	3.53	1.10	3.88
7/11	10.08.89	400	168	3.25	1.08	3.53
7/12	10.08.89	400	174	2.92	1.10	3.20
7/13	10.08.89	400	174	3.10	1.10	3.40
7/14	11.08.89	400	171	2.71	1.09	2.96

Tab. 6.6 *Radiative heat transfer measurements from NACOWA-7 test with a 2 cm layer of sodium on the vessel bottom. See Tab. 6.3 for explanations.*

Test No.	Total sodium deposit on cover plate		Remarks
	(g)	(g/m^2)	
N-8	20.5	61.8	a
N-9	22.0	66.3	b
N-10	42.1	126.9	b
N-12	9.8	29.5	a
N-13	15.0	45.2	a, c
N-14	53.3	160.6	d

Tab. 8.1: Total sodium deposit on cover plate, measured at the end of a test after lifting the cover plate.

Remarks:
a/ plate not insulated
b/ plate insulated
c/ most runs with helium cover gas
d/ enhancement, possibly due to presence of iodine

Sample	T_{pool} (°C)	T_{plate} (°C)	h_c (cm)	x (cm)	ρ Na (g/m³)
13 / 5	520	192	12.5	6	6.65
13 / 7	525	192	12.5	6	8.06
13 / 8	545	154	33	16	12.51
13 / 10	545	148	33	16	7.78
13 / 11	545	148	33	3	16.93
13 / 12	537	189	53	21	11.79
13 / 13	540	180	53	21	13.98
13 / 15	482	177	12.5	6	6.98
13 / 18	490	138	33	16	6.35
13 / 19	490	138	33	0	8.67
13 / 21	481	171	12.5	0	7.55

Tab. 10.1: *Sodium mass concentrations in cover gas samples from wash-bubbler measurements. NACOWA - 13, helium.*

Sample	T_{pool} (°C)	T_{plate} (°C)	h_c (cm)	x (cm)	ρ Na (g/m³)
13 / 6	525	161	12.5	6	16.1
13 / 9	545	152	33	16	19.2
13 / 14	540	182	53	21	16.6
13 / 16	507	183	12.5	6	18.4
13 / 17	490	138	33	16	10.7
13 / 20	481	174	12.5	6	10.4

Tab. 10.2: *Sodium mass concentrations in cover gas samples from impactor measurements. NACOWA - 13, helium.*
h_c = cover gas height,
x = position of sampling point, distance to cover plate.

Substance	Density at r.t. [g / cm³]	Melting Point [°C]	Boiling Point [°C]
Cesium	1.88	28.4	690
Iodine	4.93	113.5	184
Sodium	0.97	97.8	892
Zinc	7.1	419.4	906

Tab. 11.1: Density, melting point, and boiling point of cesium, iodine, sodium, and zinc.

Sample	T_{pool} (°C)	T_{plate} (°C)	Cover Gas Height (cm)	Gas Type	Sampling Point: Distance to Roof (cm)	Enrichment Factor EF (Zn)
13/ 1	512	179	12.5	Ar	6	20.1
13/ 2	516	179	12.5	Ar	6	12.2
13/ 4	538	156	33	Ar	16	6.4
13/ 5	520	192	12.5	He	6	32.2
13/ 7	525	192	12.5	He	6	38.8
13/ 8	545	154	33	He	16	18.9
13/10	545	148	33	He	16	16.9
13/11	545	148	33	He	3	22.9
13/12	537	189	53	He	21	10.4
13/13	540	180	53	He	21	11.0
13/15	482	177	12.5	He	6	19.0
13/18	490	138	33	He	16	23.8
13/19	490	138	33	He	0	16.6
13/21	481	171	12.5	He	0	13.2

Tab. 13.1: *Enrichment factors for zinc from wash-bubbler samples during NACOWA - 13*

sample	T_{pool} [°C]	T_{plate} [°C]	Cover Gas Height (cm)	Gas Type	Enrichment Factor EF (Zn)
13 / 3	538	161	33	Ar	15.6
13 / 6	525	192	12.5	He	30.5
13 / 9	545	152	33	He	9.9
13 / 14	540	182	53	He	8.6
13 / 16	507	183	12.5	He	17.9
13 / 17	490	138	33	He	10.3
13 / 20	481	174	12.5	He	11.0

Tab. 13.2: *Enrichment factors for zinc from impactor samples (preseparator stage only) during NACOWA - 13.*

Sample	T_{pool} [°C]	T_{plate} [°C]	Cover Gas Height (cm)	Gas Type	Enrichment Factor EF (Zn)
14 / 1	426	159	12.5	Ar	14.0
14 / 2	485	142	12.5	Ar	2.8
14 / 3	533	140	33	Ar	5.3
14 / 7	535	138	33	Ar	27.2
14 / 8	535	140	33	Ar	9.6

Tab. 13.3: *Enrichment factors for zinc from wash-bubbler samples during NACOWA - 14.*

LIST OF FIGURES

The figure numbers are related to the chapter where the figure is discussed.

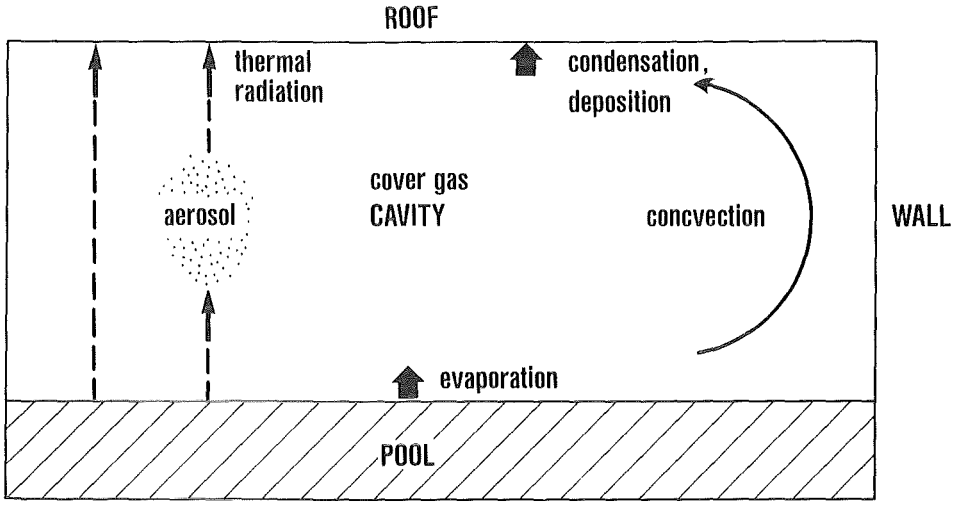

Fig. 1.1 Typical geometry of the fast reactor cover gas space.

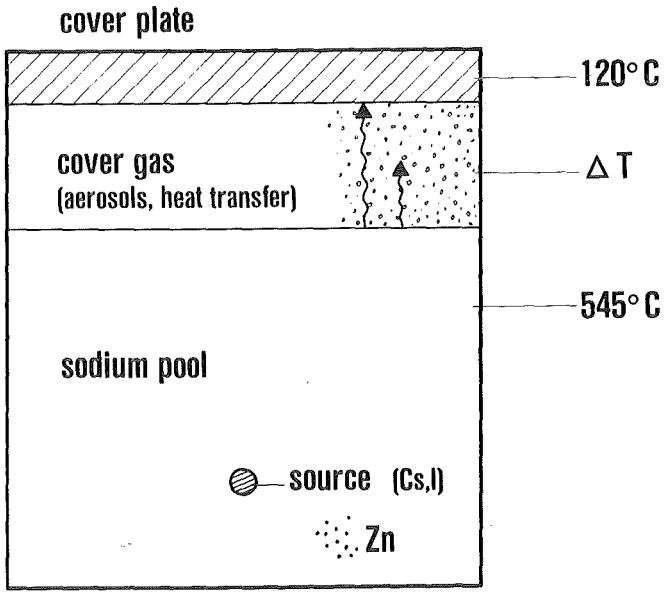

Fig. 1.2 Simplified sketch to illustrate the main conditions of the NACOWA programme in relation to EFR.

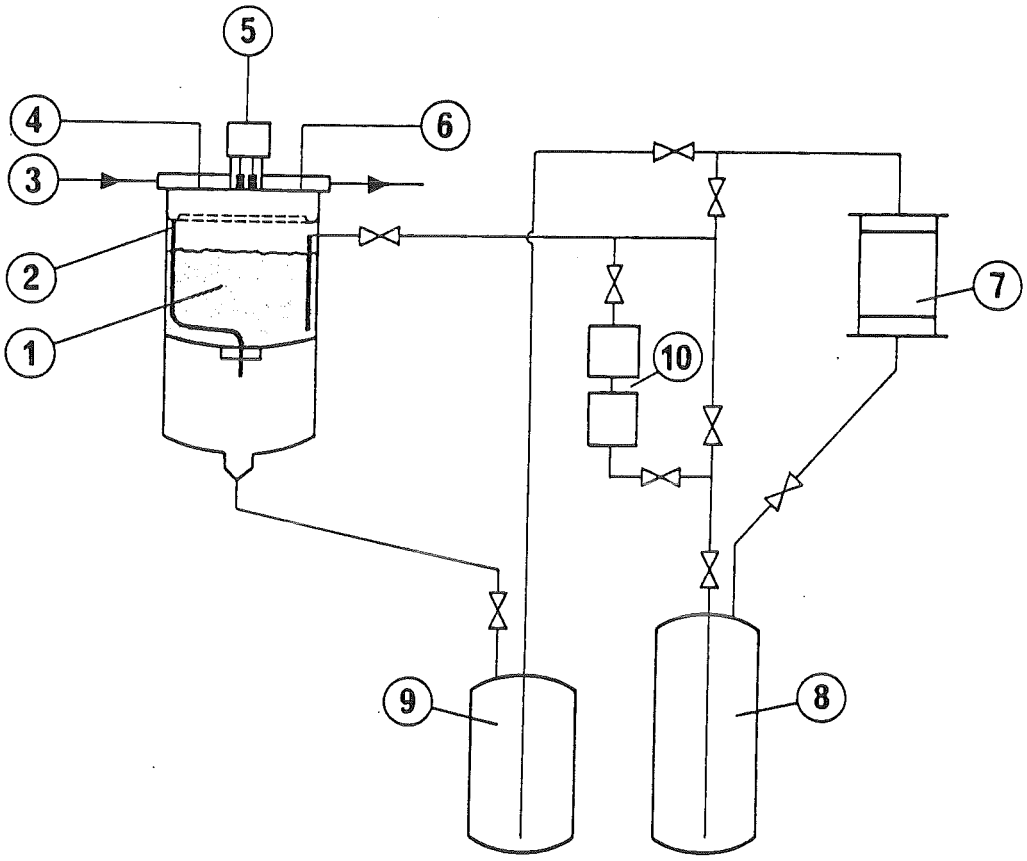

Fig. 2.1 Diagram of the entire NACOWA facility including sodium storage and handling.

1 sodium test vessel (0.6 m ∅ , 1.1 m h)
2 sodium overflow ring
3 air cooling
4 aerosol measurement
5 thermo-electronical radiometer
6 temperature measurement
7 sodium supply
8 sodium storage tank 500 liters
9 sodium dump tank 300 liters
10 filter section

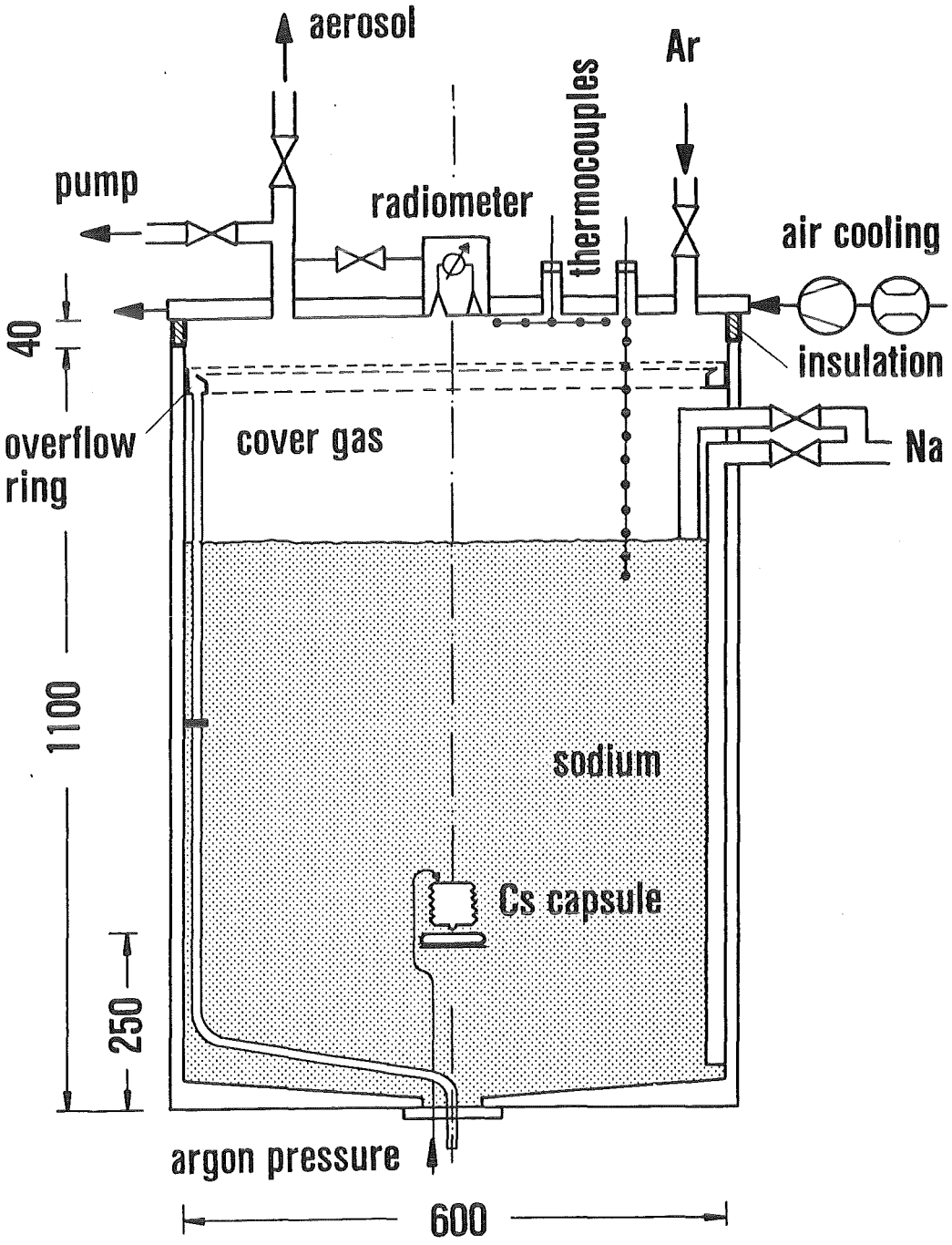

Fig. 2.2 NACOWA test vessel.
(Dimensions in mm).

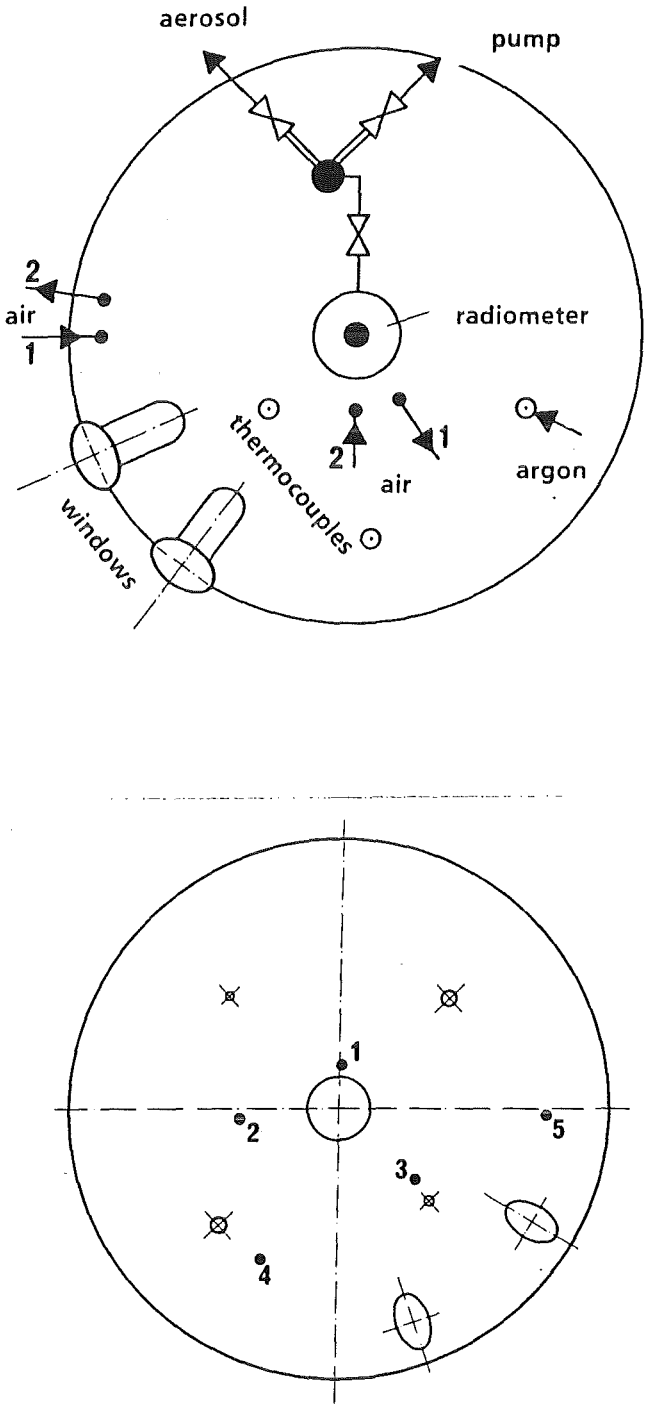

Fig. 2.3 Cover plate, top and bottom view.
The numbers on the bottom view indicate positions of thermocouples.

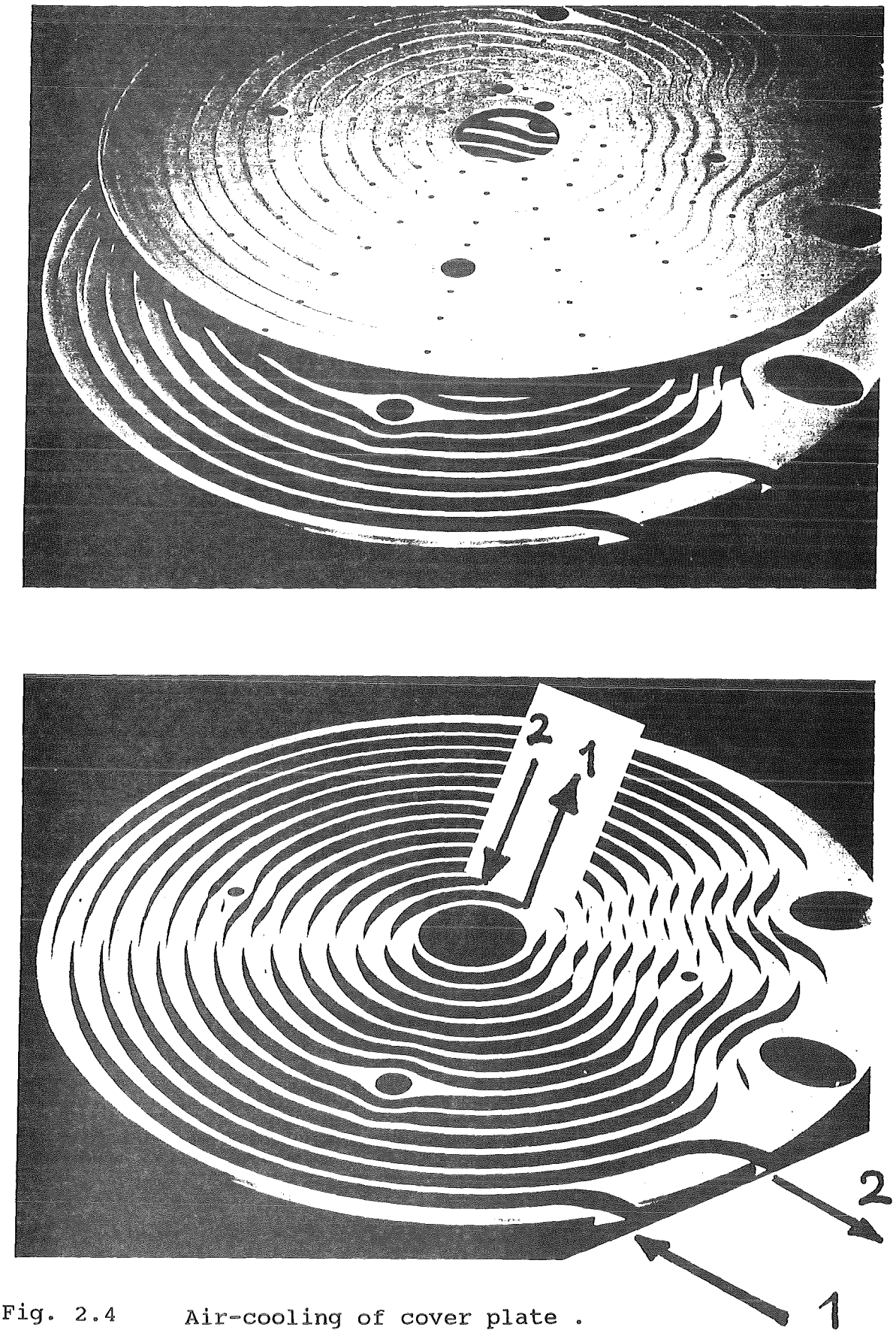

Fig. 2.4 Air-cooling of cover plate .

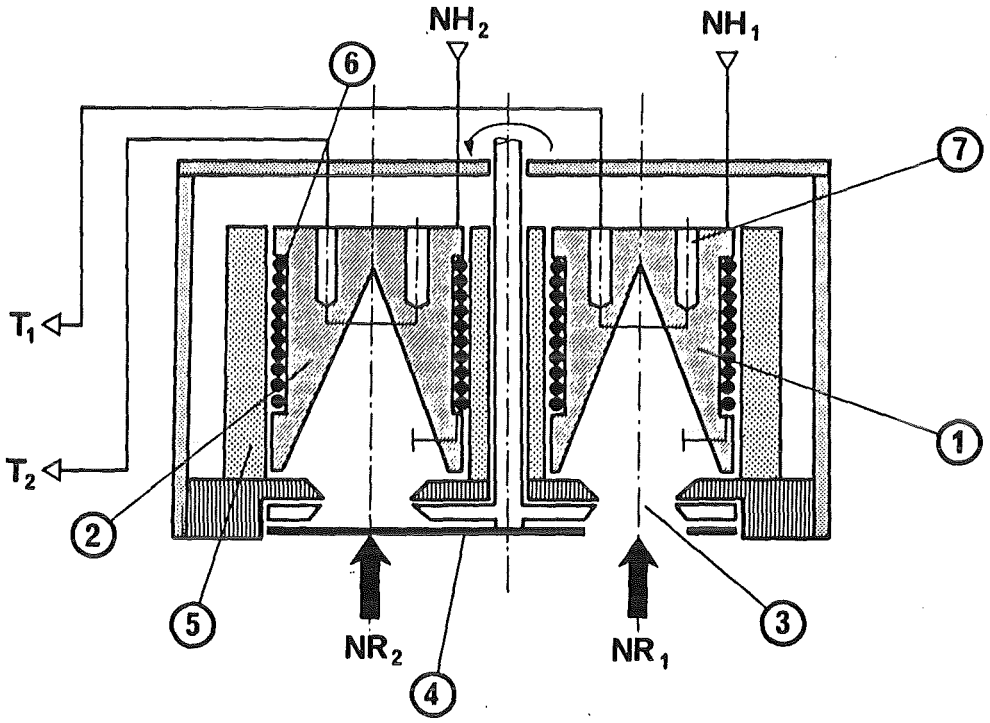

Fig. 2.5 **Thermo-electronical radiometer**

1	absorber	2	reference absorber
3	aperture	4	reflector
5	copper block	6	heater
	7 temperature sensors		

NH = thermal input by electric heating
NR = incoming radiation

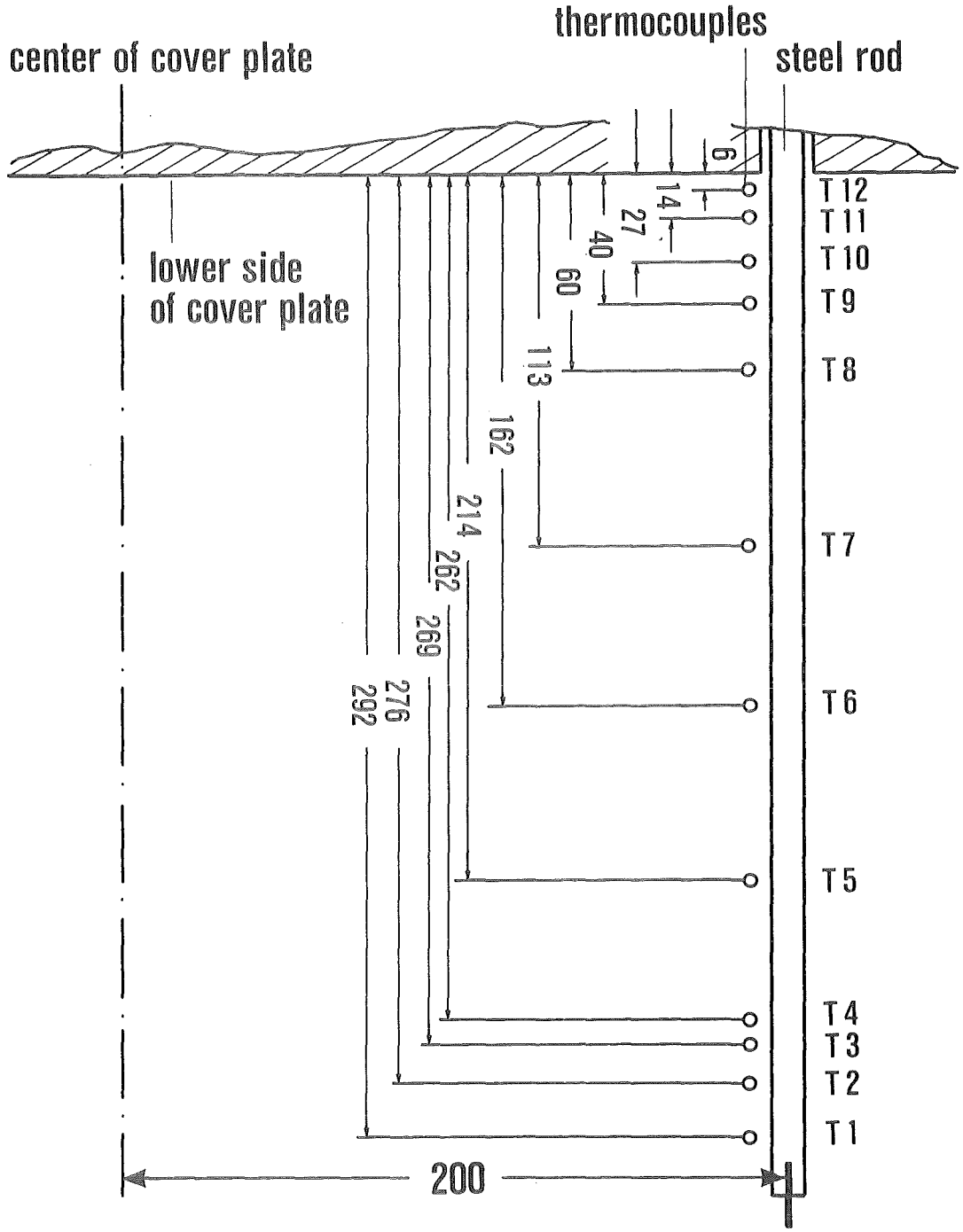

Fig. 2.6 Vertical arrangement of thermocouples in the cover gas region

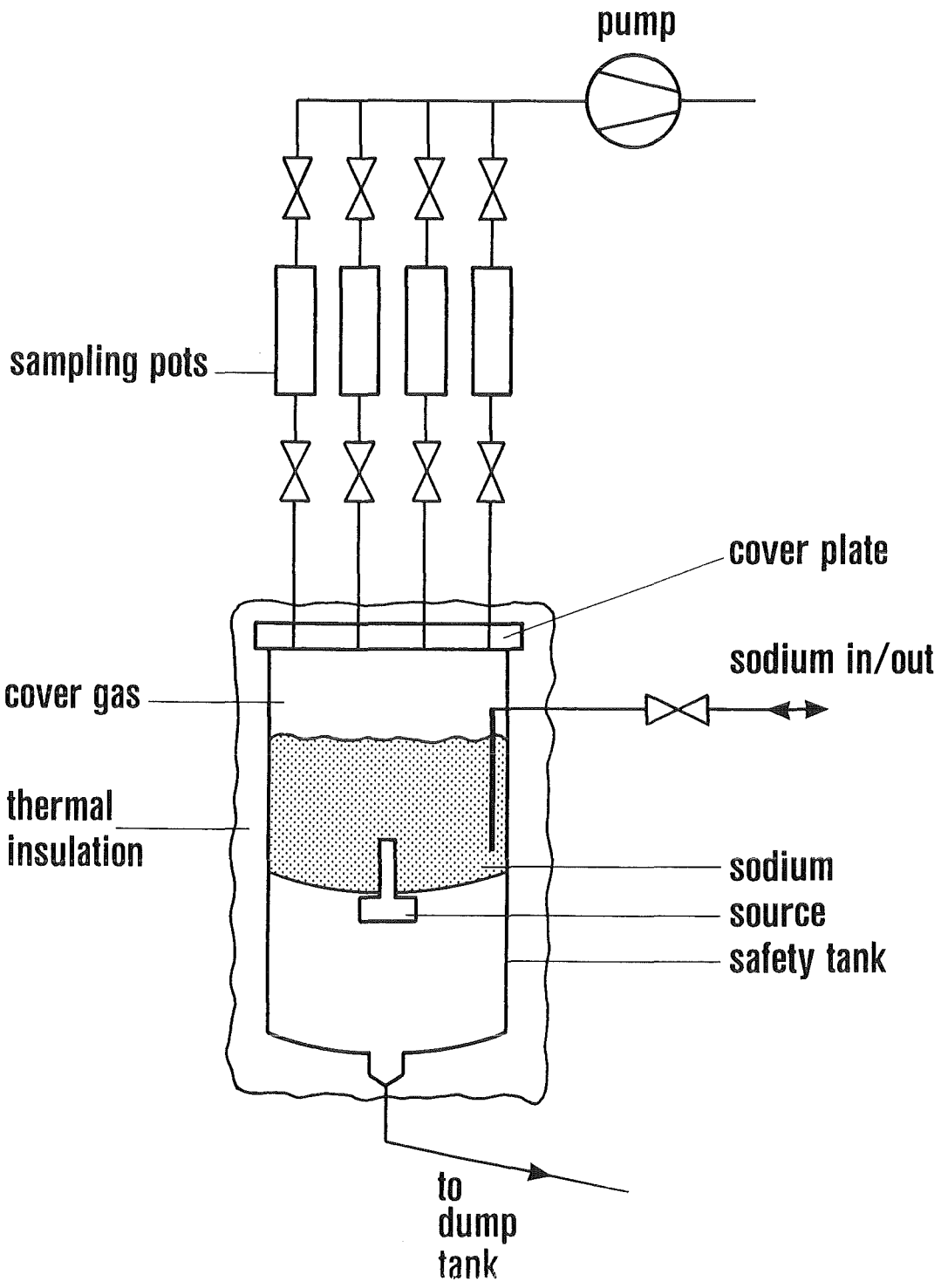

Fig. 2.7 Sketch of FAUST setup to collect cover gas samples under high plate temperature (test NACOWA-15)

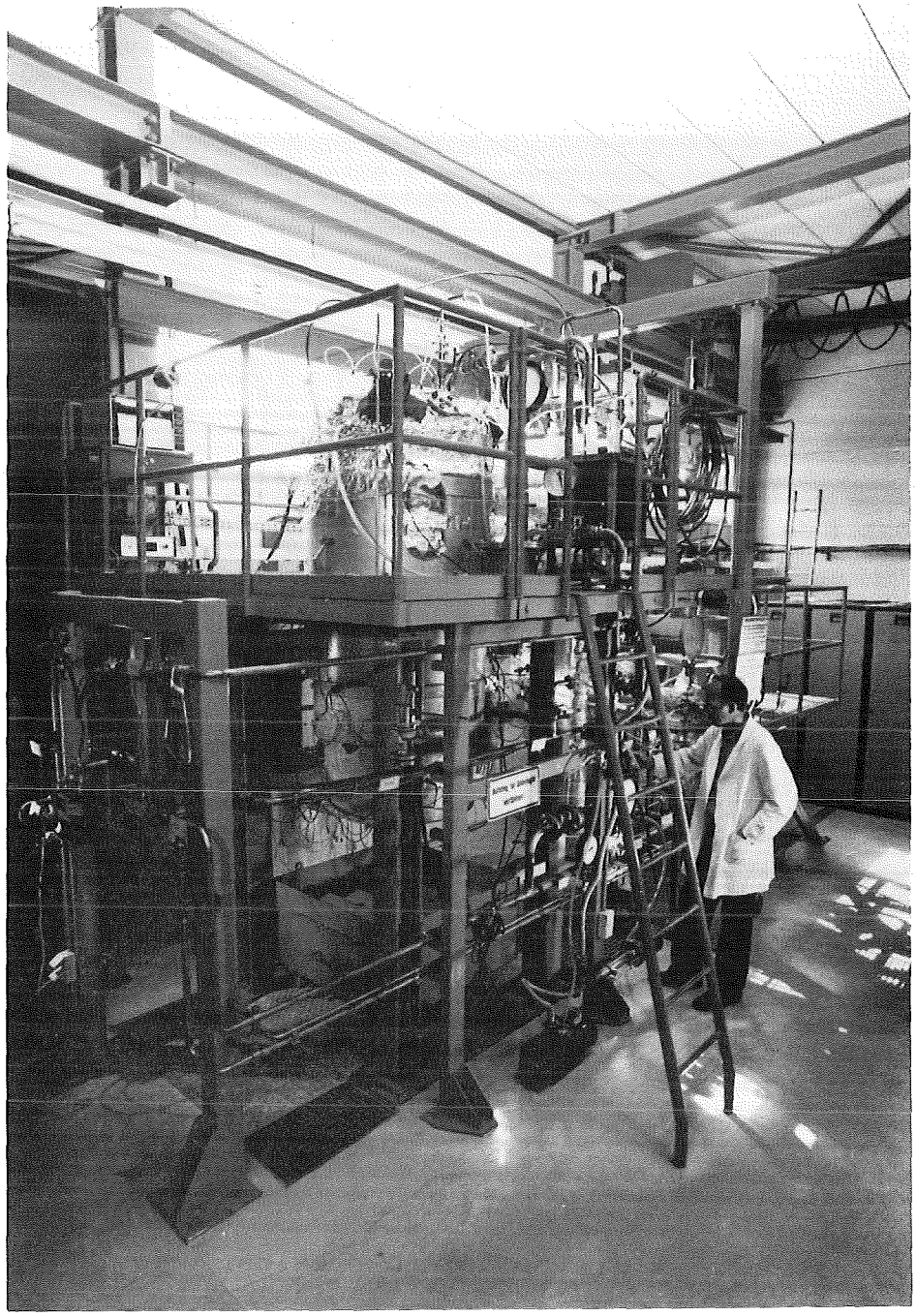

Fig. 2.8 Foto of the NACOWA facility.

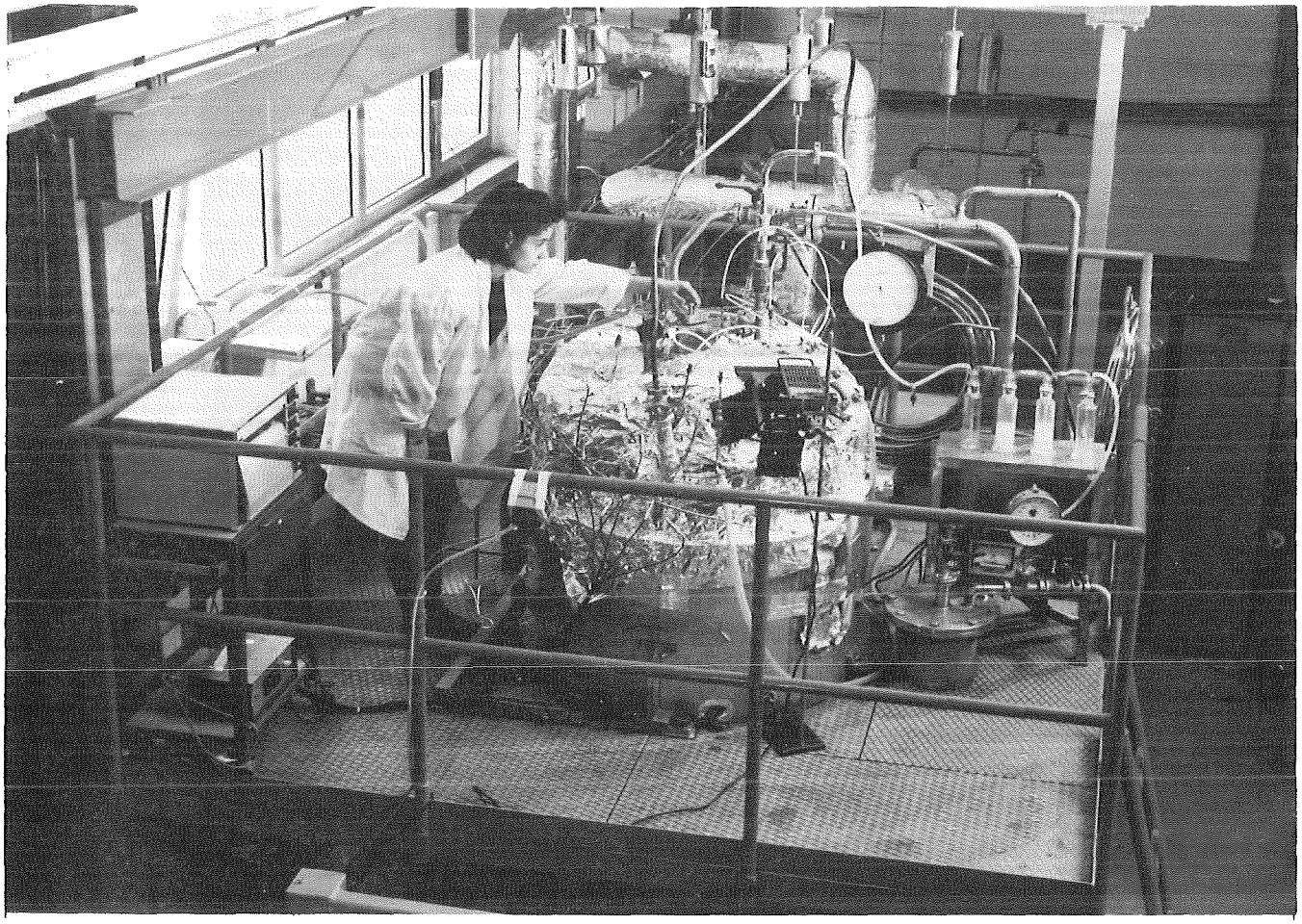

Fig. 2.9 Foto of cover plate area during test with full thermal insulation.

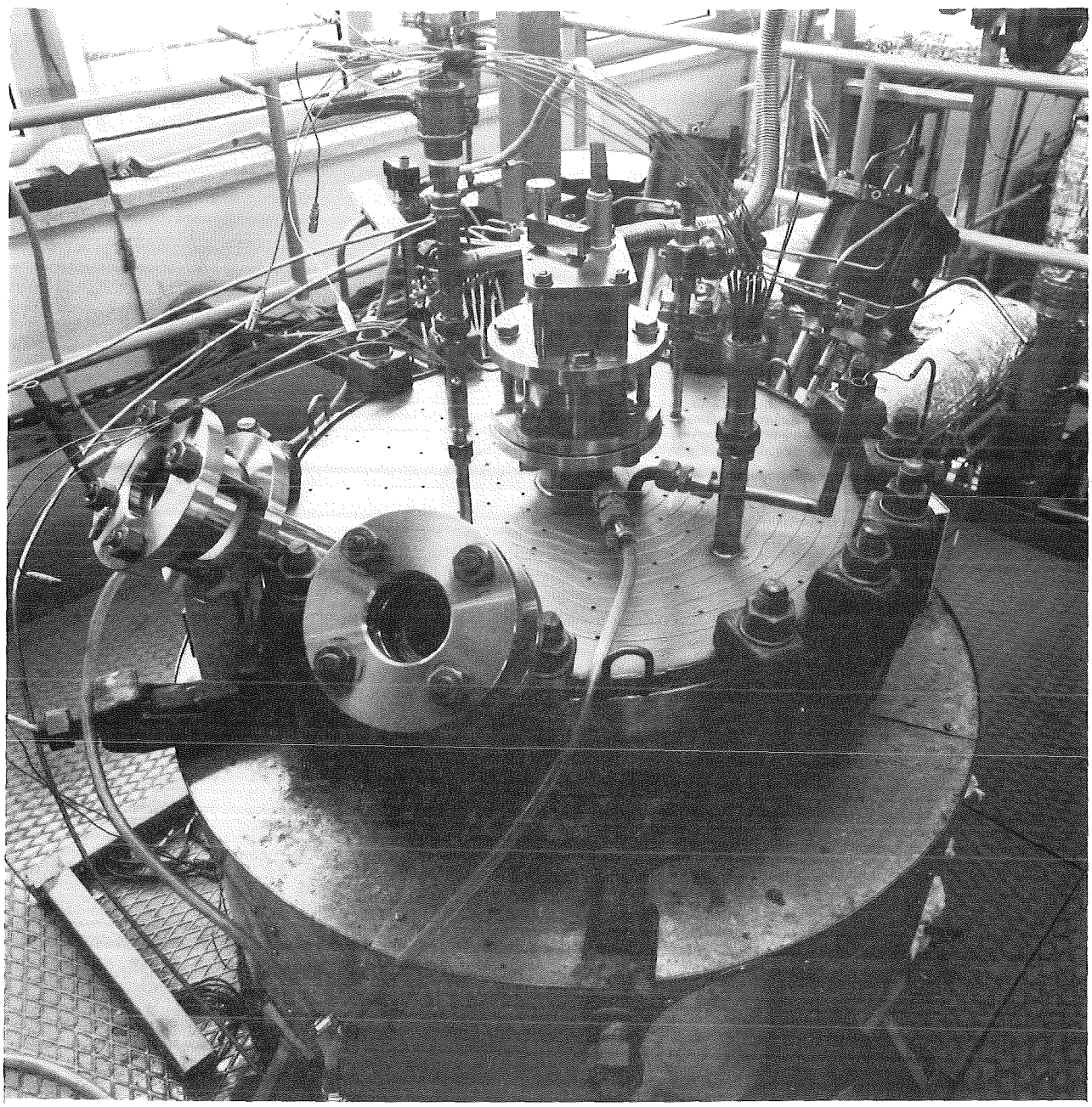

Fig. 2.10 Cover plate and installations:
View ports, radiometer, penetration for thermocouples, connections for air-cooling, penetration for cover gas sampling.

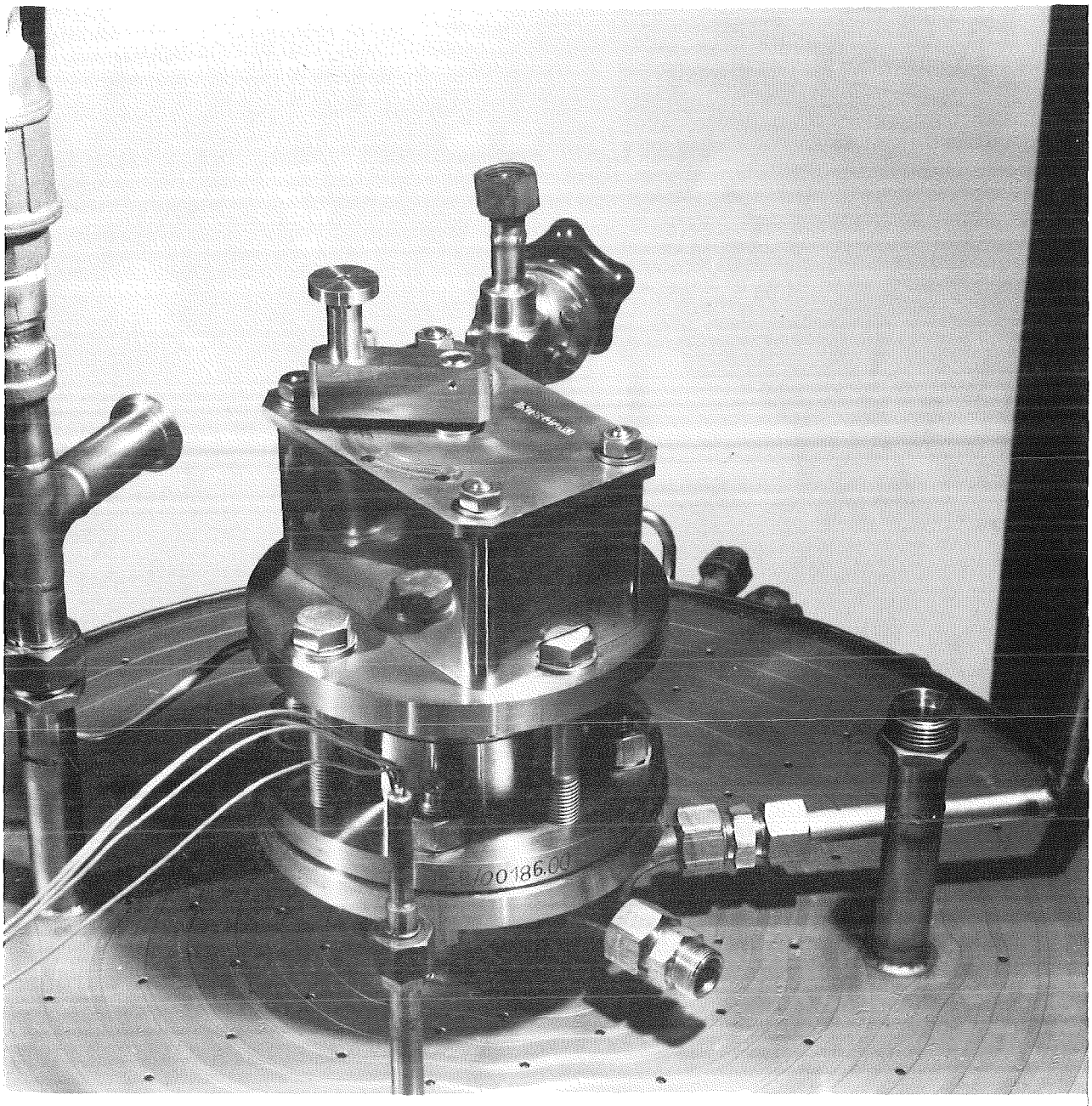

Fig. 2.11 Thermo-electronical radiometer TER

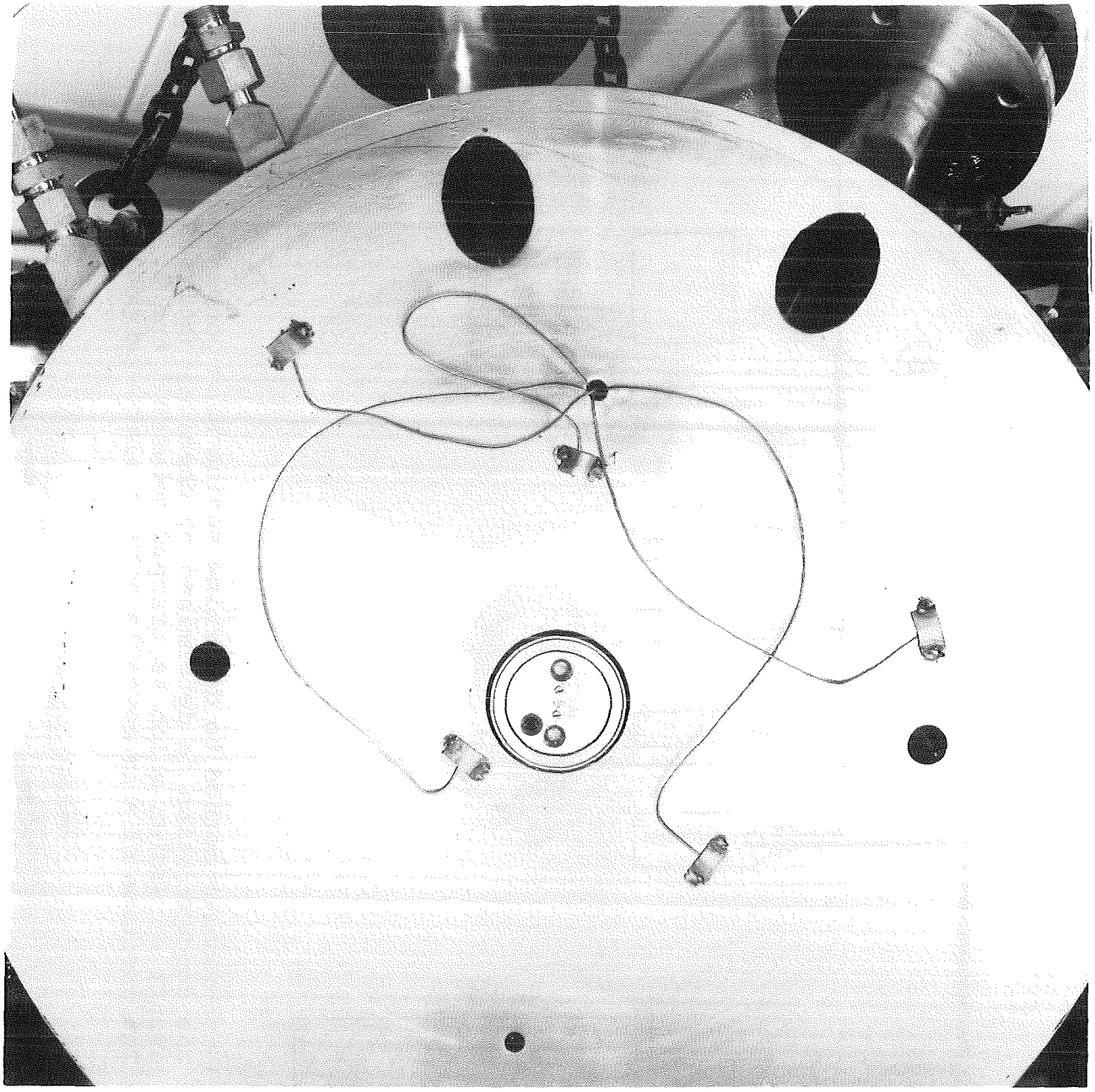

Fig. 2.12 Lower-side view of cover plate with thermocouples, radiometer and view ports.

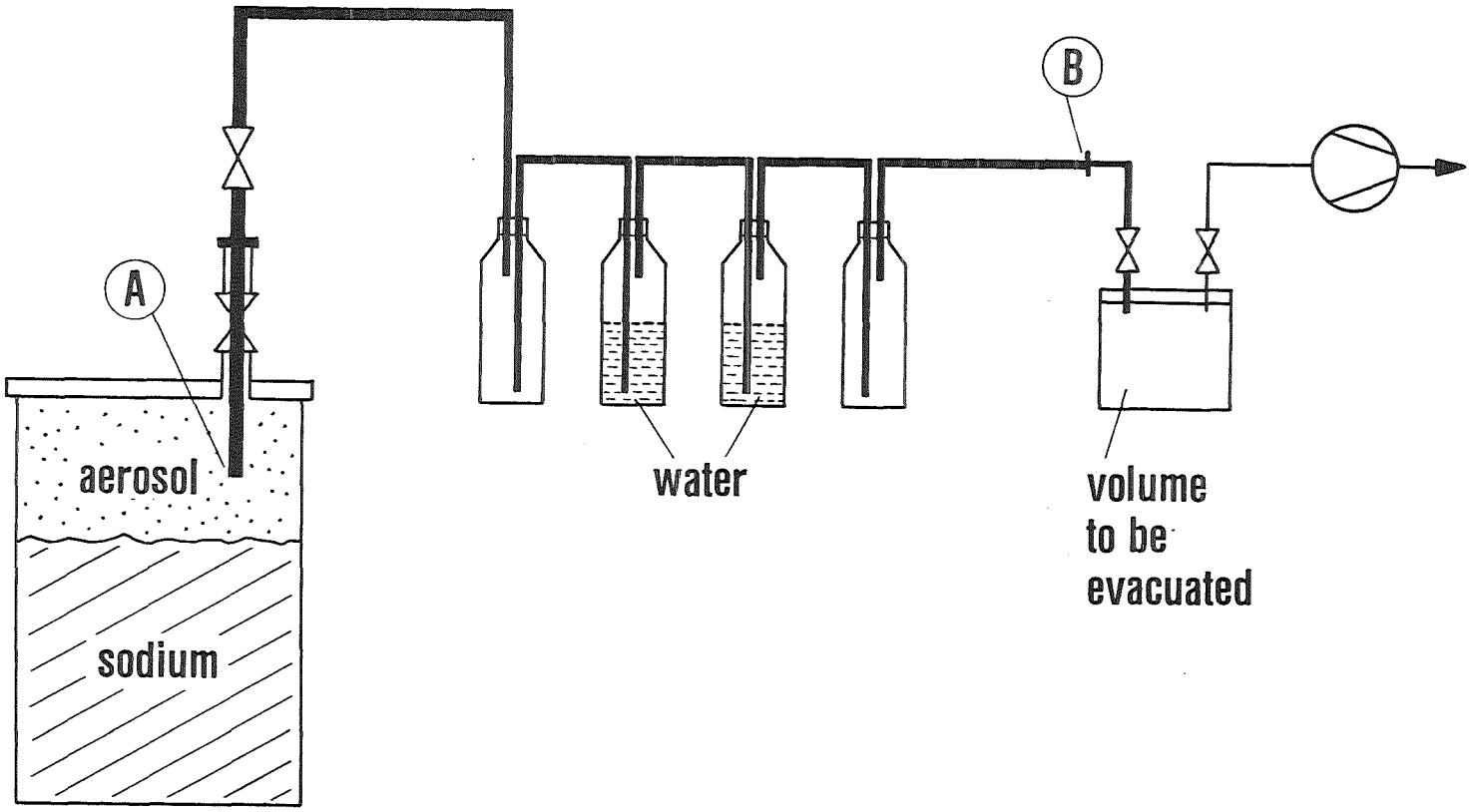

Fig. 4.1 Wash-bubbler method to determine sodium mass concentrations. The concentration is determined by chemical analysis of the amount of sodium which is trapped between A and B. The position of A is moveable between plate and pool surface.

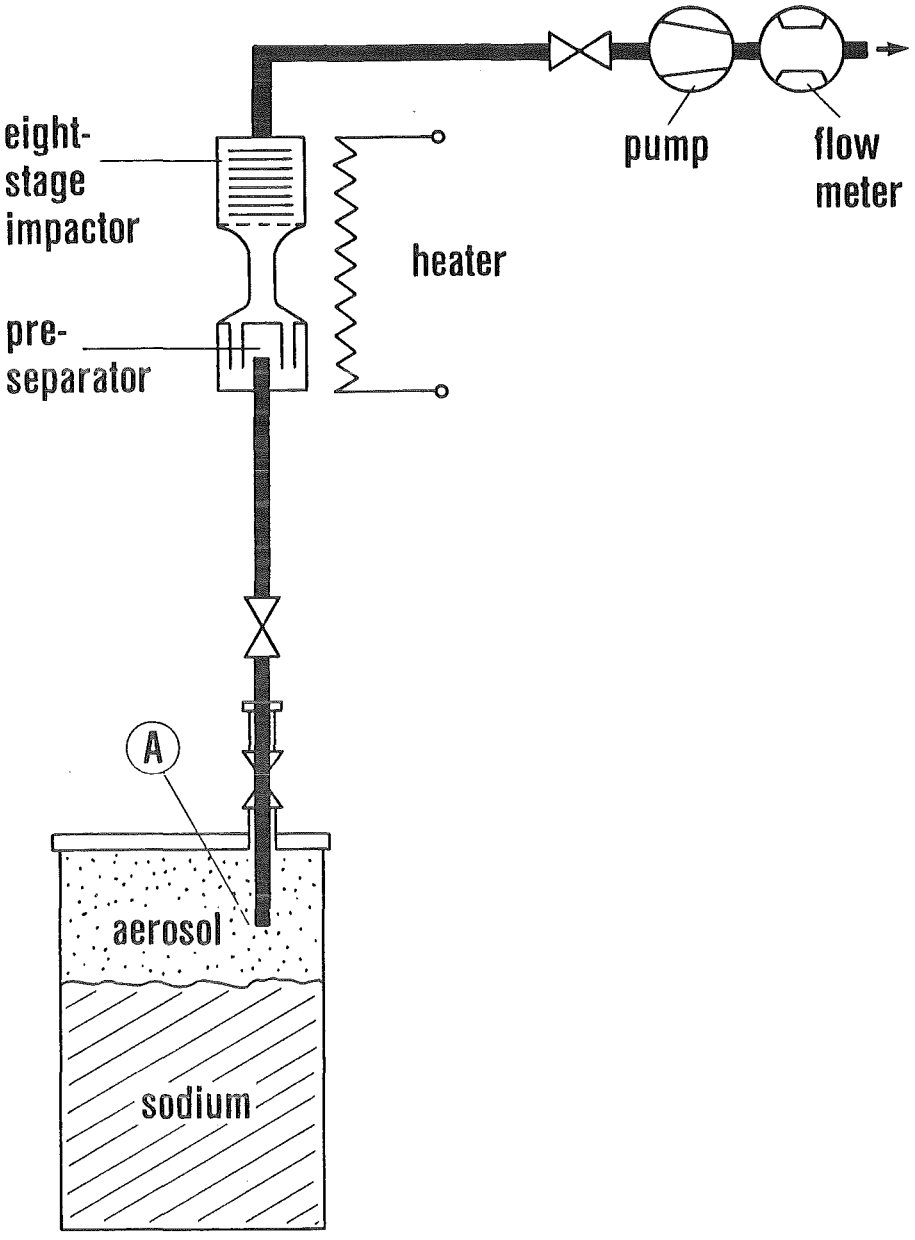

Fig. 4.2 Arrangement of Andersen impactor to determine particle size spectra and mass concentrations. The position of A is moveable between plate and pool surface.

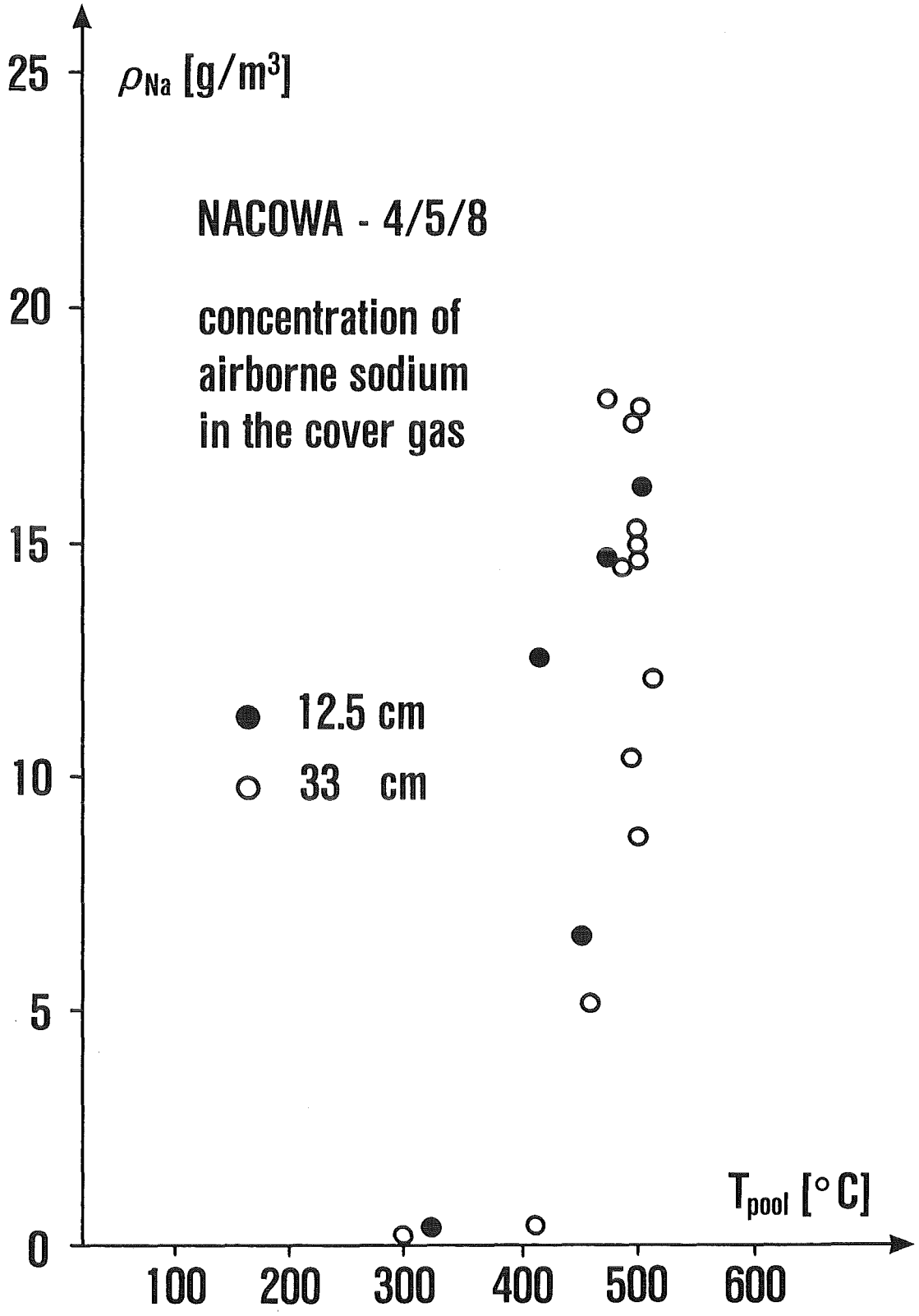

Fig. 4.3 Sodium mass concentrations, determined from wash-bubbler measurements during tests N-4, N-5 and N-8 .

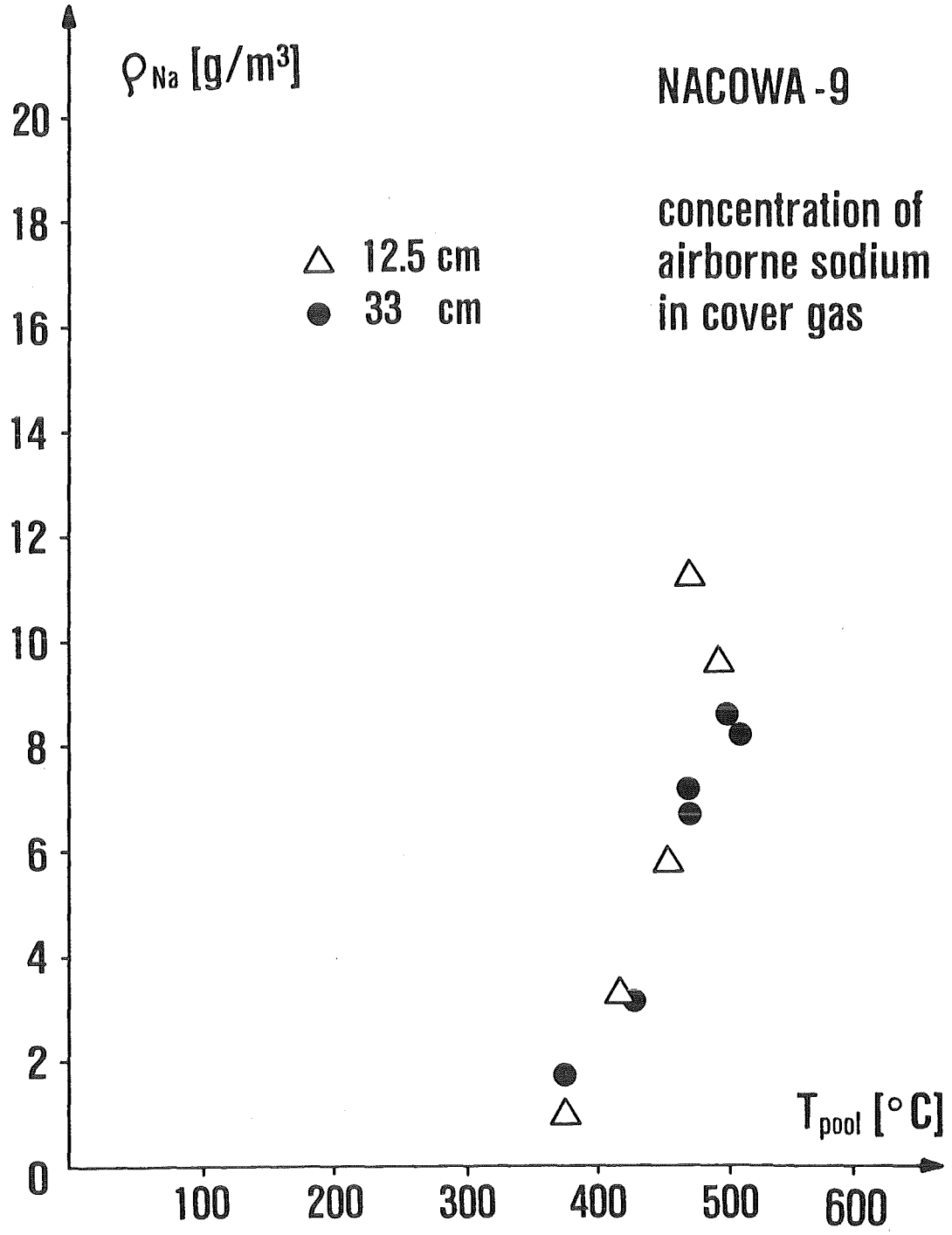

Fig. 4.4 Sodium mass concentrations, determined from wash-bubbler measurements during test N9.

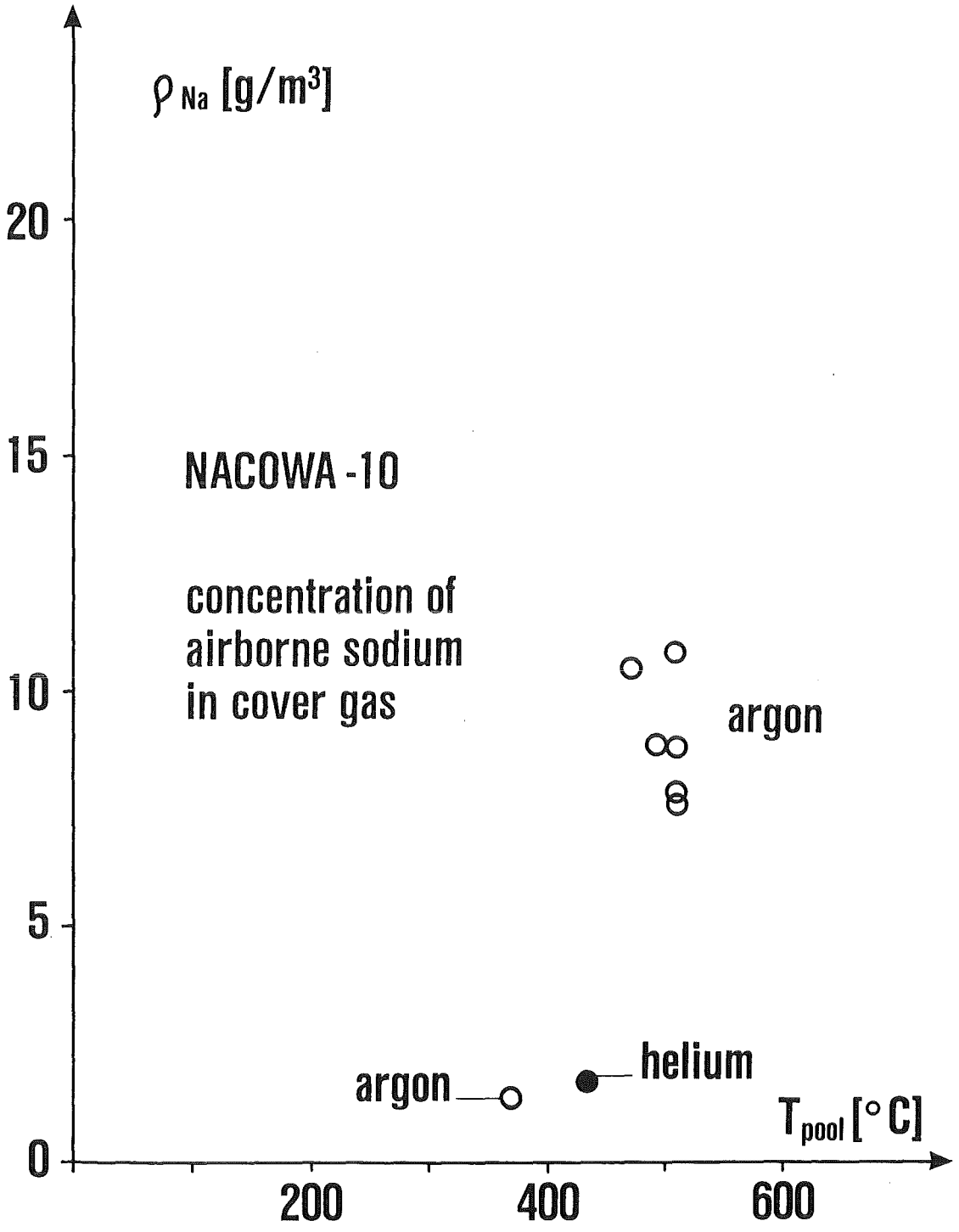

Fig. 4.5 Sodium mass concentrations, determined from wash-bubbler measurements during test N-10, plate temperatures up to 294 °C.

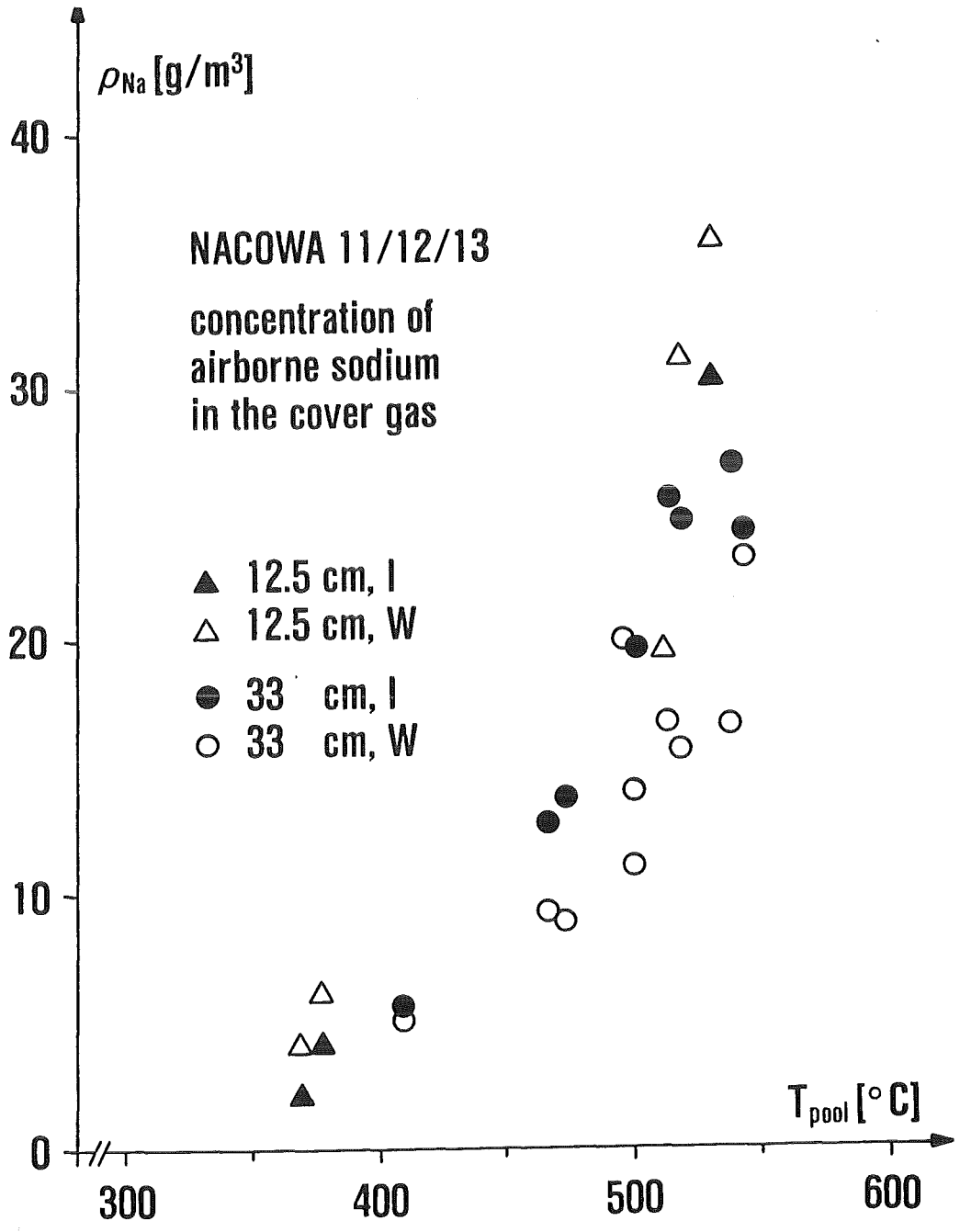

Fig. 4.6 Sodium mass concentrations, determined from wash-bubbler and impactor measurements during tests N11, N12 and N13.

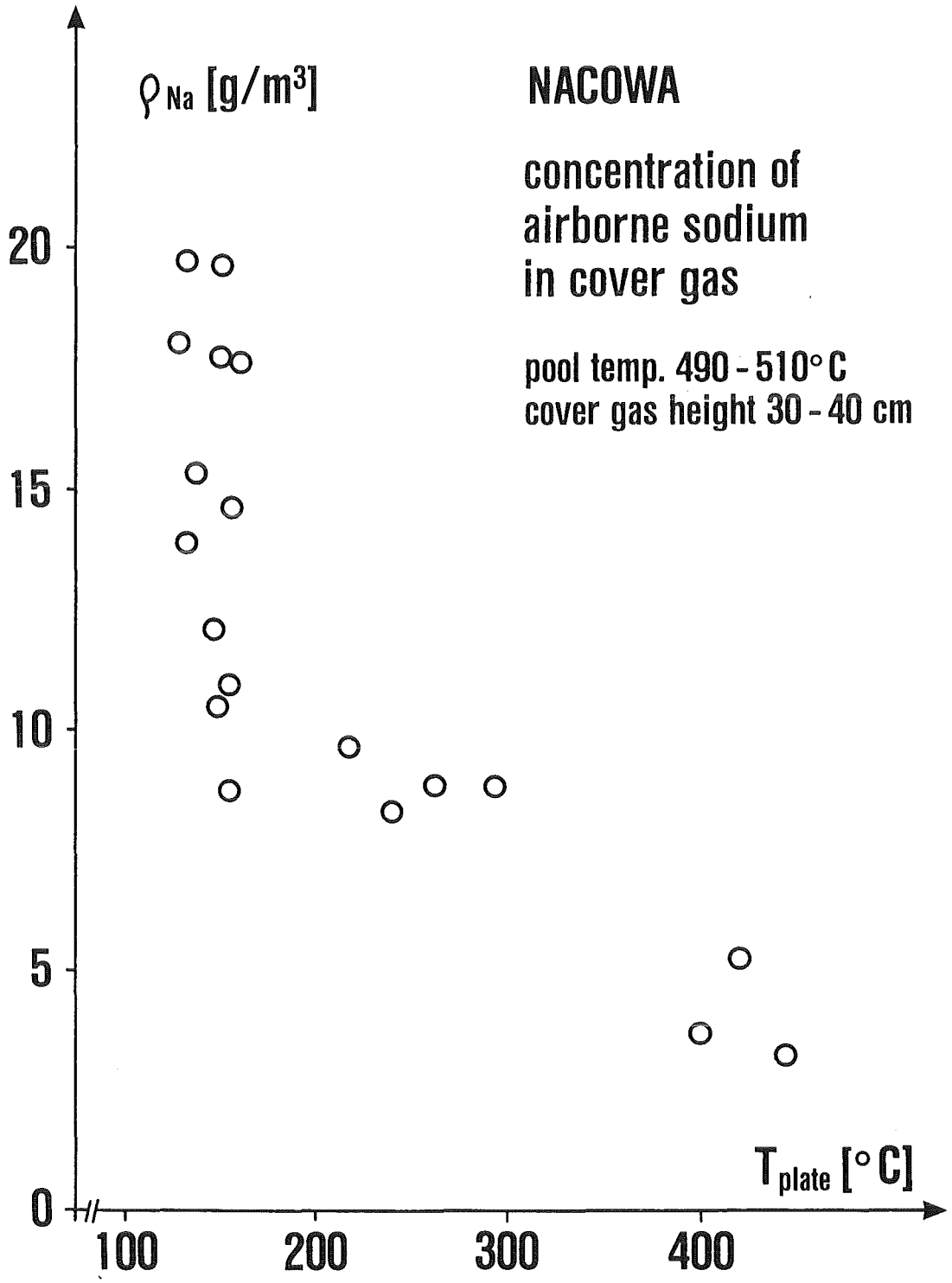

Fig. 4.7 Sodium mass concentrations at 490°C to 510°C pool temperature versus plate temperature, data from several NACOWA tests.

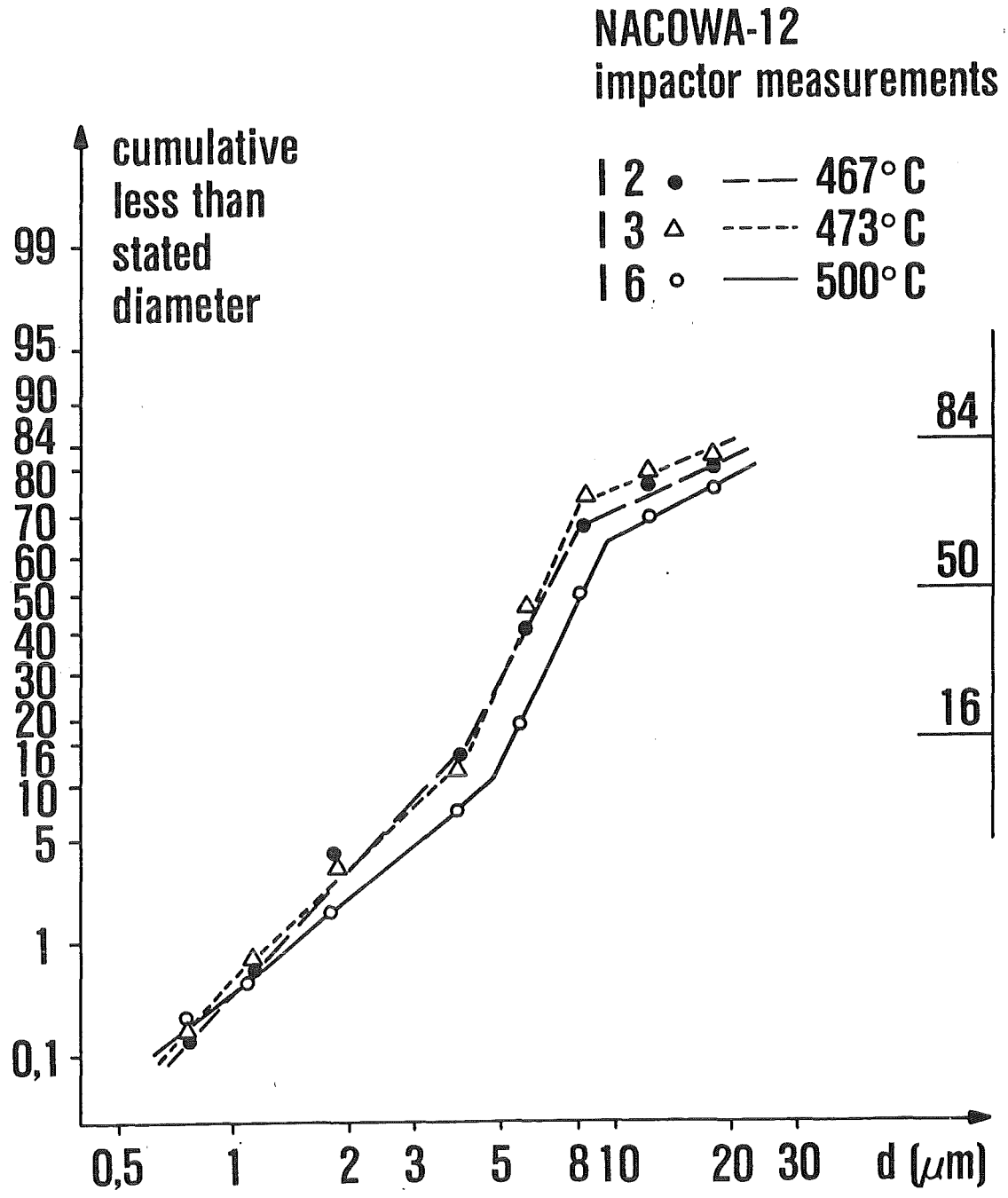

Fig. 5.1 Particle size spectra from impactor measurements, test NACOWA 12 .

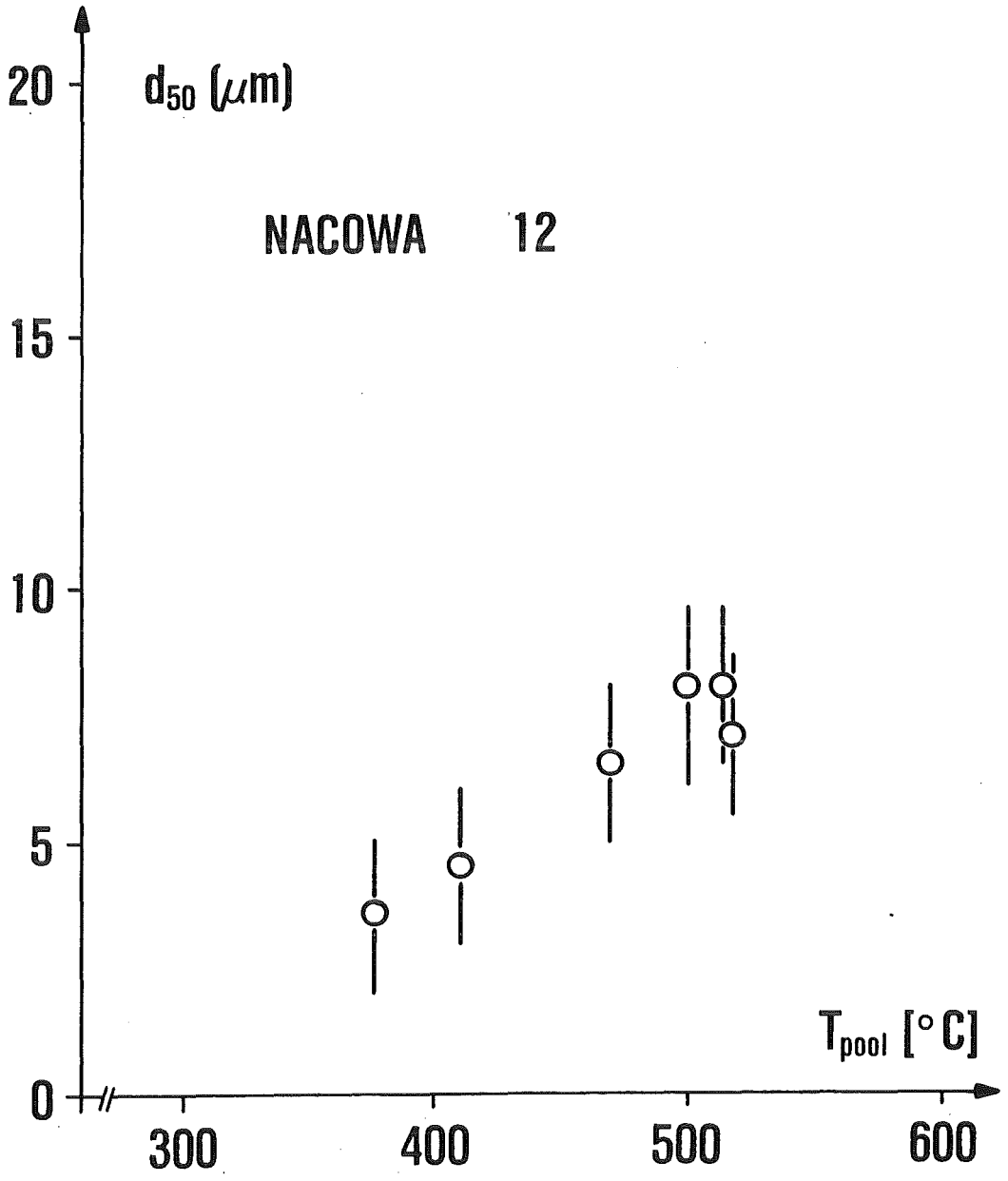

Fig. 5.2 50 % values of size spectra versus pool temperature, test NACOWA 12 .

Circular area A_2 parallel to area element ΔA_1

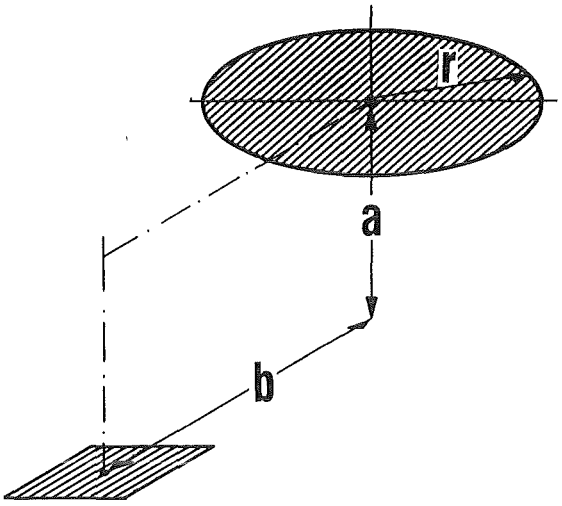

$$B = \frac{b}{a}$$

$$R = \frac{r}{a}$$

$$\varphi_{12} = \frac{1}{2} - \frac{1 + B^2 - R^2}{2\sqrt{B^4 + 2B^2(1-R^2) + (1+R^2)^2}}$$

Circular area A_2 perpendicular to area element ΔA_1

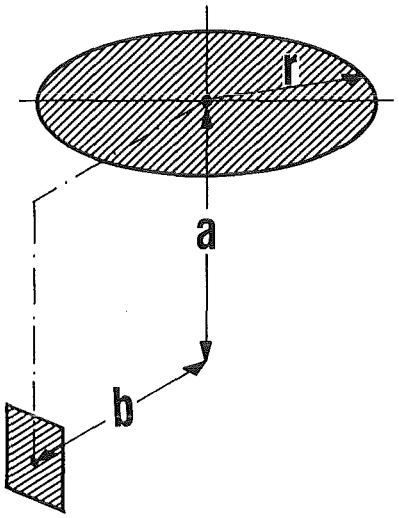

$$B = \frac{b}{a}$$

$$R = \frac{r}{a}$$

$$\varphi_{12} = \frac{1}{2B} \cdot \left[\frac{1 + B^2 + R^2}{\sqrt{B^4 + 2B^2(1-R^2) + (1+R^2)^2}} - 1 \right]$$

Fig. 6.1 View factors which are used in the NACOWA computer code.

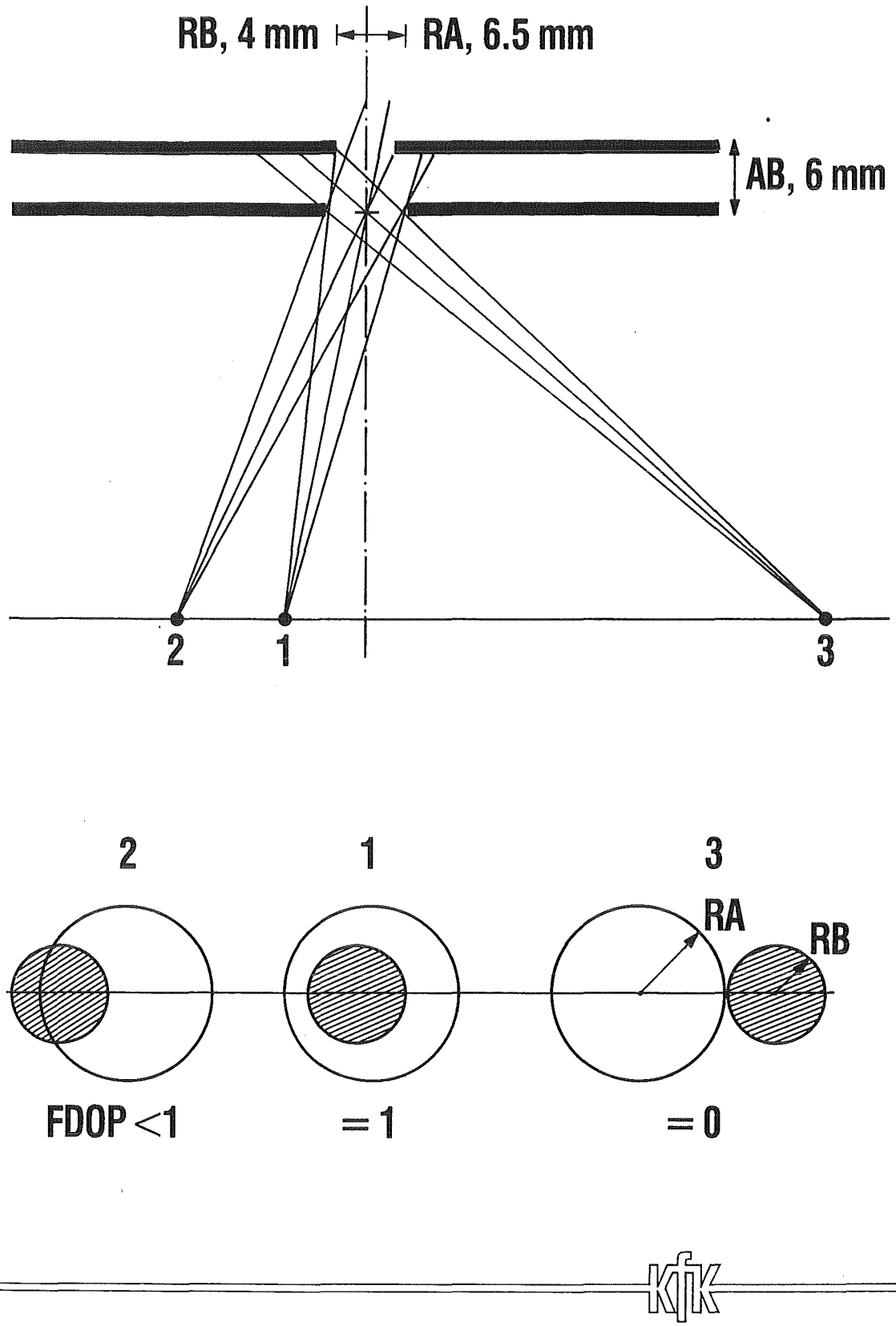

Fig. 6.2 Geometry of the double aperture of the thermo-electronical radiometer and cutoff-effect (function FDOP).

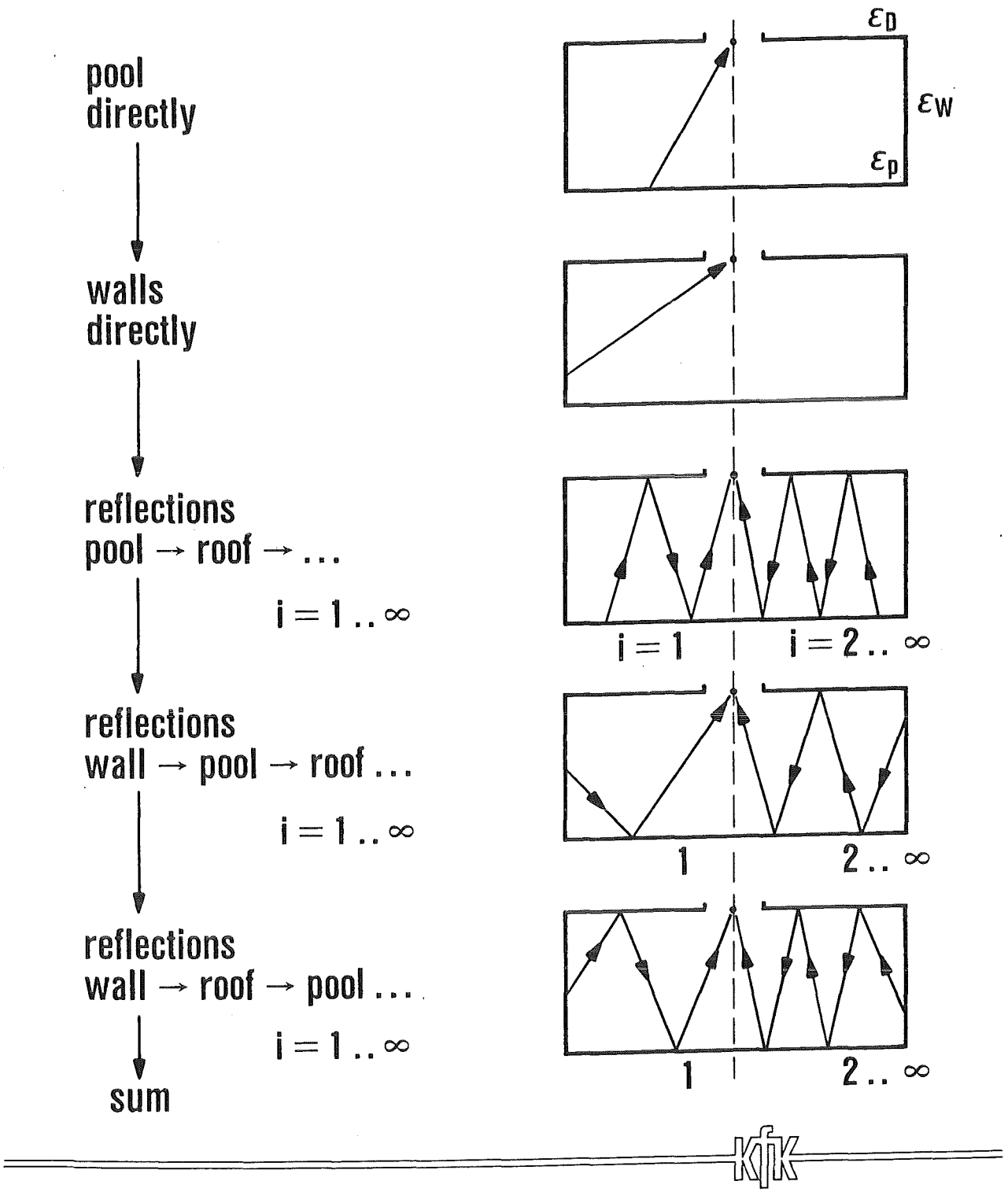

Fig. 6.3 NACOWA computer code: different contributions to the amount of radiative heat which is measured by the radiometer.

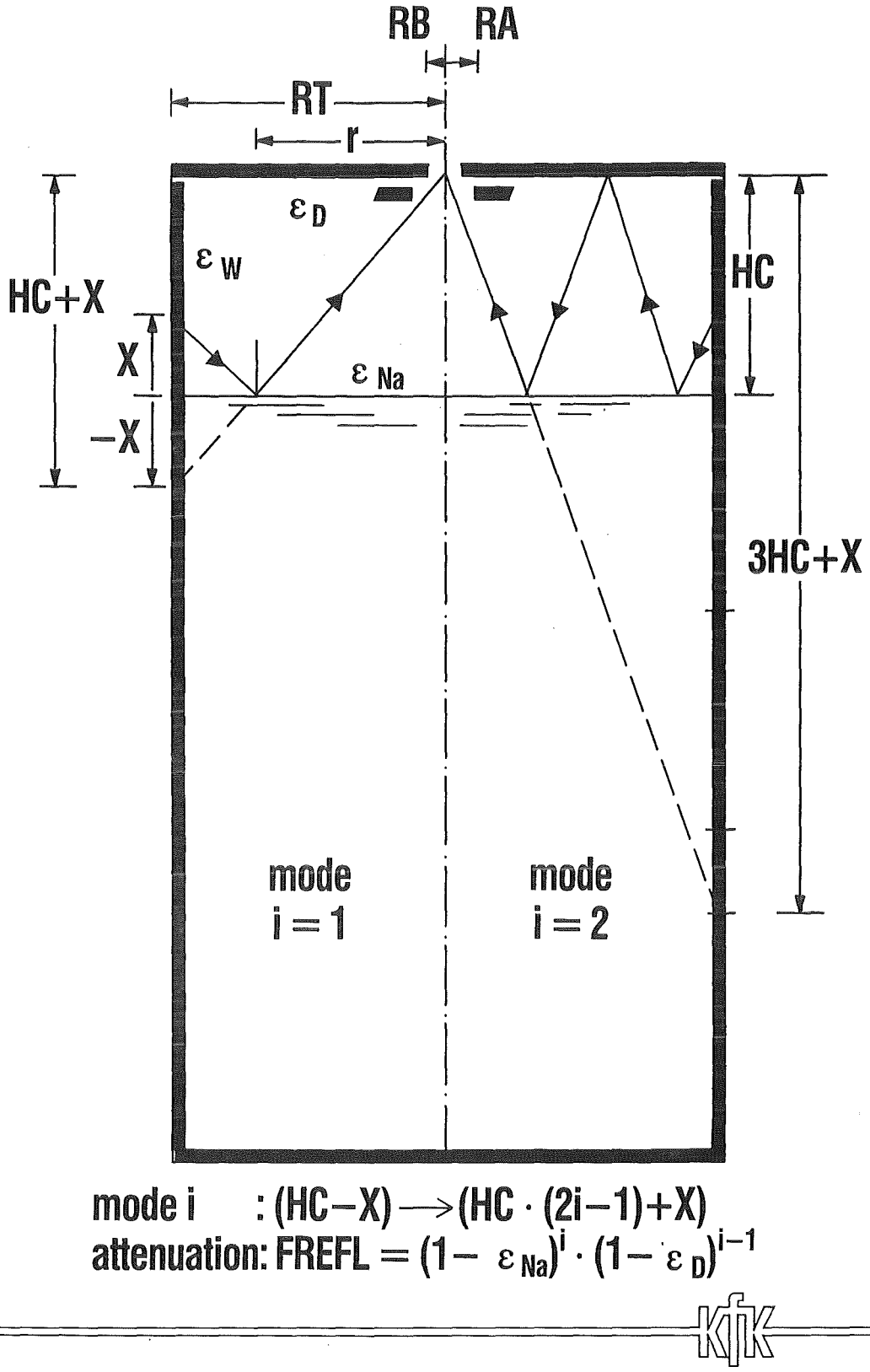

Fig. 6.4 Geometrical relations to calculate the reflection modes.

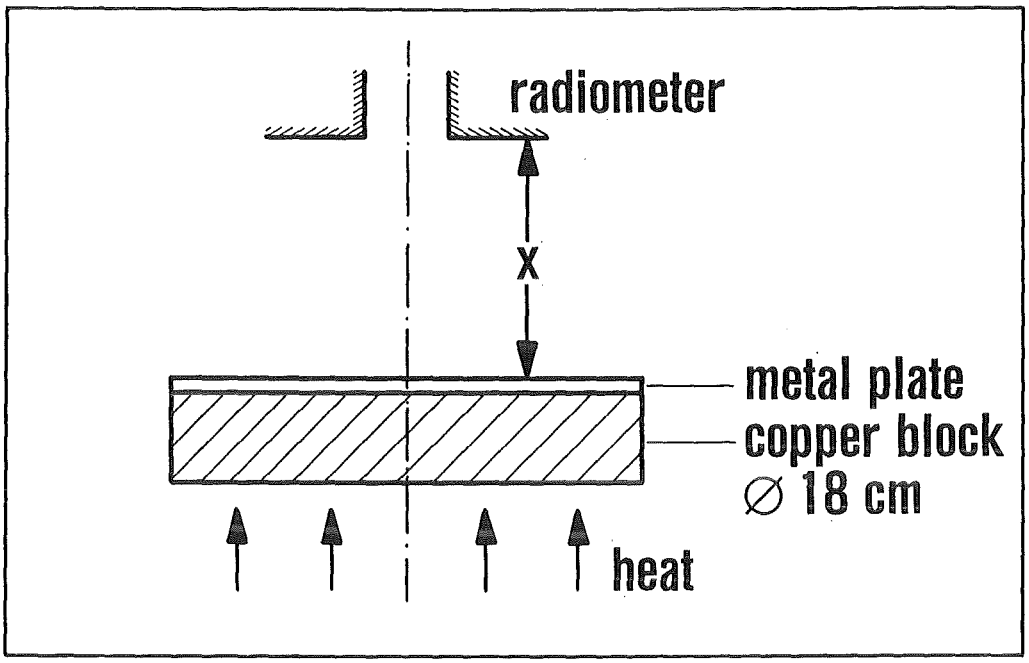

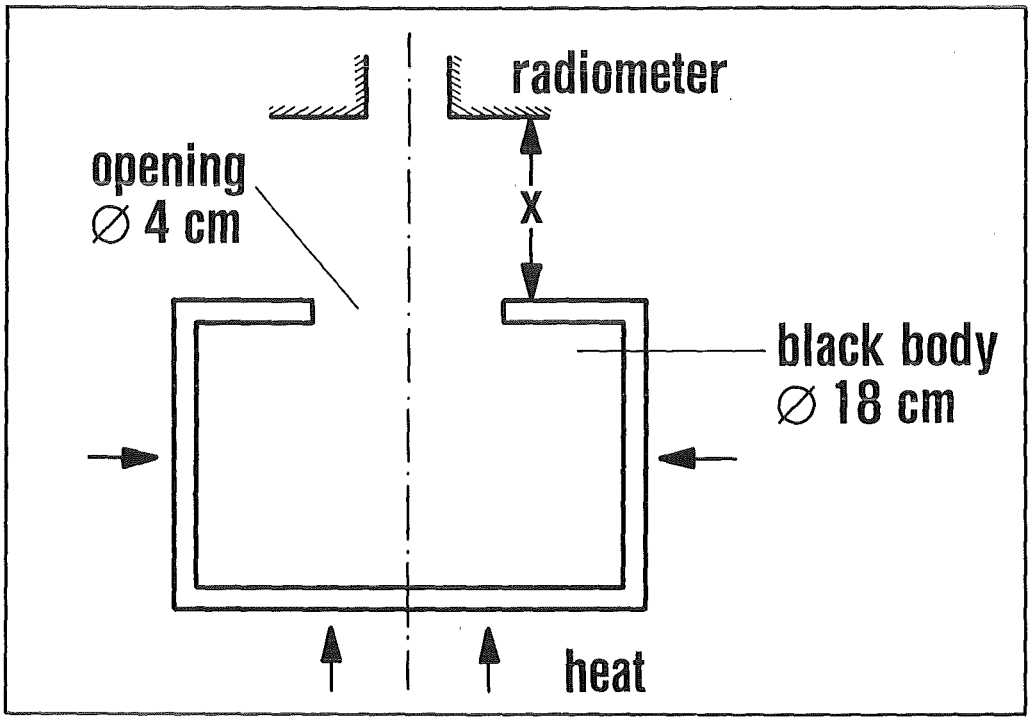

Fig. 6.5 Small-scale setup with heated metal plates and cavity radiator to test the radiometer and to verify the computer code.

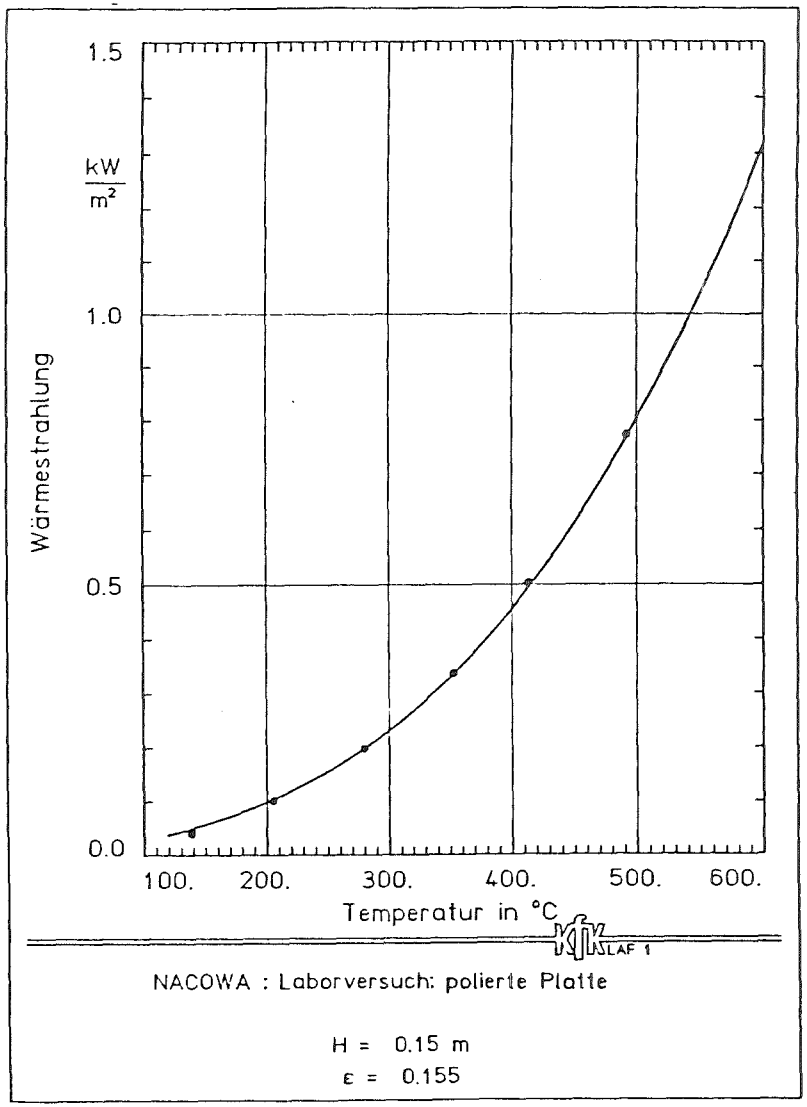

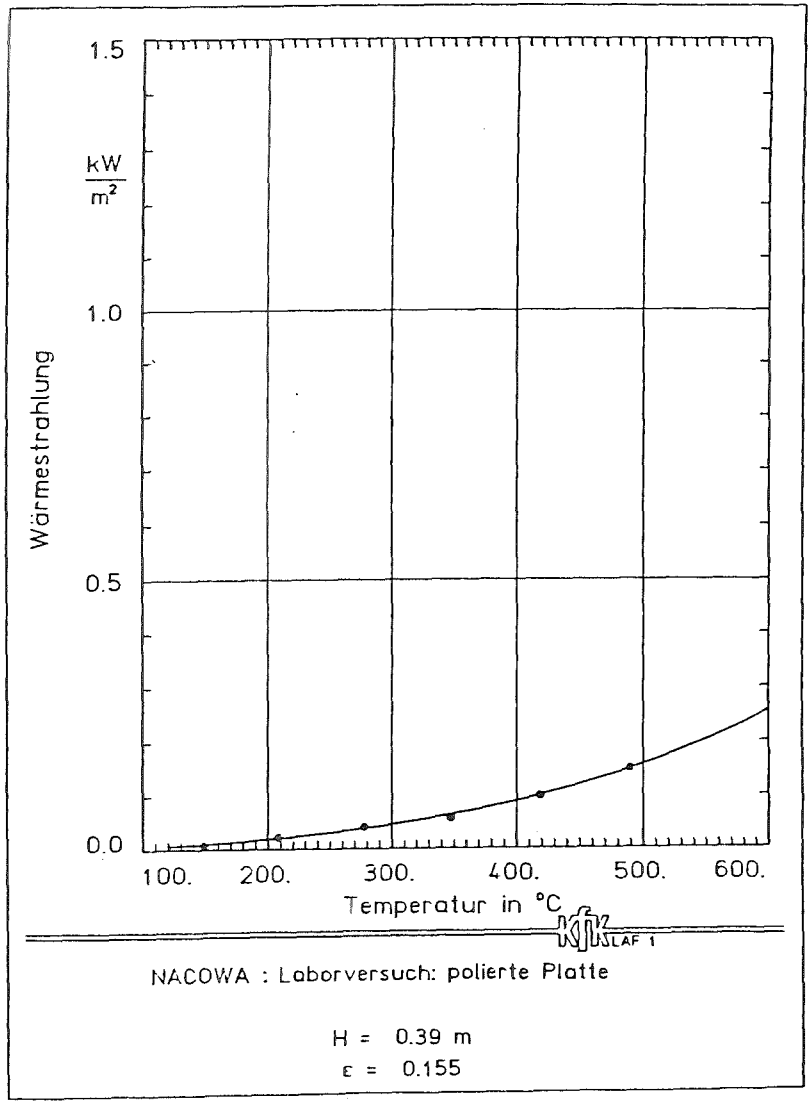

Fig. 6.6 **Small-scale tests with polished steel metal plate: Experimental results for distances x = 0.15 m and 0.39 m and calculations with emissivity 0.155**

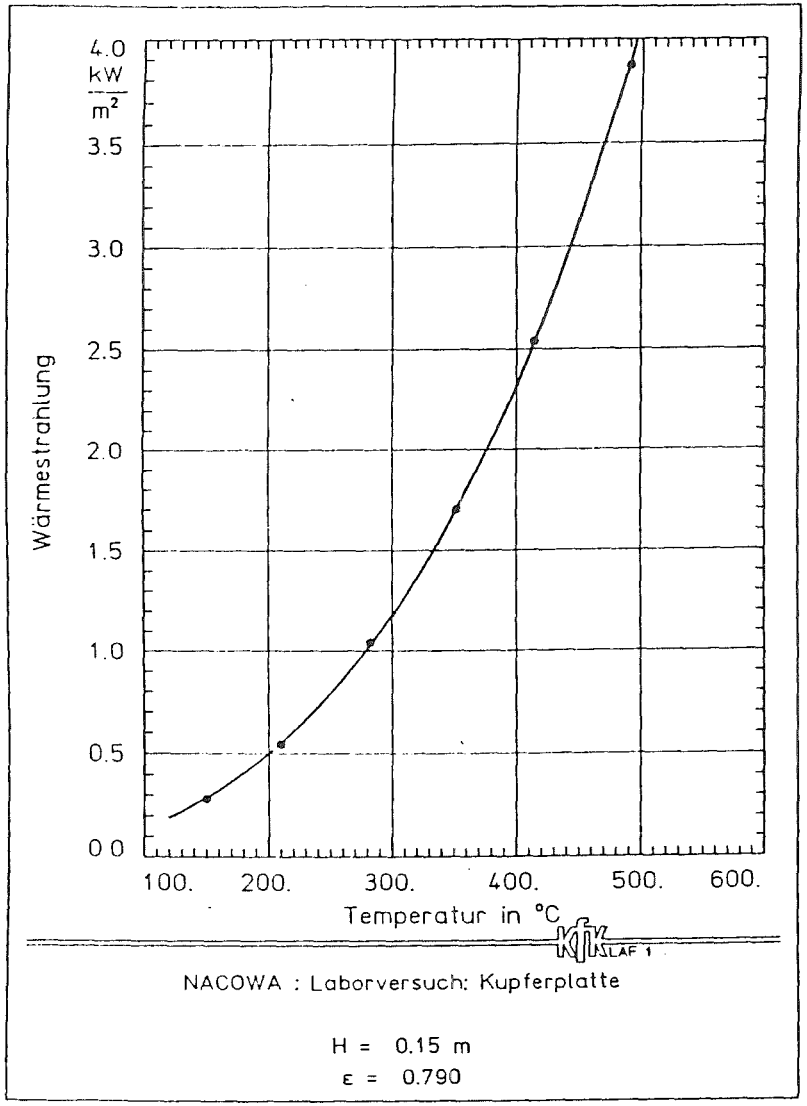

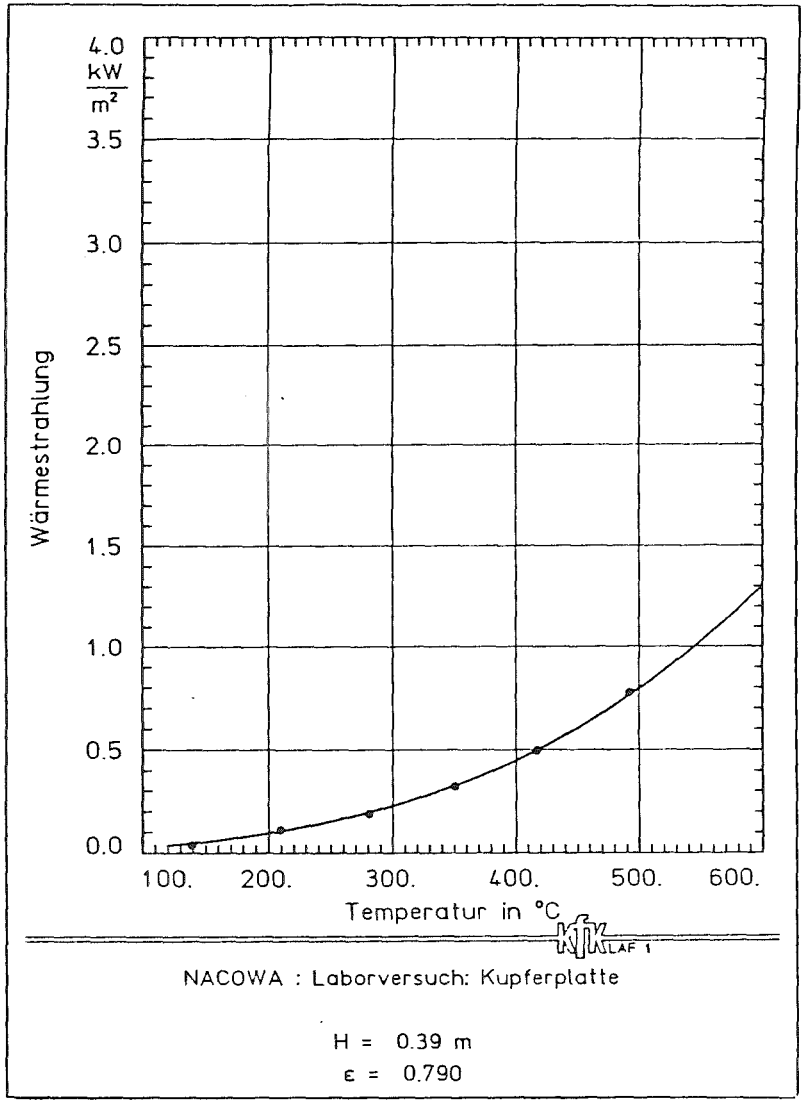

Fig. 6.7 Small-scale tests with oxidized copper plate: Experimental results for distances x = 0.15 m and 0.39 m and calculations with emissivity 0.79

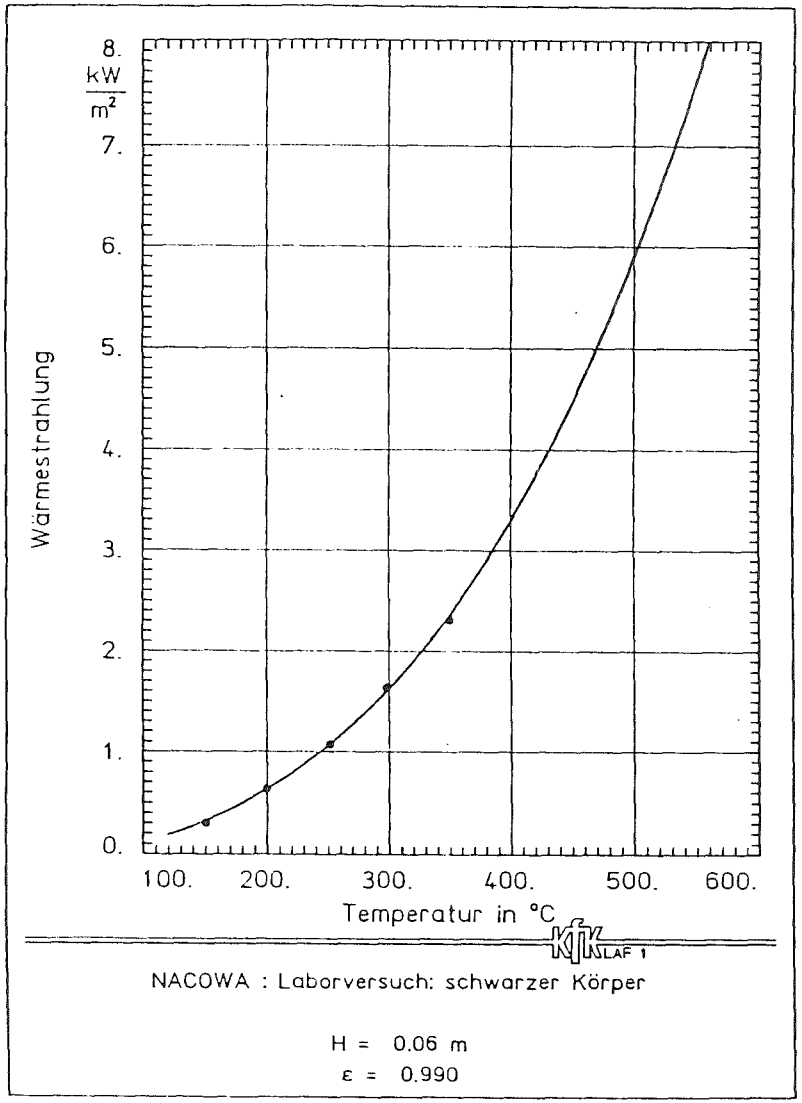

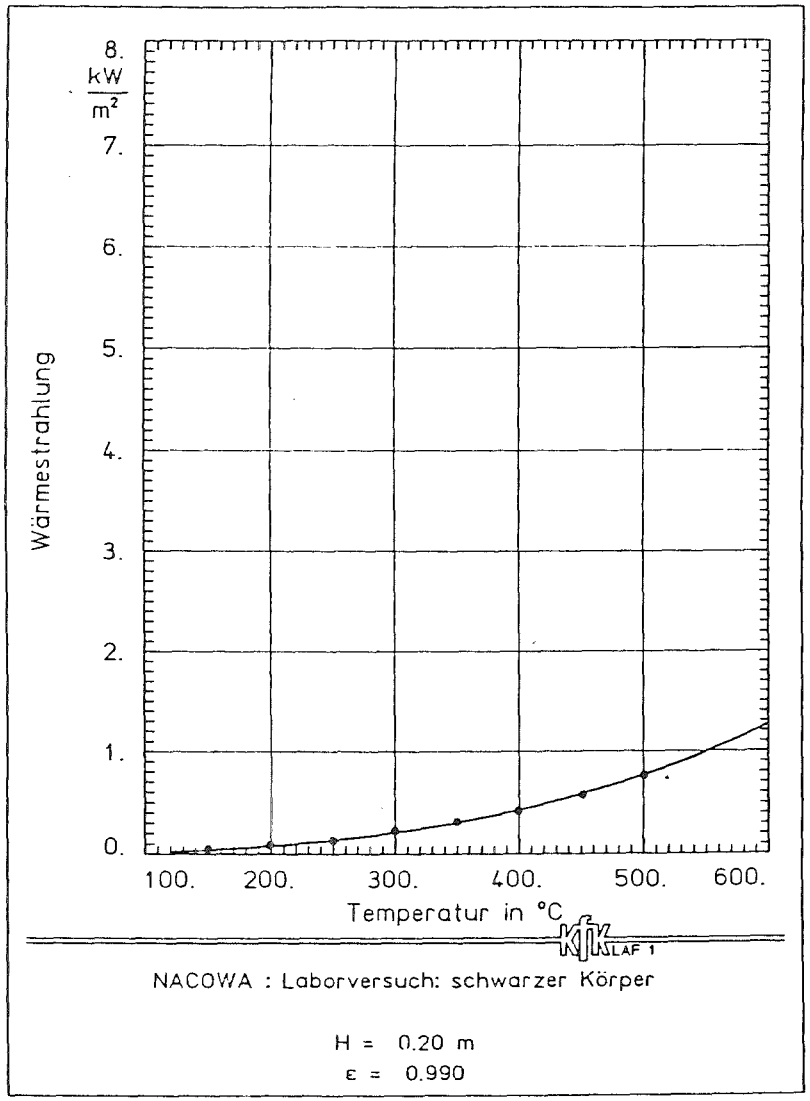

Fig. 6.8 **Small-scale tests with cavity radiator as black body: Experimental results for distances x = 0.06 m and 0.20 m and calculations with emissivity 0.99**

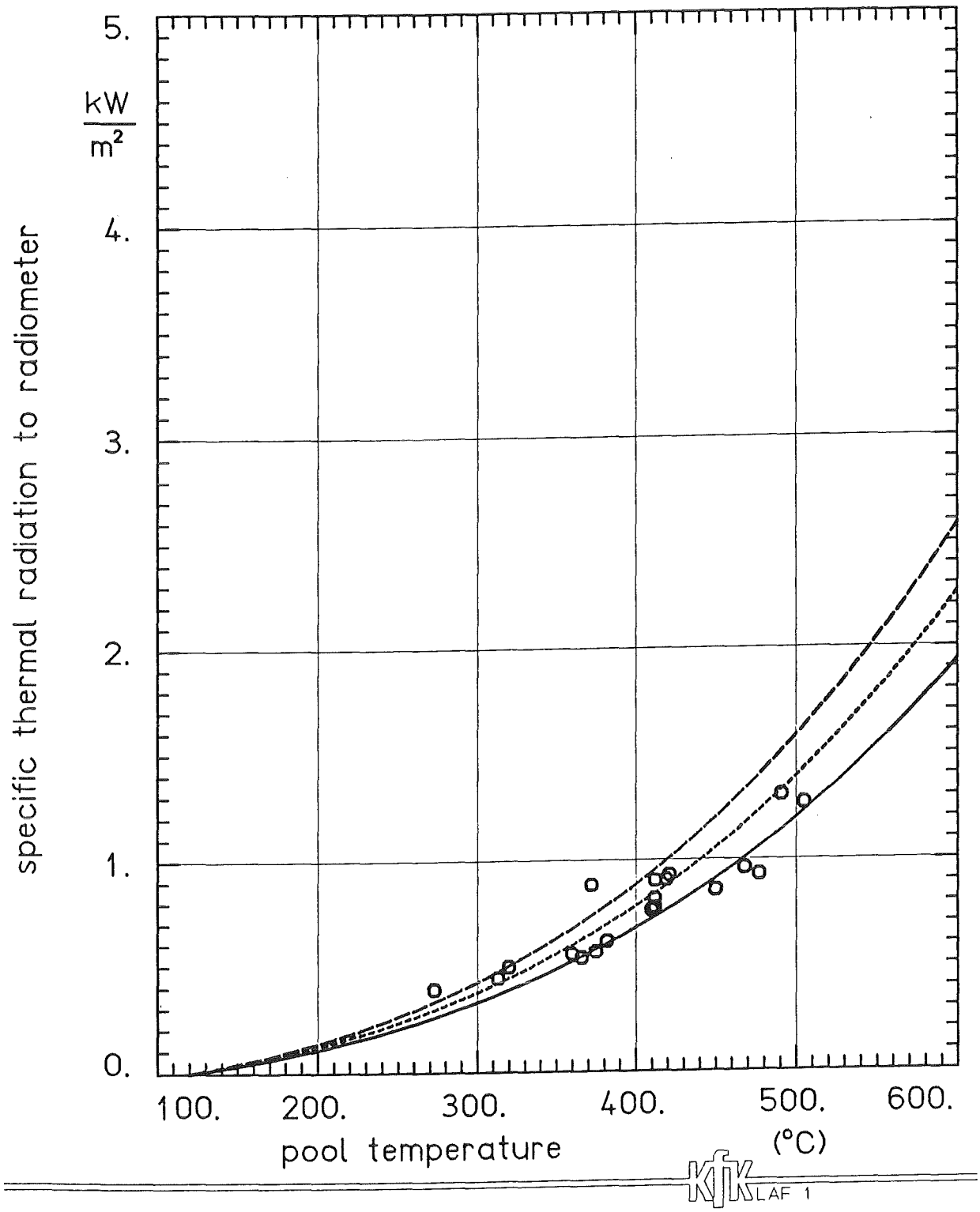

Fig. 6.9 Radiative heat transfer calculations and experimental results

cover gas height : 0.125 m

emissivities : sodium 0.03 to 0.07 (Δ 0.02), wall 0.40, roof 0.25

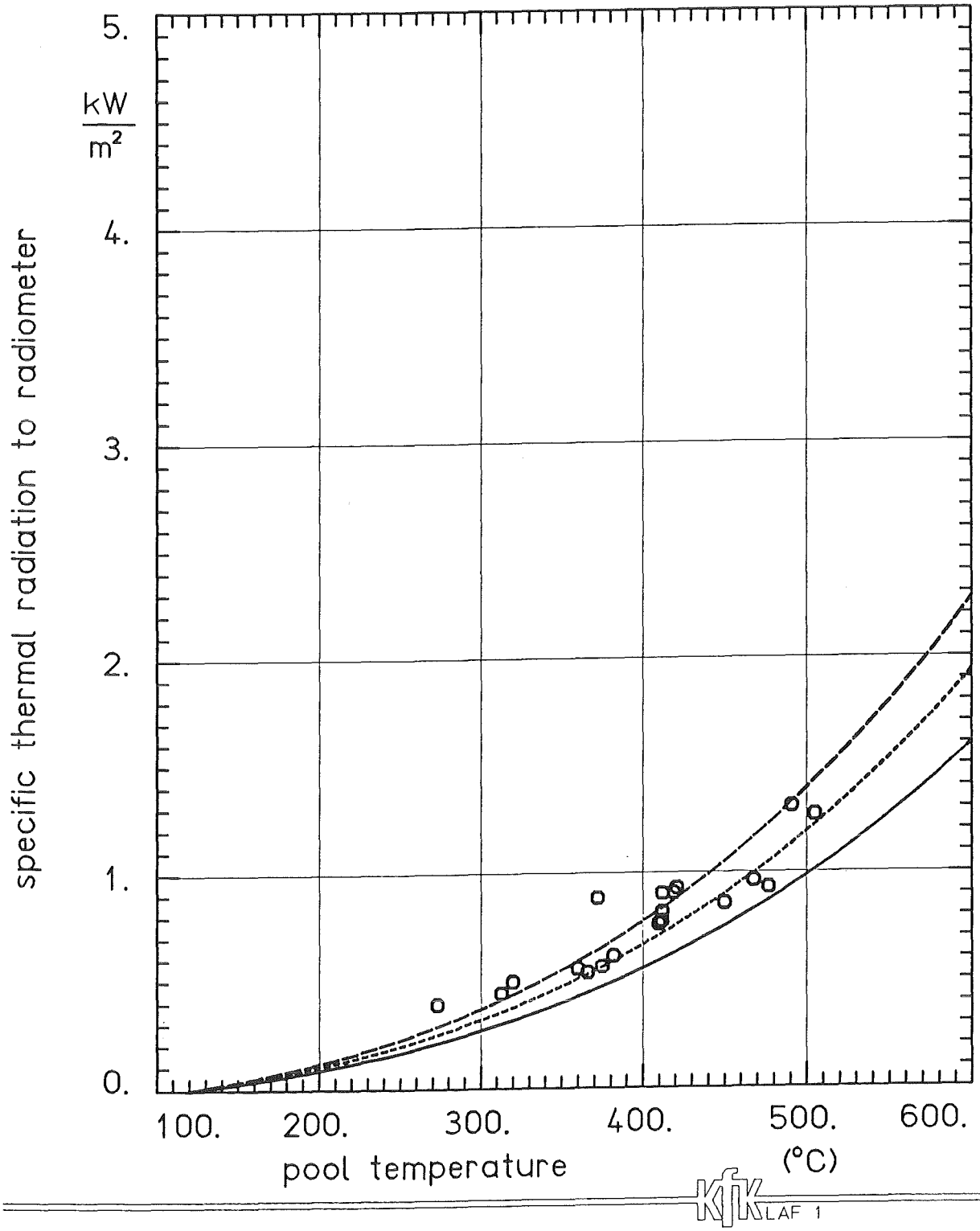

Fig. 6.10 Radiative heat transfer calculations and experimental results

cover gas height : 0.125 m

emissivities : sodium 0.03 to 0.07 (Δ 0.02), wall 0.30, roof 0.25

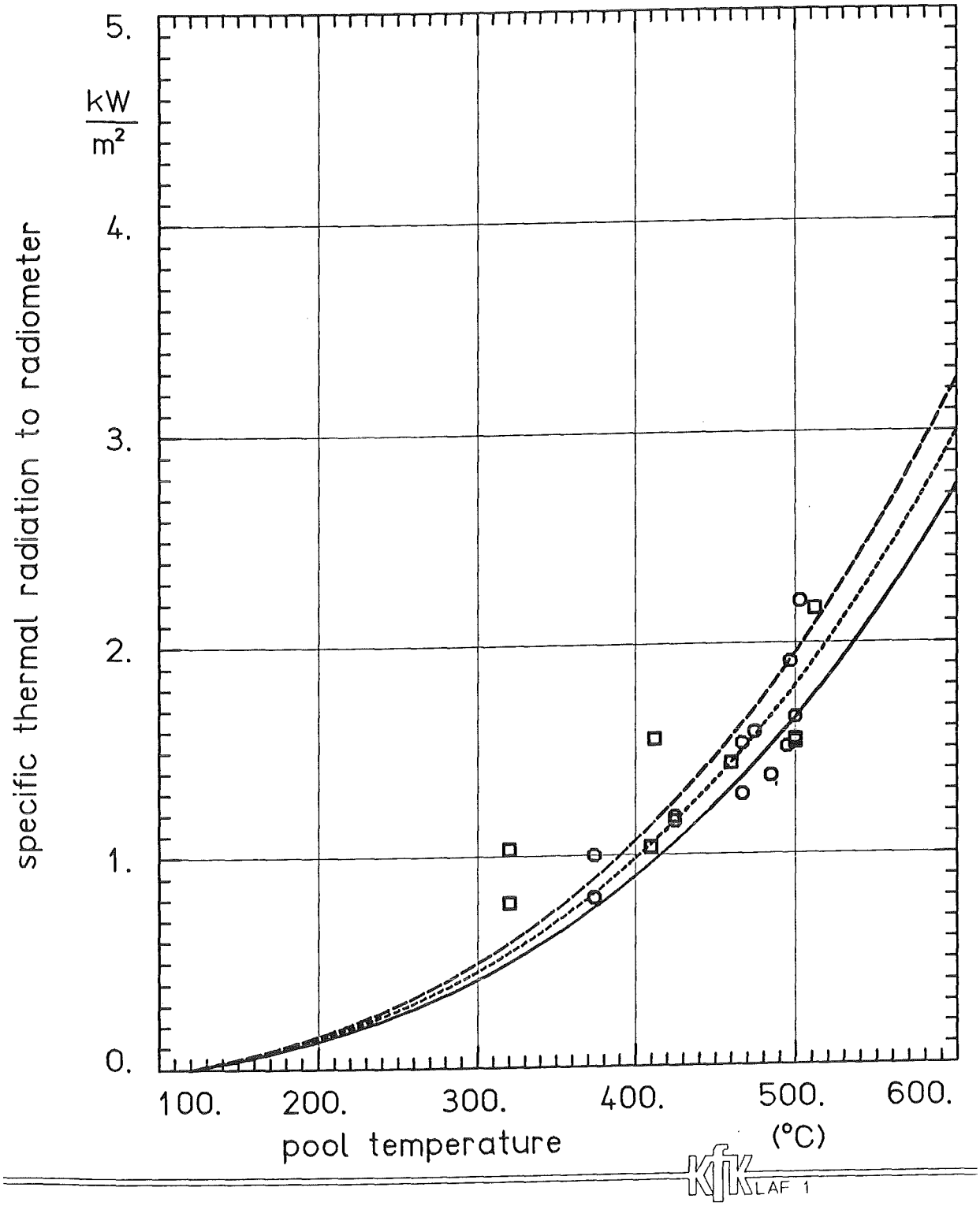

Fig. 6.11 Radiative heat transfer calculations and experimental results

cover gas height : 0.331 m

emissivities : sodium 0.03 to 0.07 (Δ 0.02), wall 0.14, roof 0.25

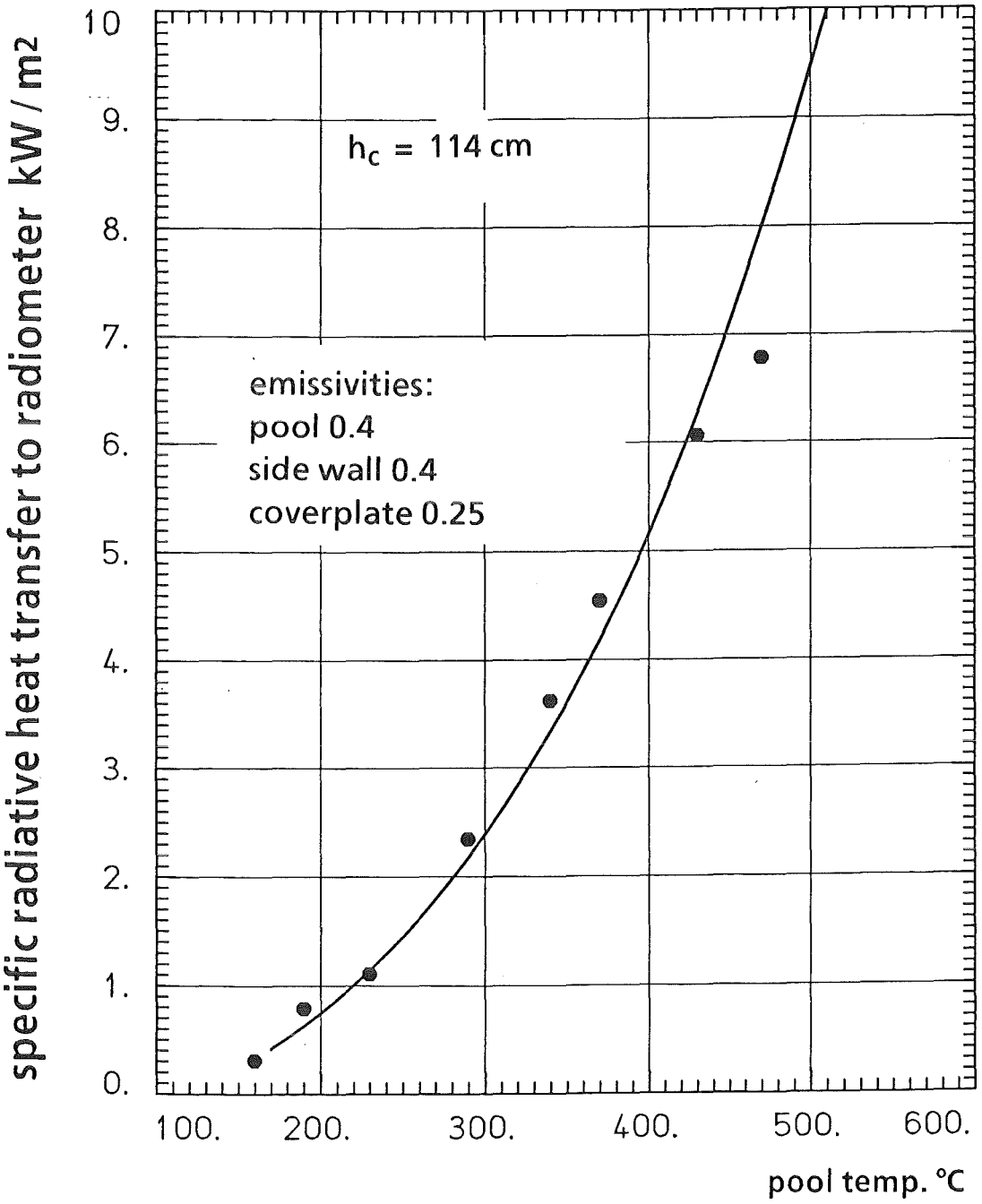

Fig. 6.12 Empty-vessel test NACOWA 6 : Radiative heat transfer calculations and experimental results.

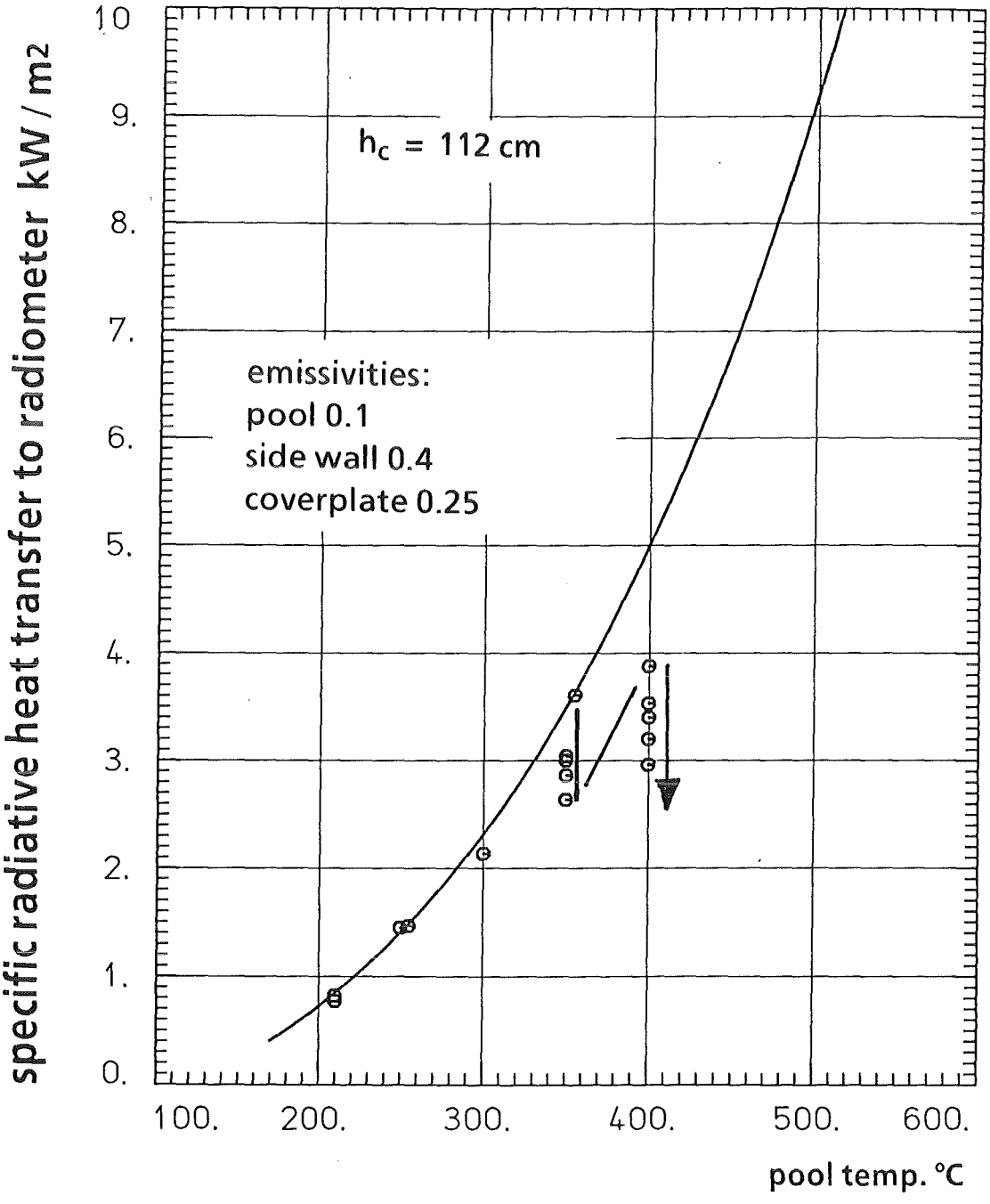

Fig. 6.13 NACOWA-7 test with a shallow (2 cm) layer of sodium: radiative heat transfer calculations and experimental results.
The arrow indicates the time behaviour.

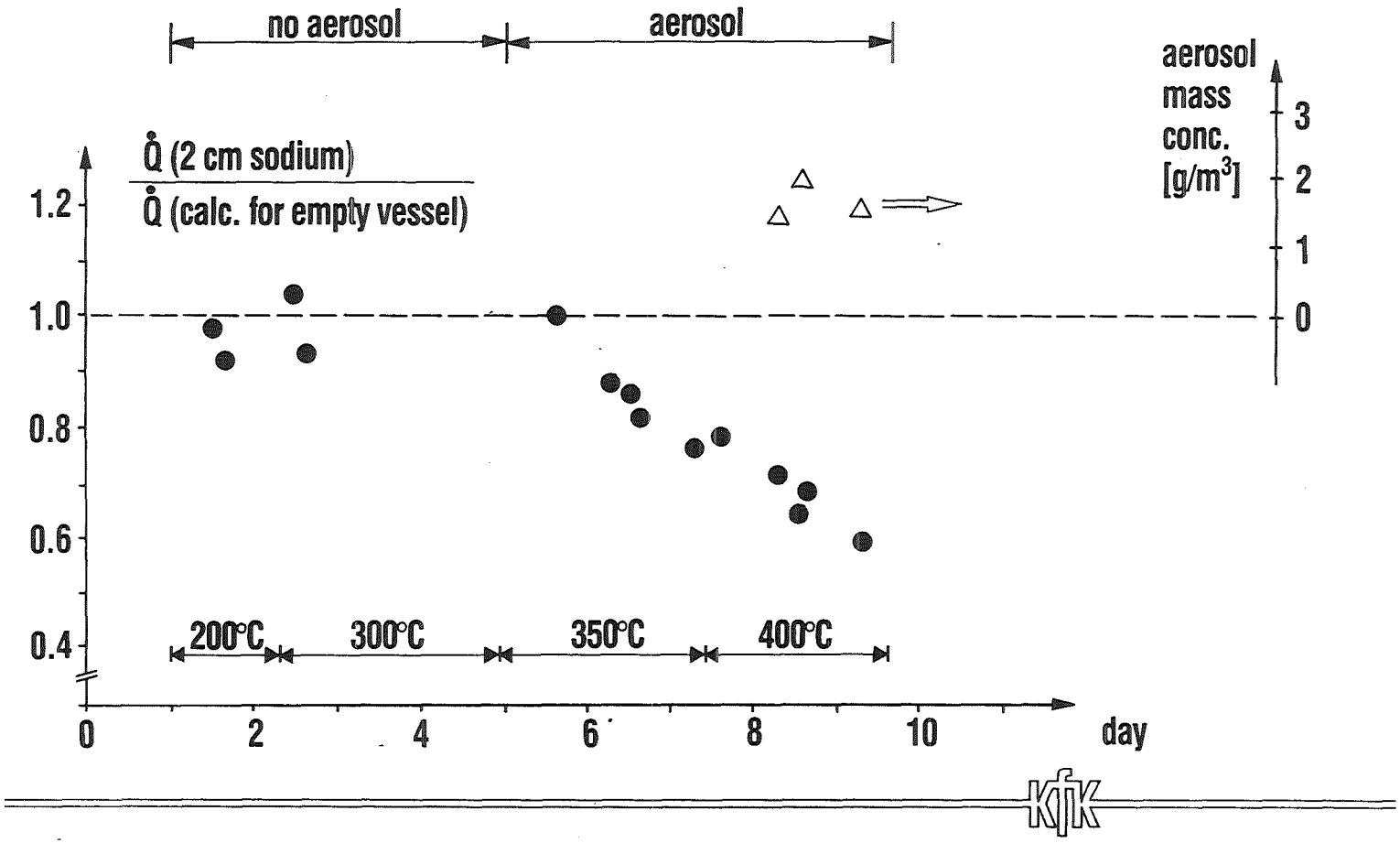

Fig. 6.14 NACOWA-7 test with a shallow (2 cm) layer of sodium: Time behaviour of radiative heat transfer and effect of sodium deposition on the steel walls.

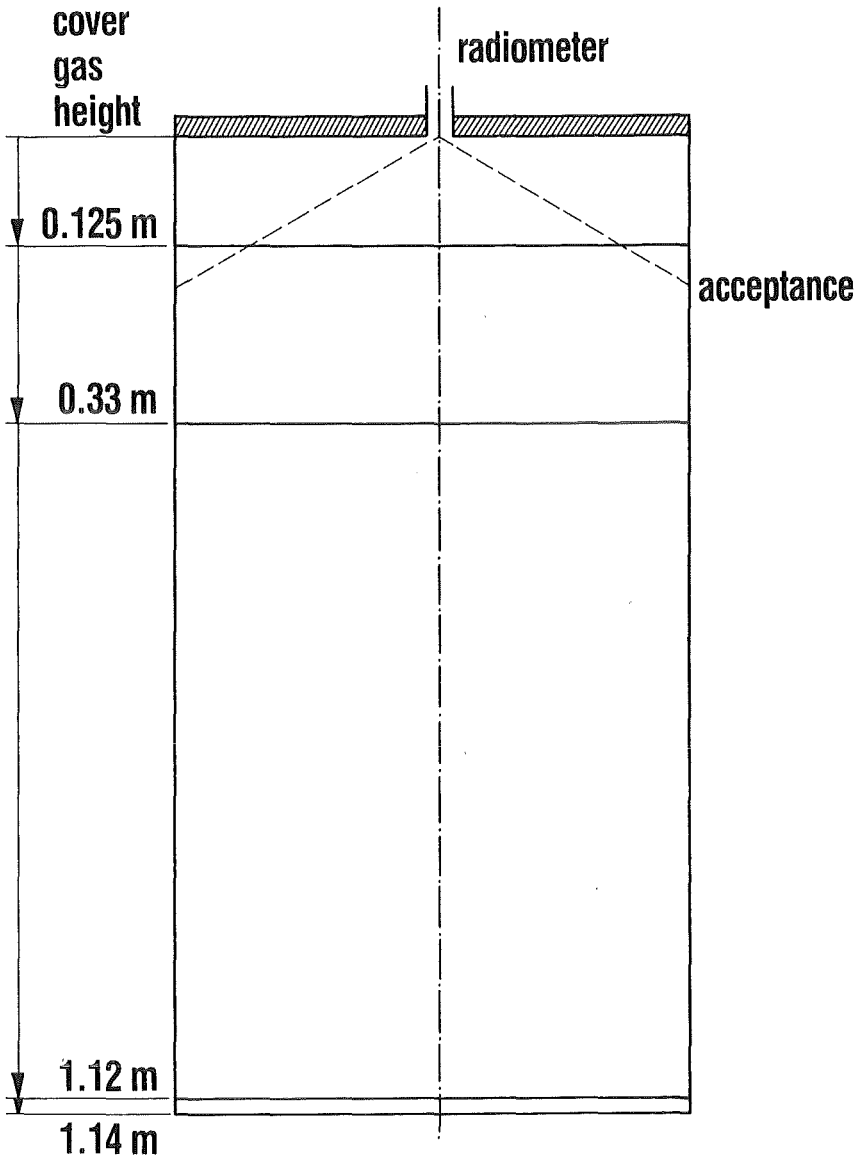

Fig. 6.15 Different cover gas heights (sodium levels) and radiometer acceptance.

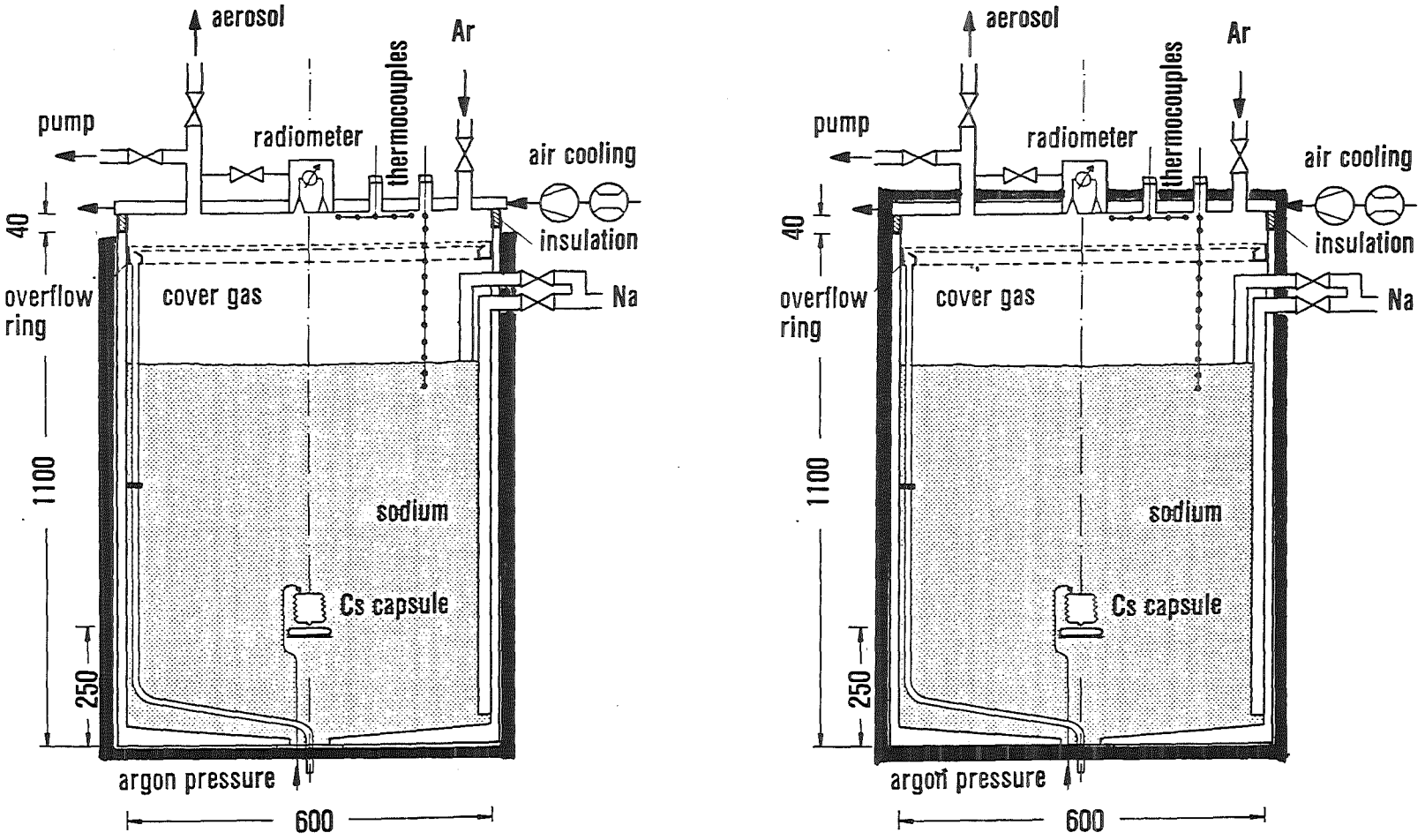

Fig. 7.1 Thermal insulation of test vessel:
Right: Full insulation, NACOWA 9 and 10
Left: No insulation on cover plate, other tests .

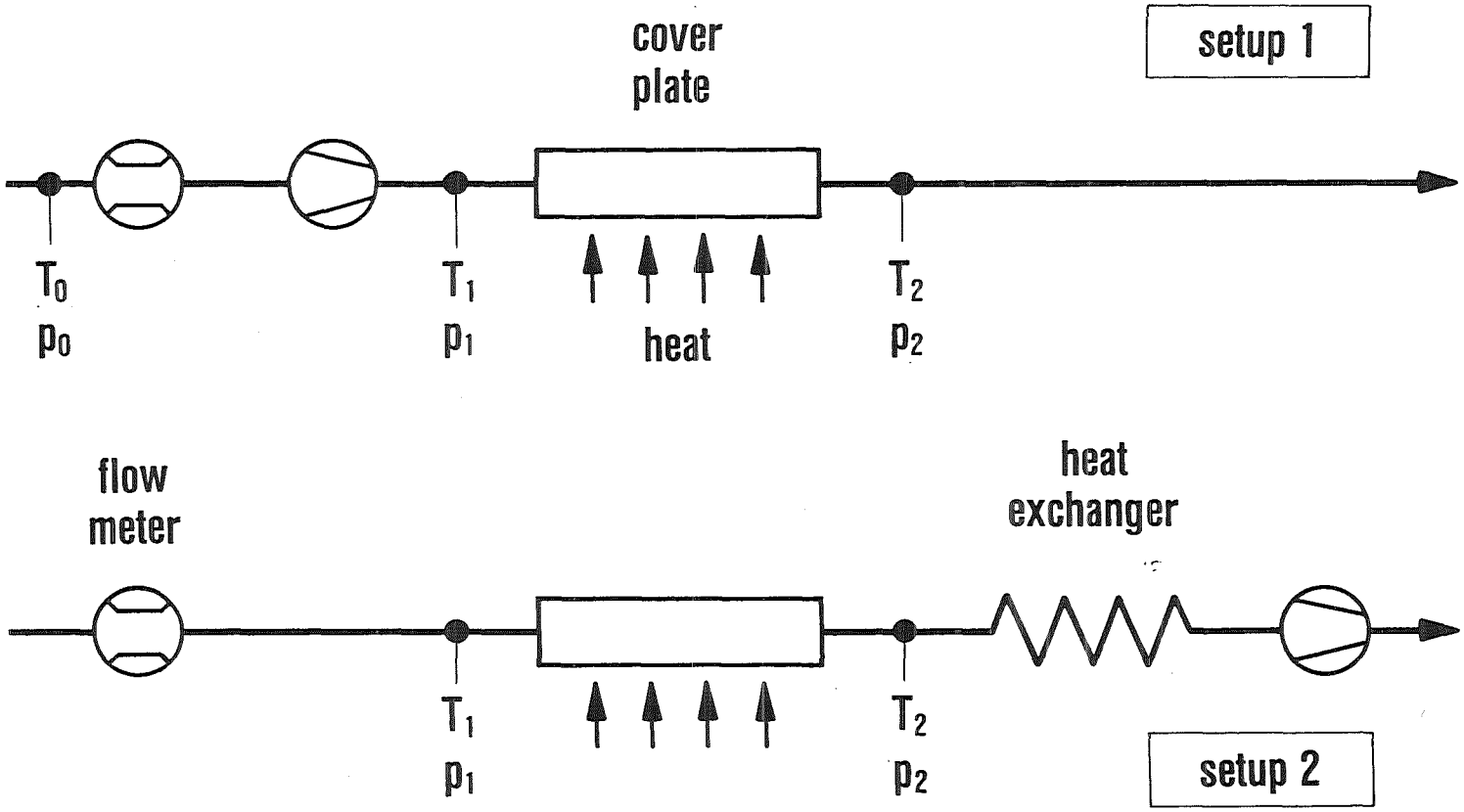

Fig. 7.2 Two methods to determine the total heat transfer to the cover plate .

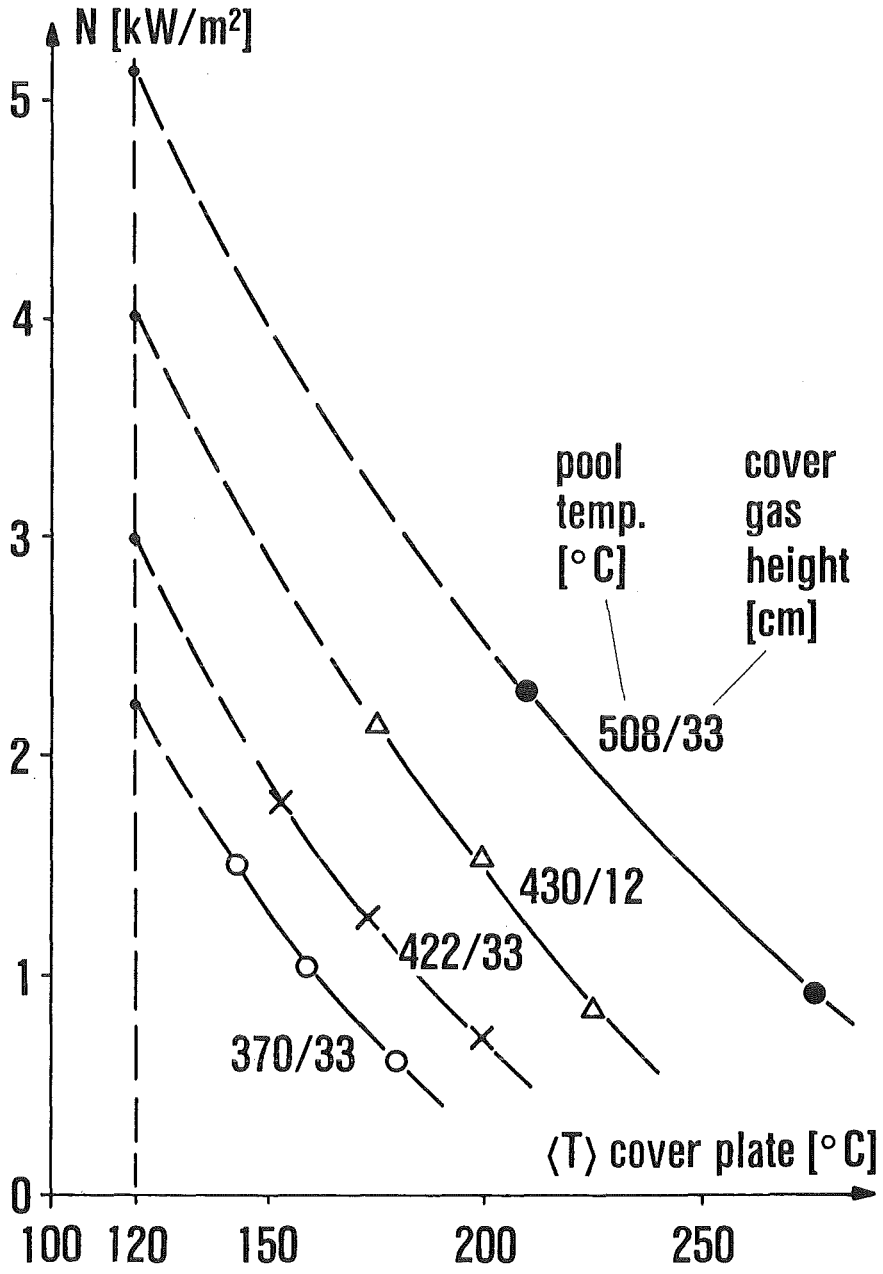

Fig. 7.3 Total heat transfer: Experimental results from test NACOWA 10 and eyeball extrapolation to 120°C .

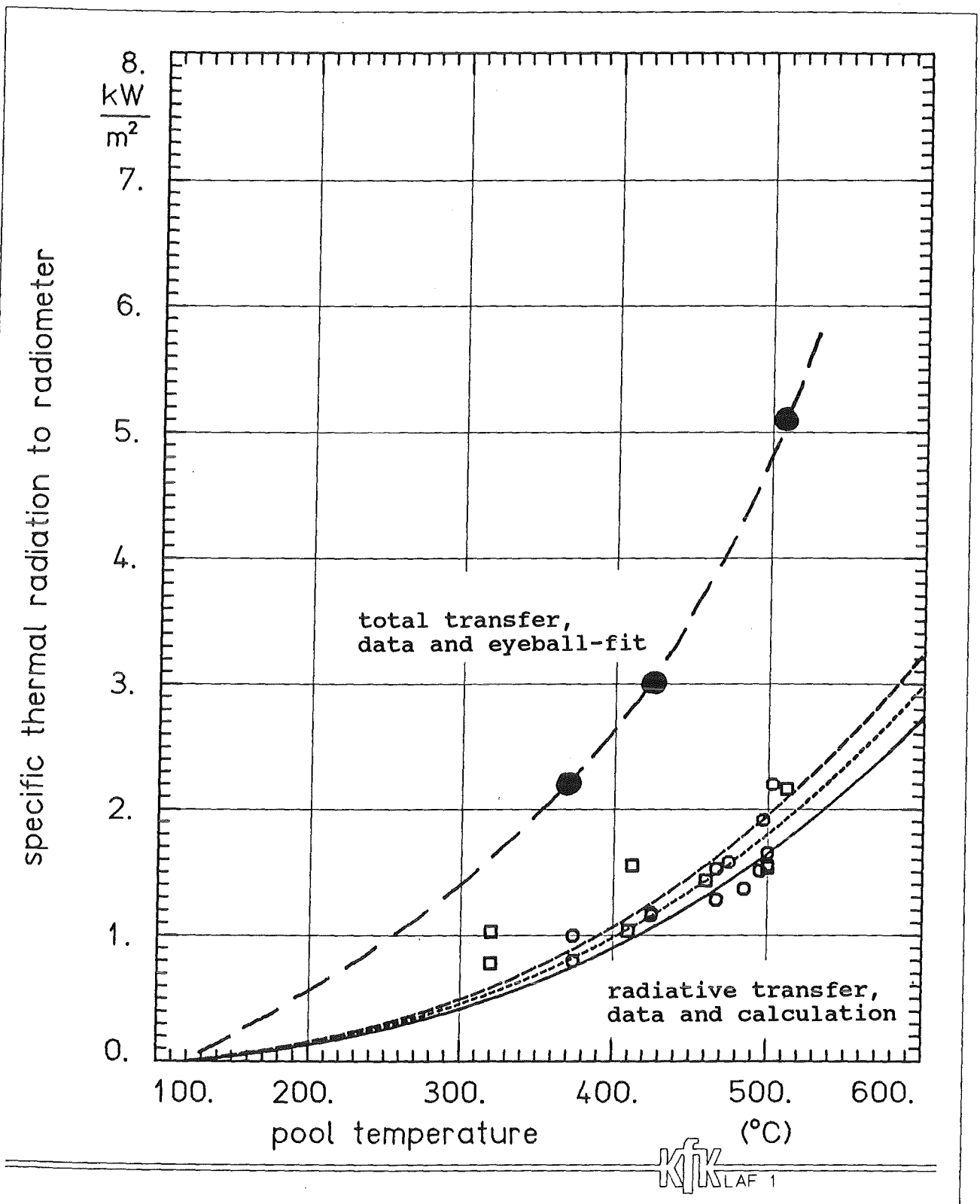

Fig. 7.4 **Total and radiative heat transfer.**

cover gas height : 0.331 m

emissivities : sodium 0.03 to 0.07 (Δ 0.02), wall 0.14, roof 0.25

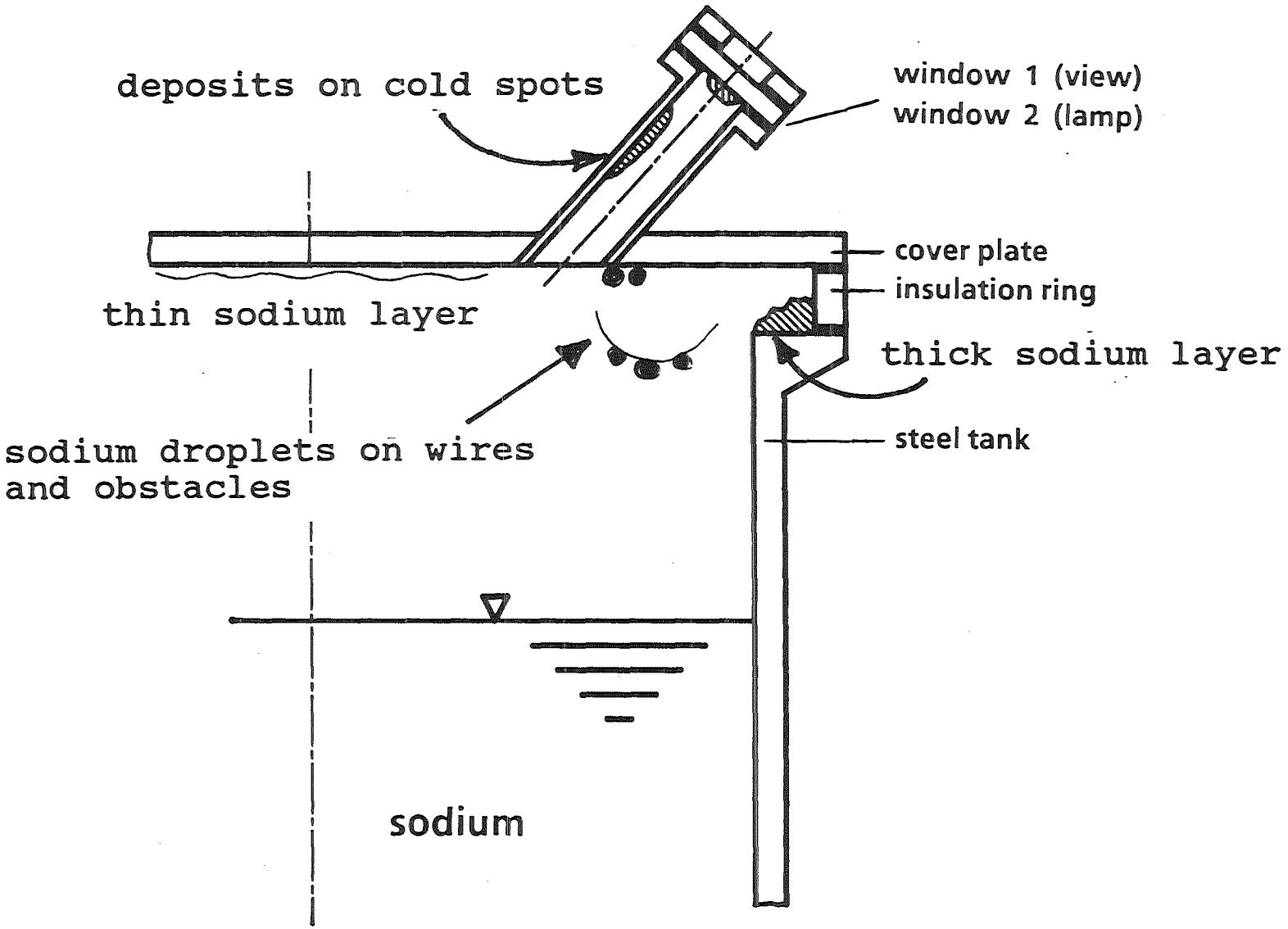

Fig. 8.1 Cross section of cover gas area to illustrate sodium deposition.

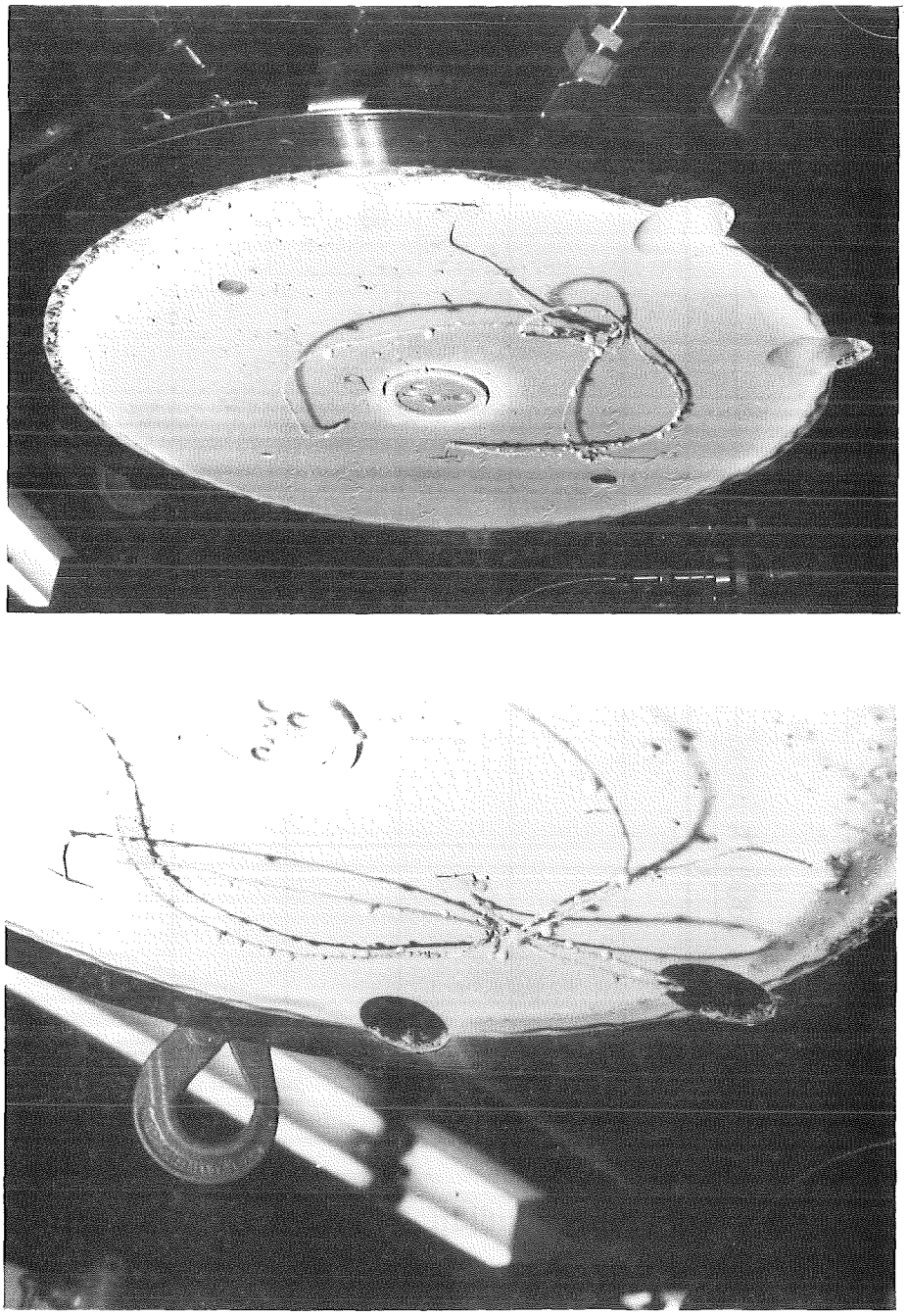

Fig. 8.2 Sodium deposits on the lower side of the cover plate.

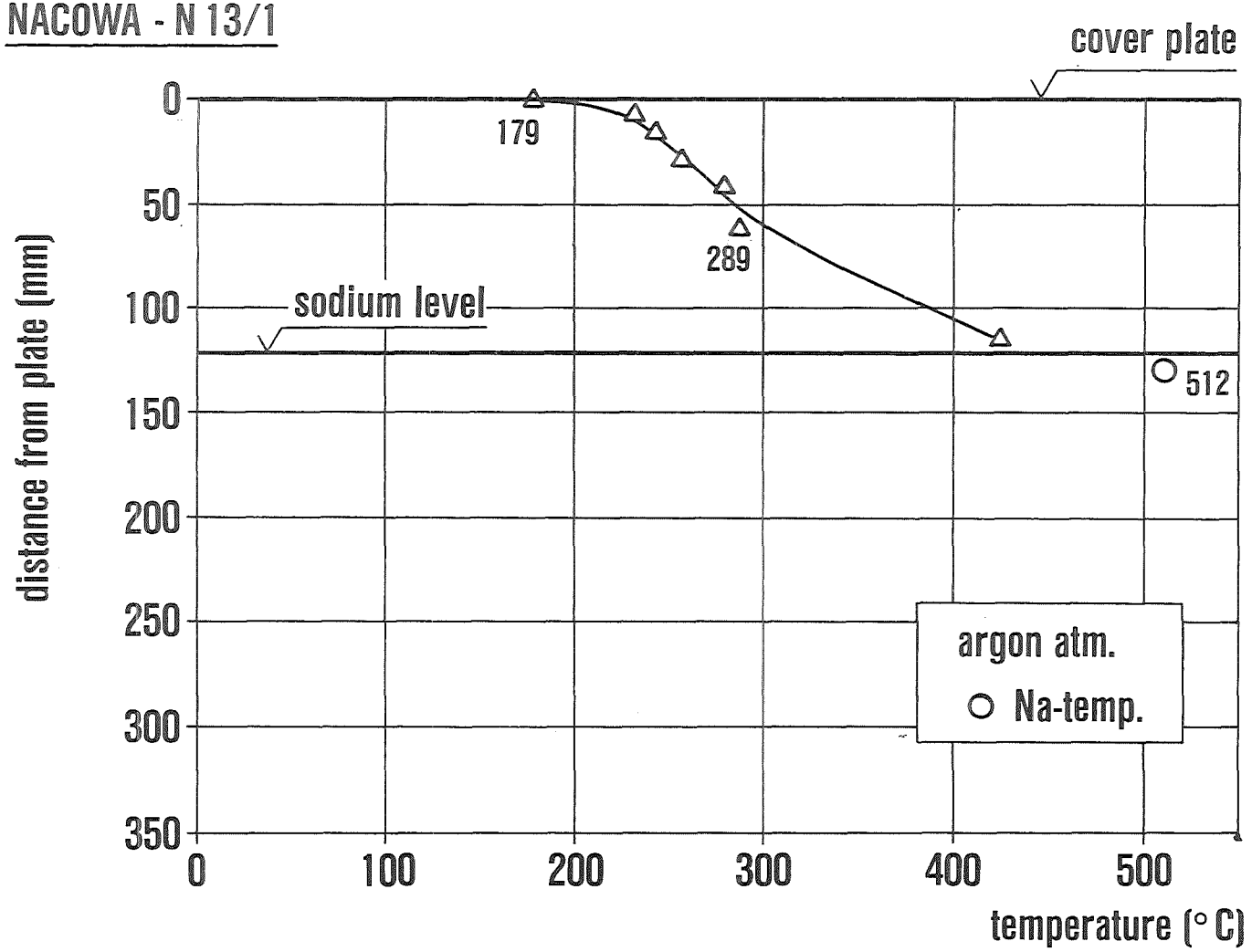

Fig. 9.1 Temperature profile across cover gas, argon, 12.5 cm.

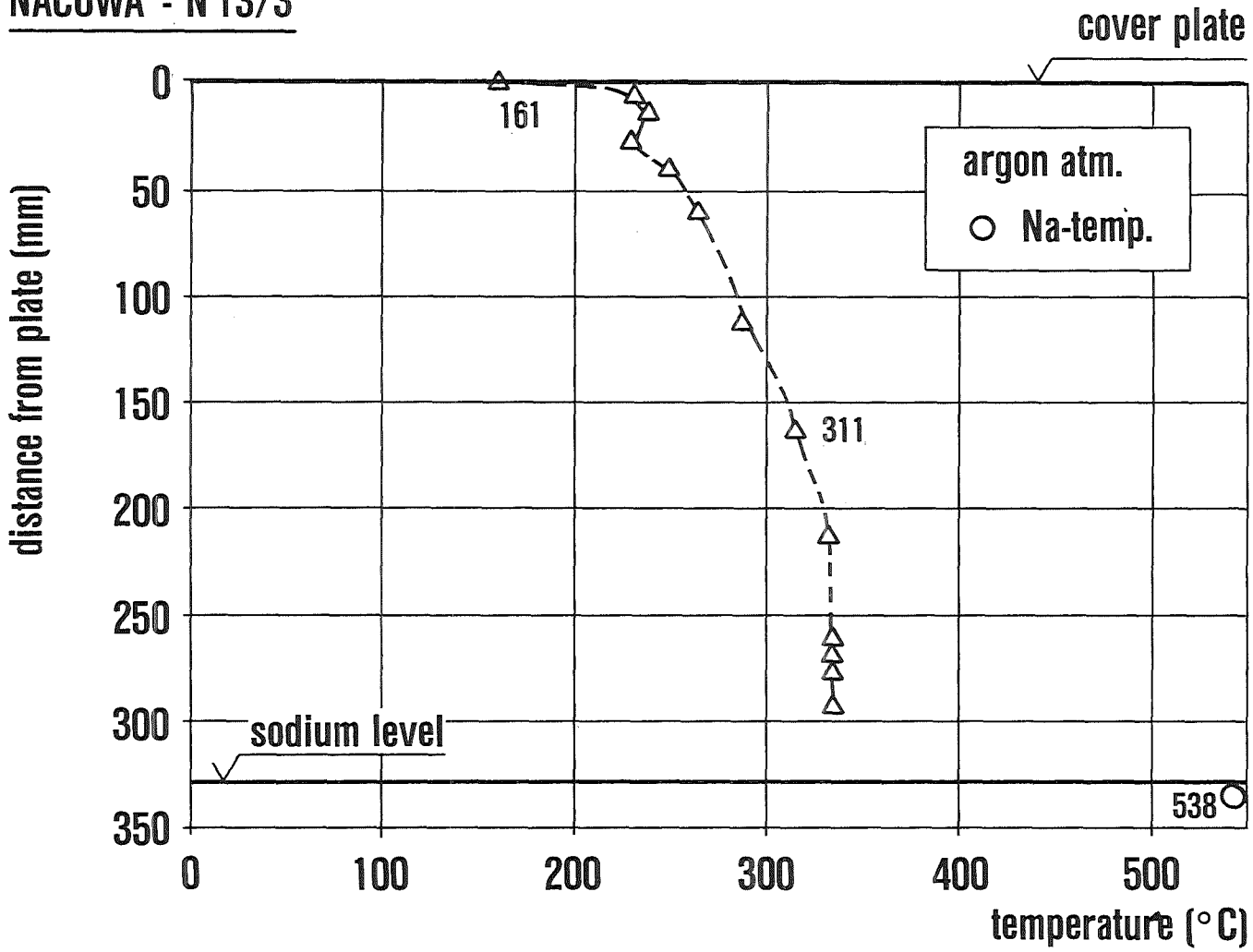

Fig. 9.2 Temperature profile across cover gas, argon, 33 cm.

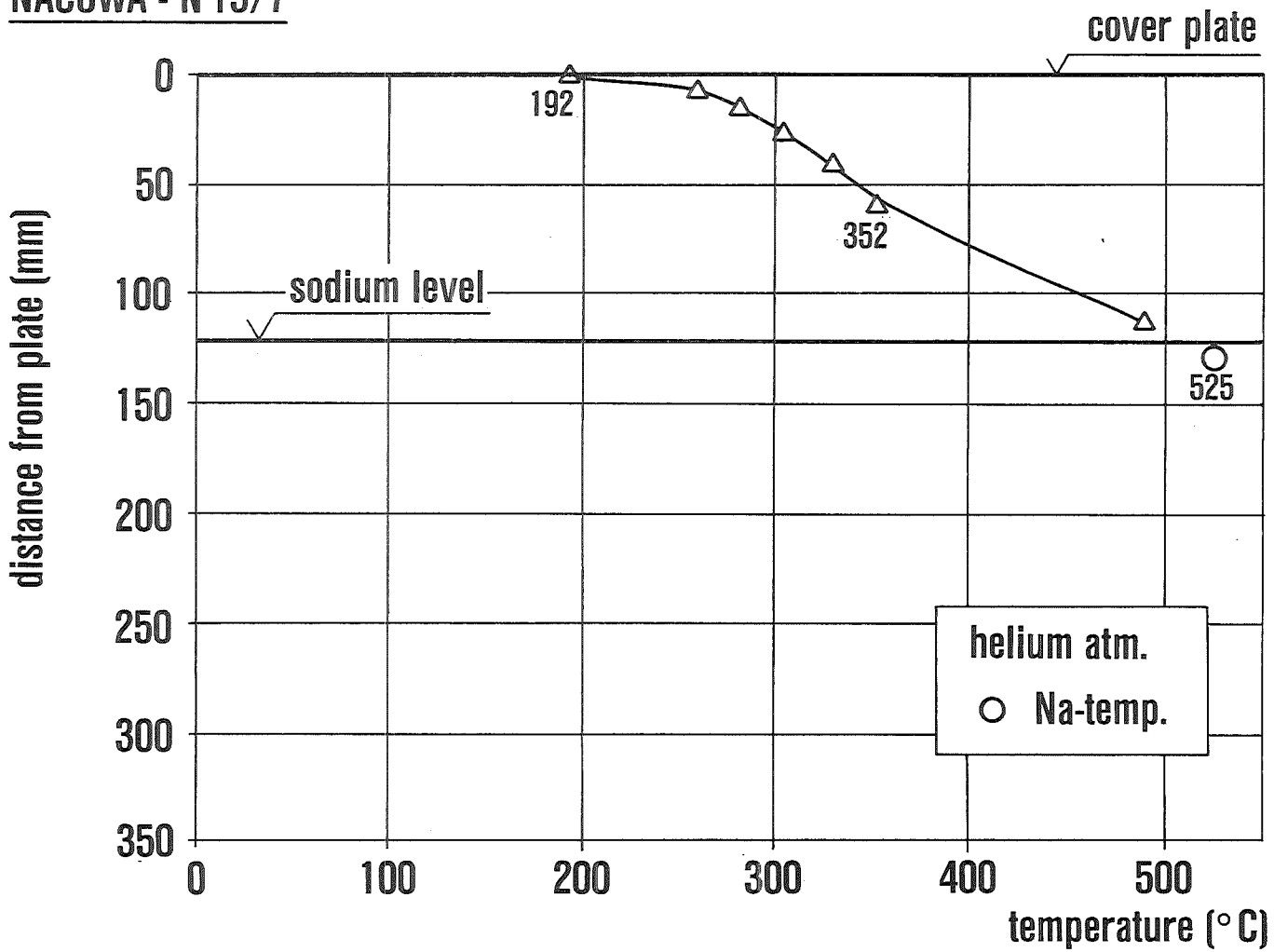

Fig. 9.3 Temperature profile across cover gas, helium, 12.5 cm.

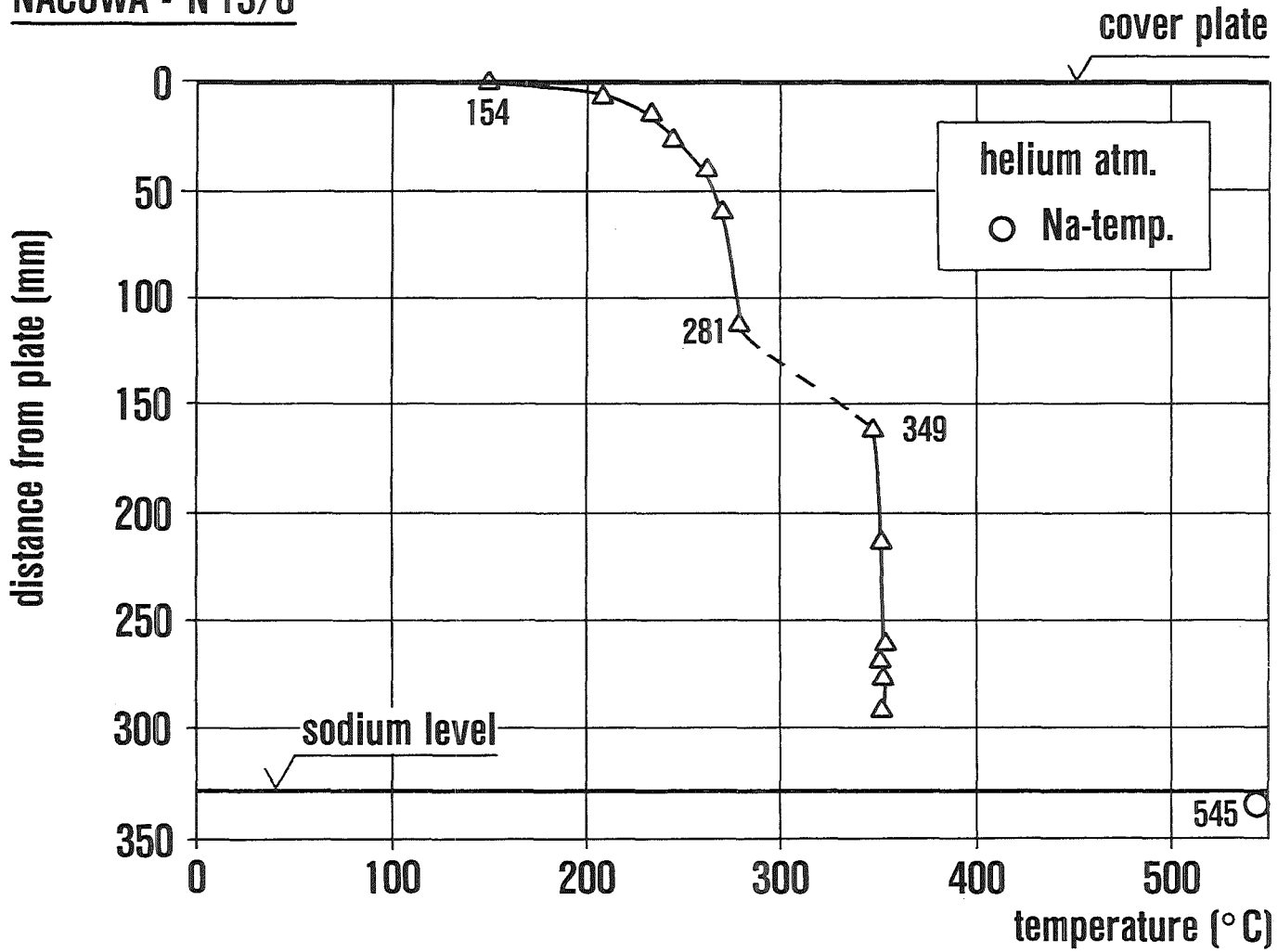

Fig. 9.4 Temperature profile across cover gas, helium, 33 cm.

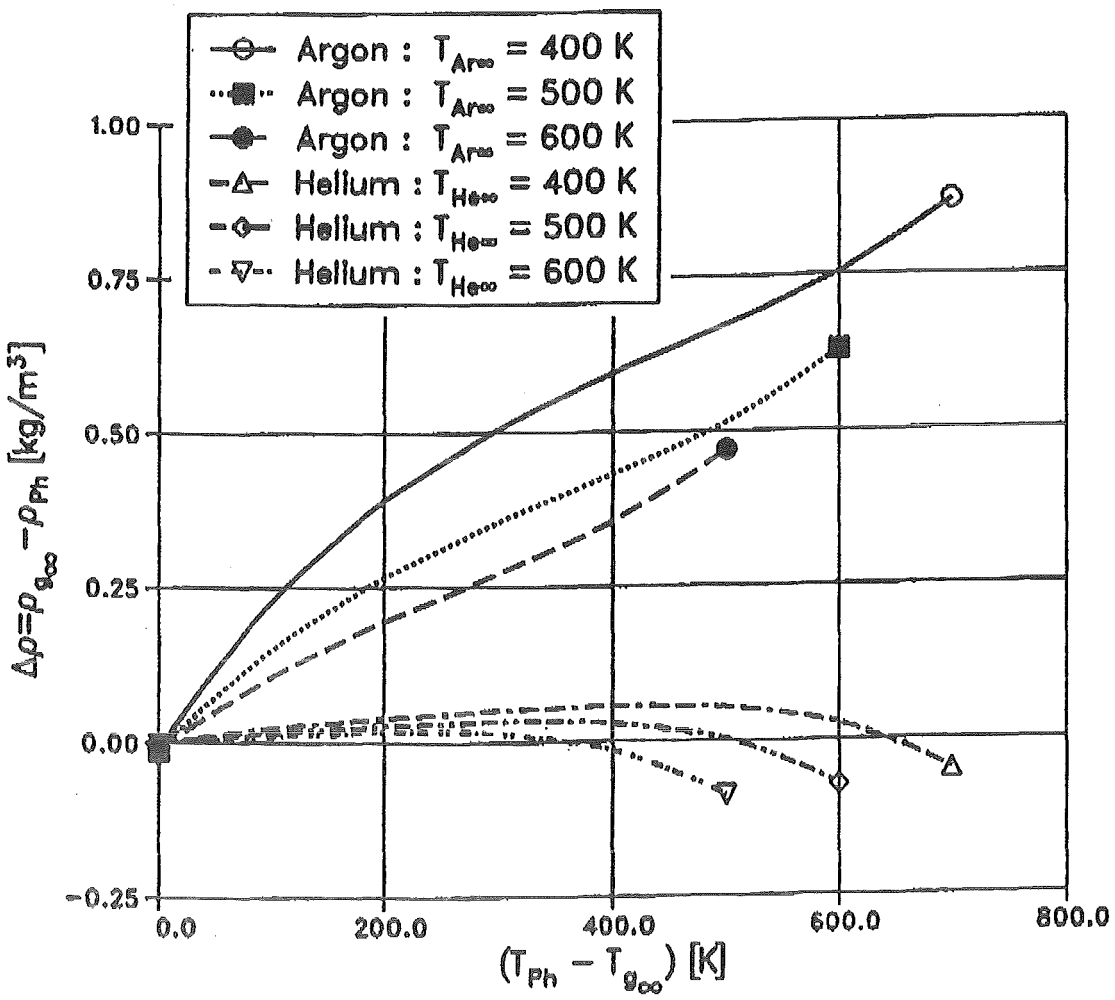

Fig. 10.1 Difference in density $\Delta\varrho$ between the density of the atmosphere at `far distance` from the pool, $\varrho_{g\infty}$, and the density ϱ_{Ph} of the mixture of inert gas and sodium vapour at the pool surface as a function of the temperature difference ($T_{Ph} - T_{g\infty}$) for the systems sodium-argon and sodium-helium. Parameter of the calculations is the temperature of the atmosphere at far distance.

REVOLS - calculation, see ref. 10.1 .

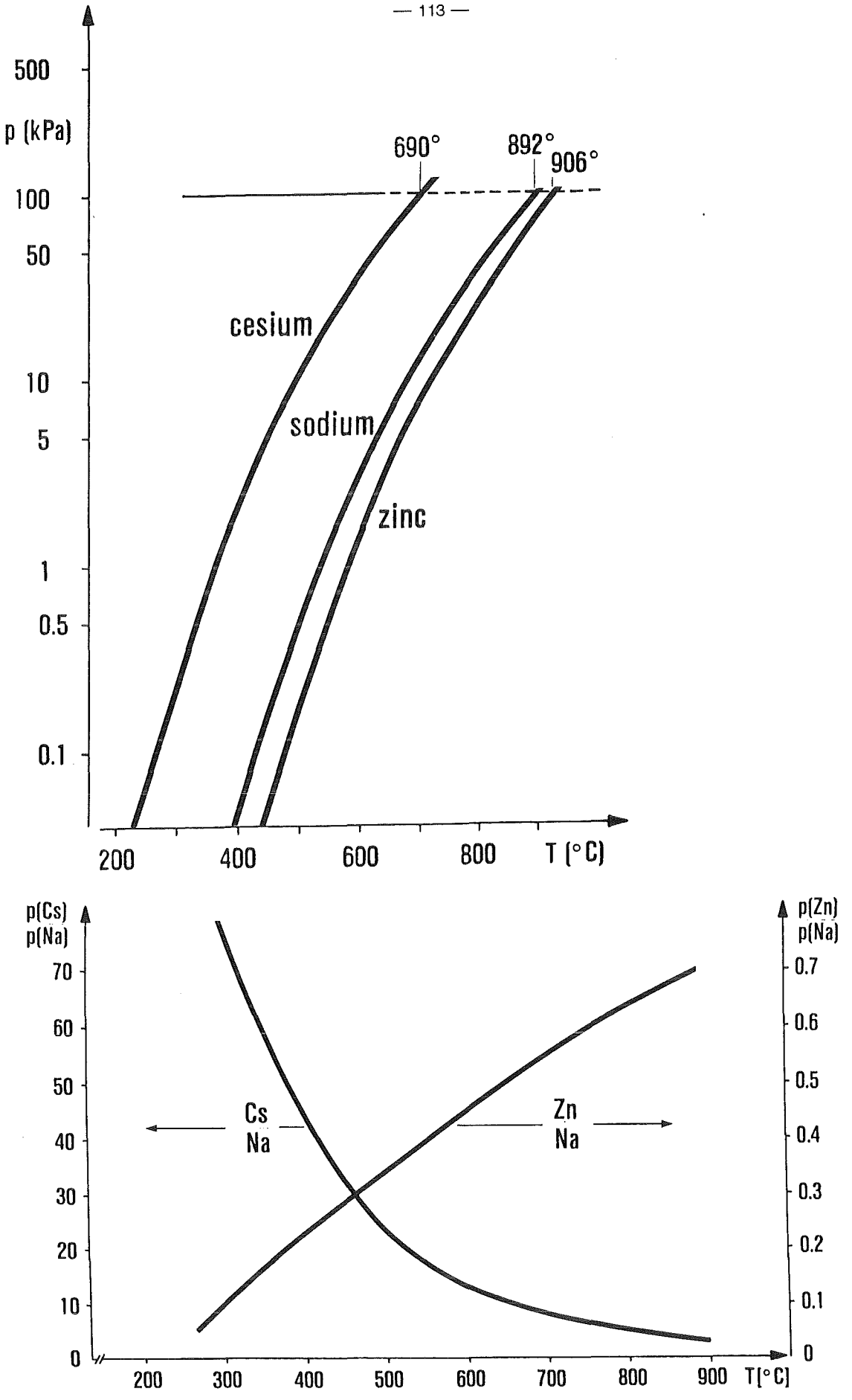

Fig. 11.1 Vapour pressure of cesium, sodium, and zinc, and ratio of vapour pressures.

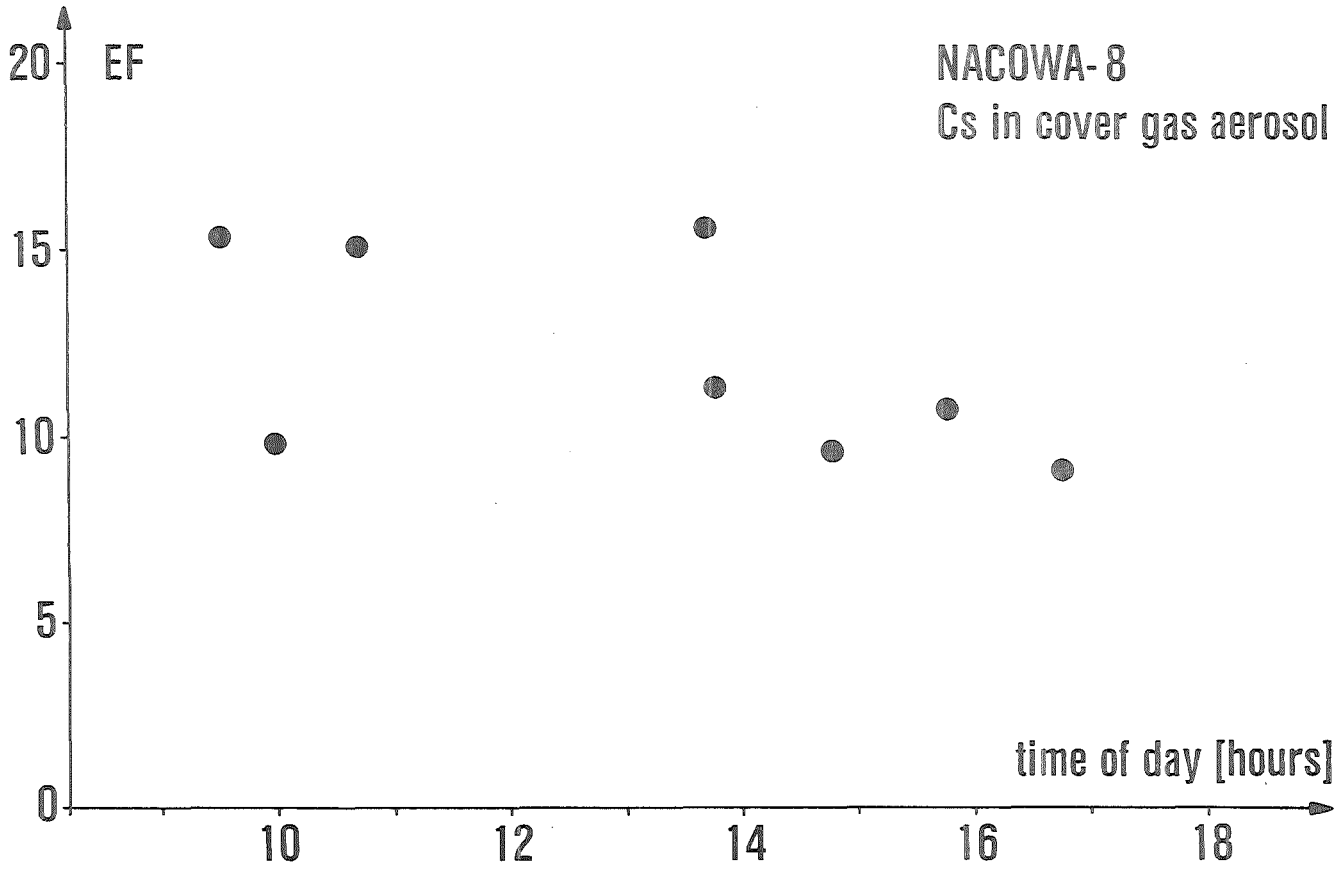

Fig. 11.2 Cesium enrichment factors from cover gas samples taken during test NACOWA 8 .

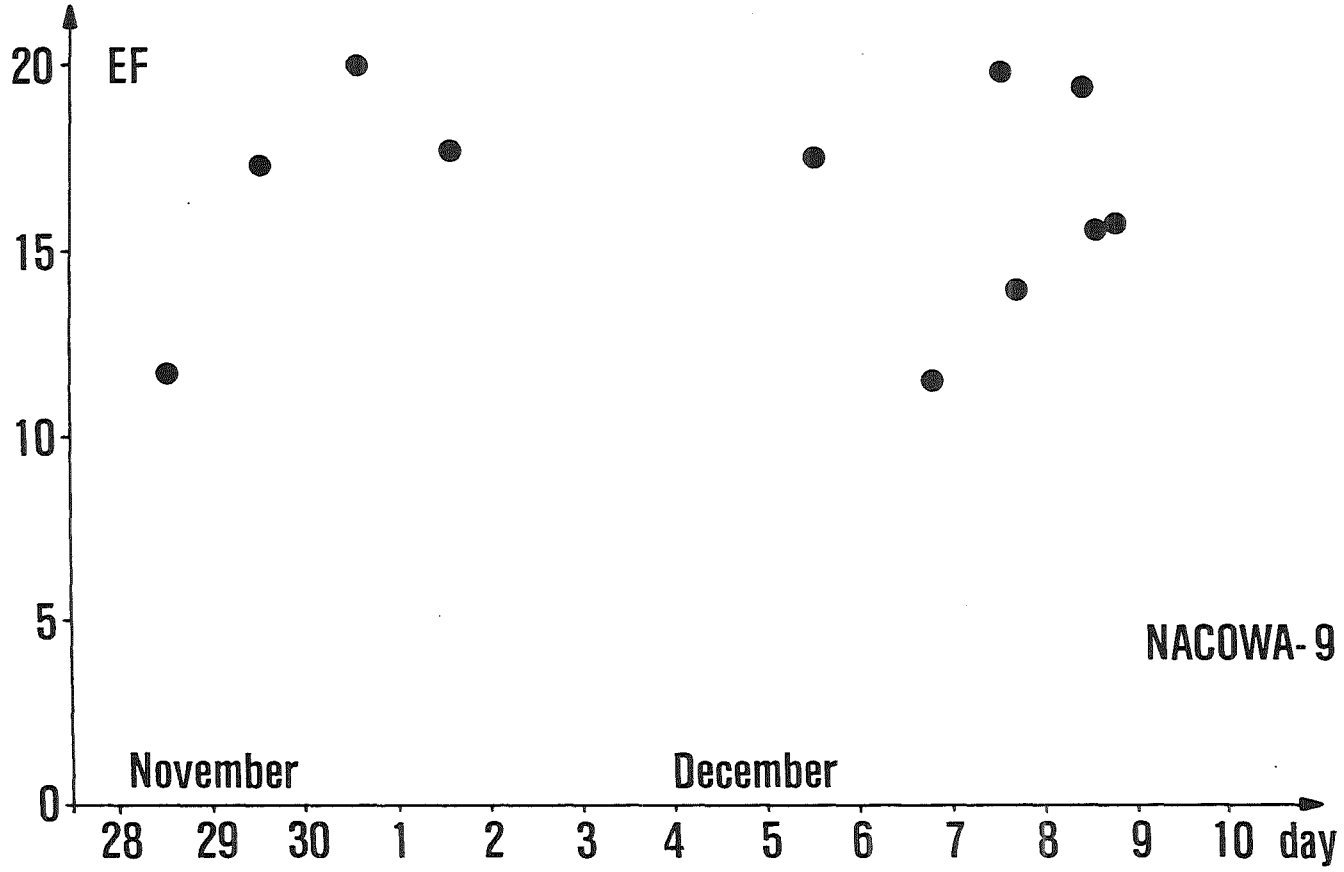

Fig. 11.3 Cesium enrichment factors from cover gas samples taken during test NACOWA 9 .

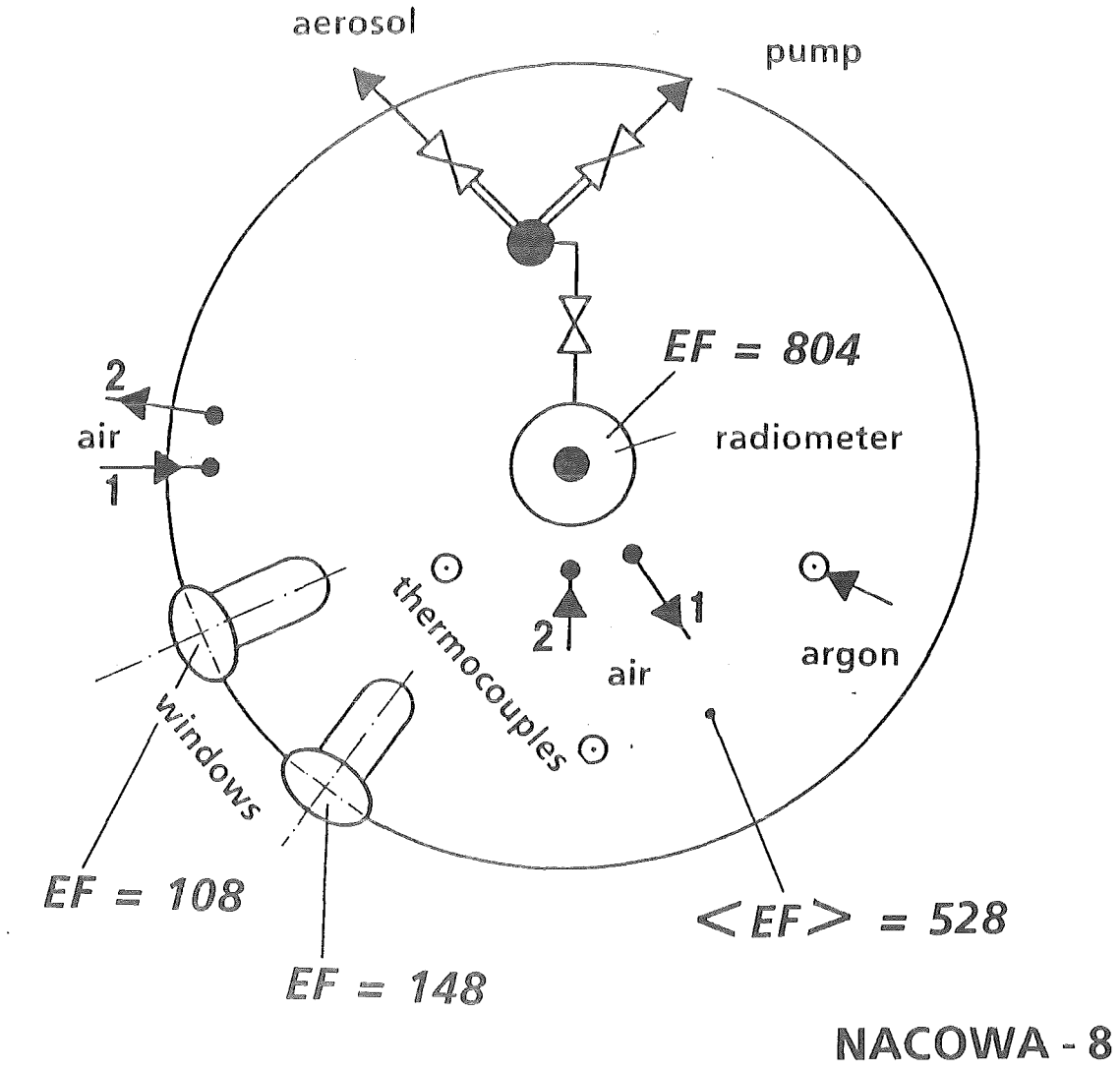

Fig. 11.4 Cesium enrichment factors from deposits on lower side of cover plate, test NACOWA 8 .

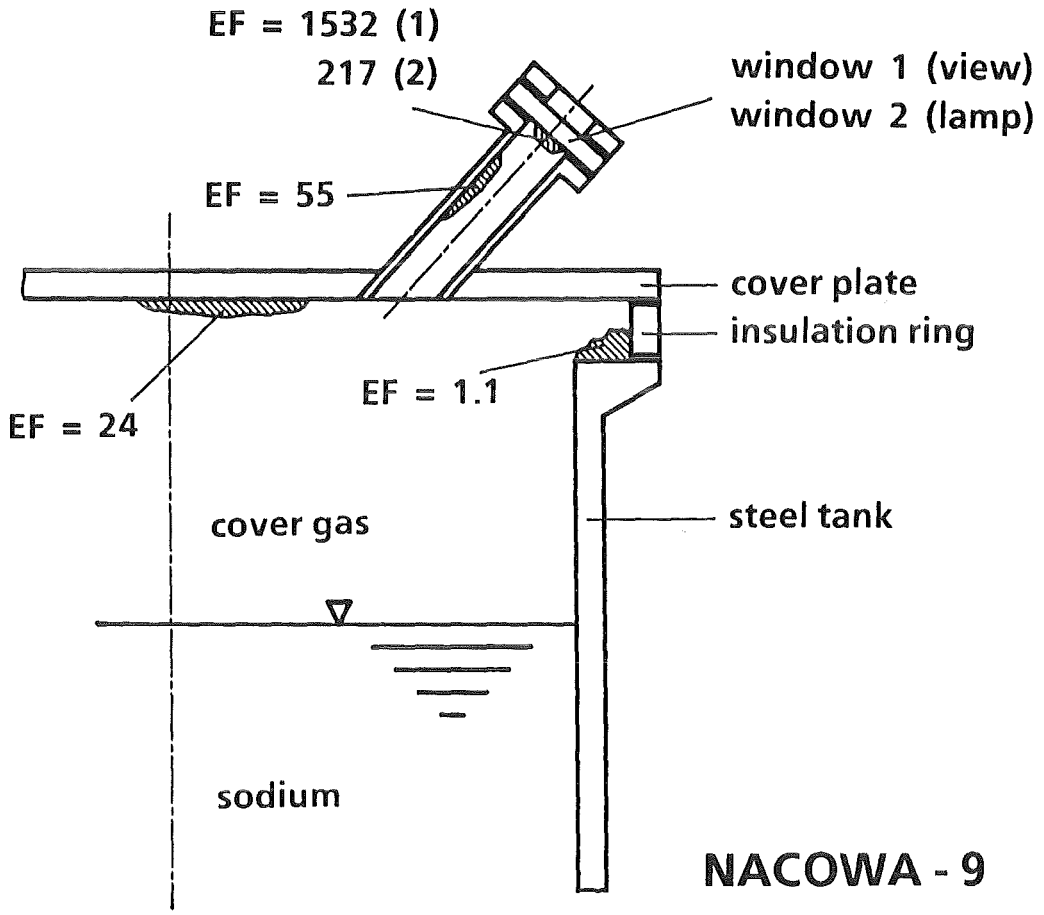

Fig. 11.5 Cesium enrichment factors from deposits on cover plate and upper rim of test vessel, NACOWA 9 .

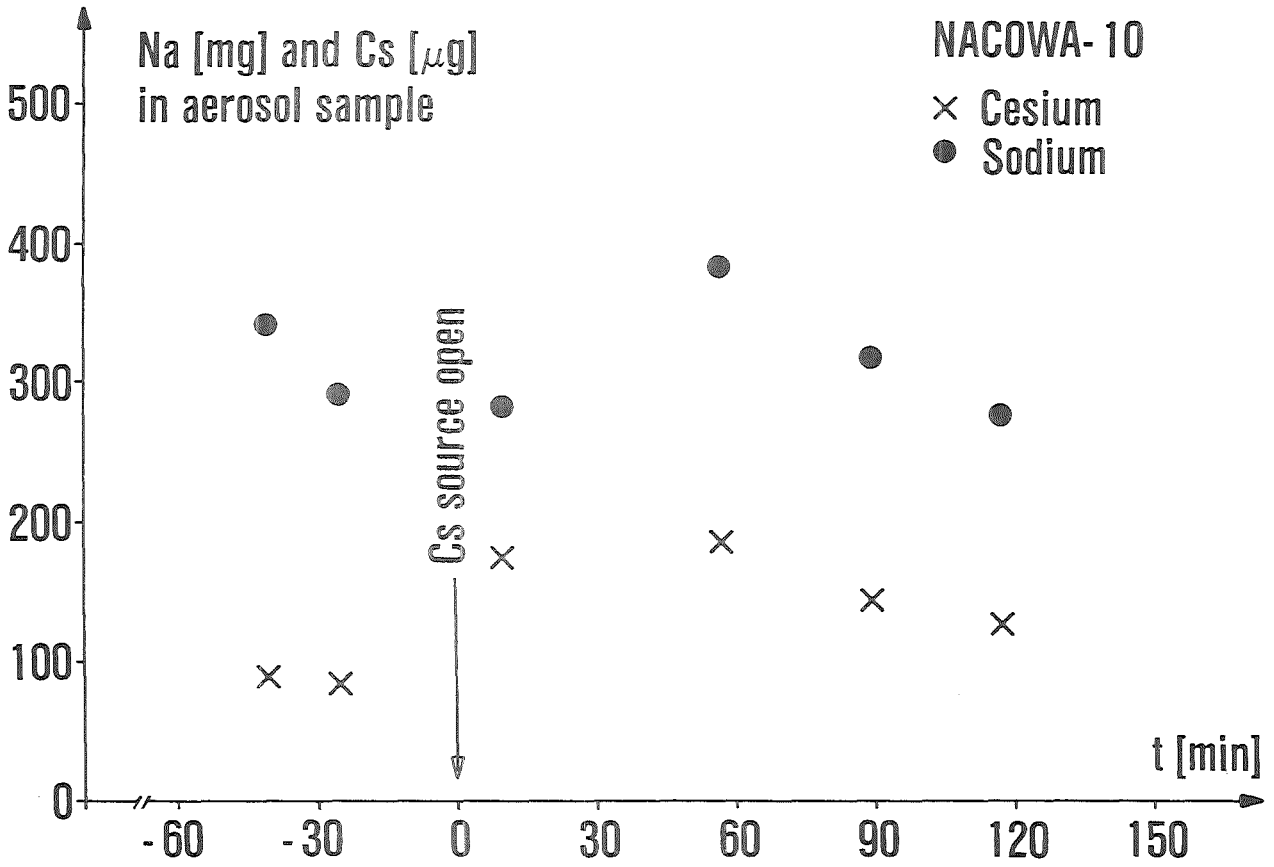

Fig. 11.6 Amounts of sodium and cesium in aerosol samples taken during test NACOWA 10 .

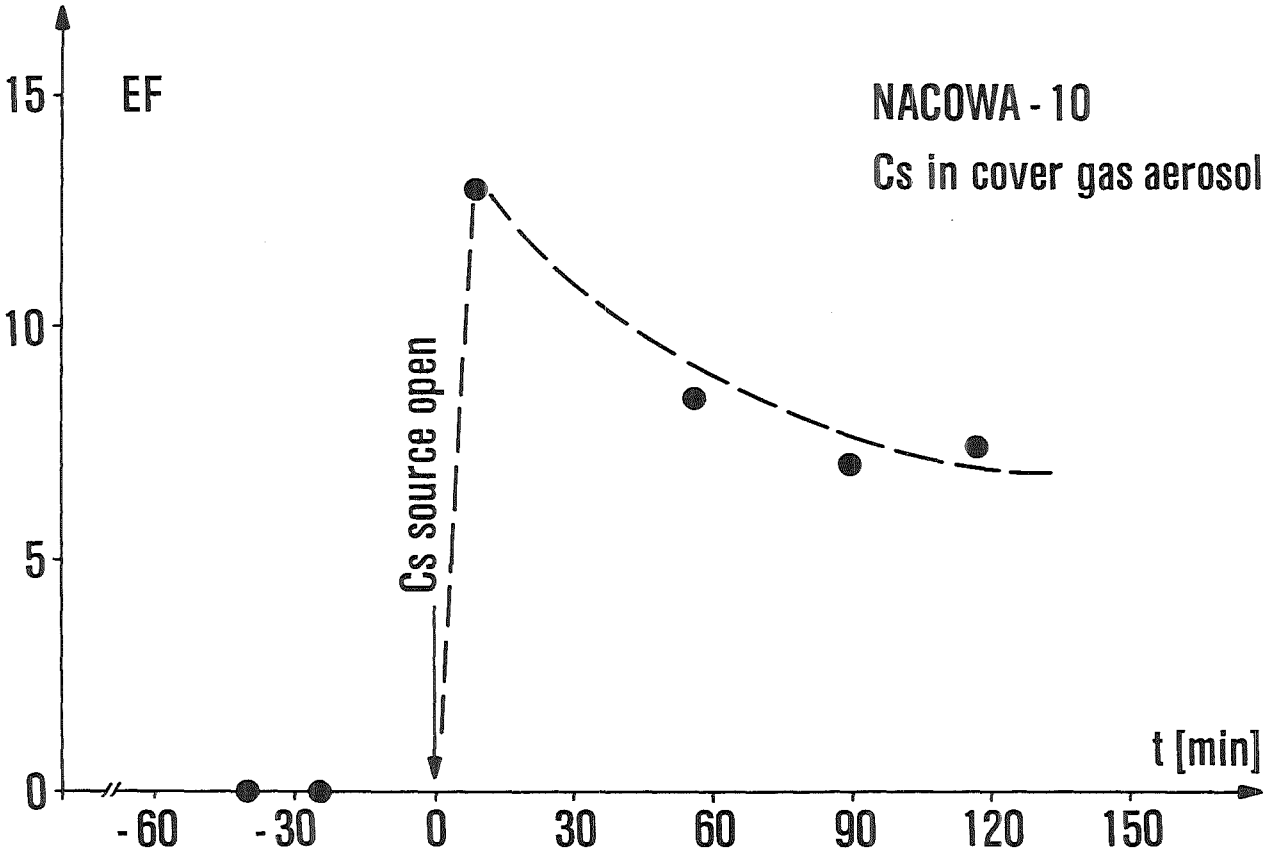

Fig. 11.7 Cesium enrichment factors from cover gas samples taken during test NACOWA 10, with background correction.

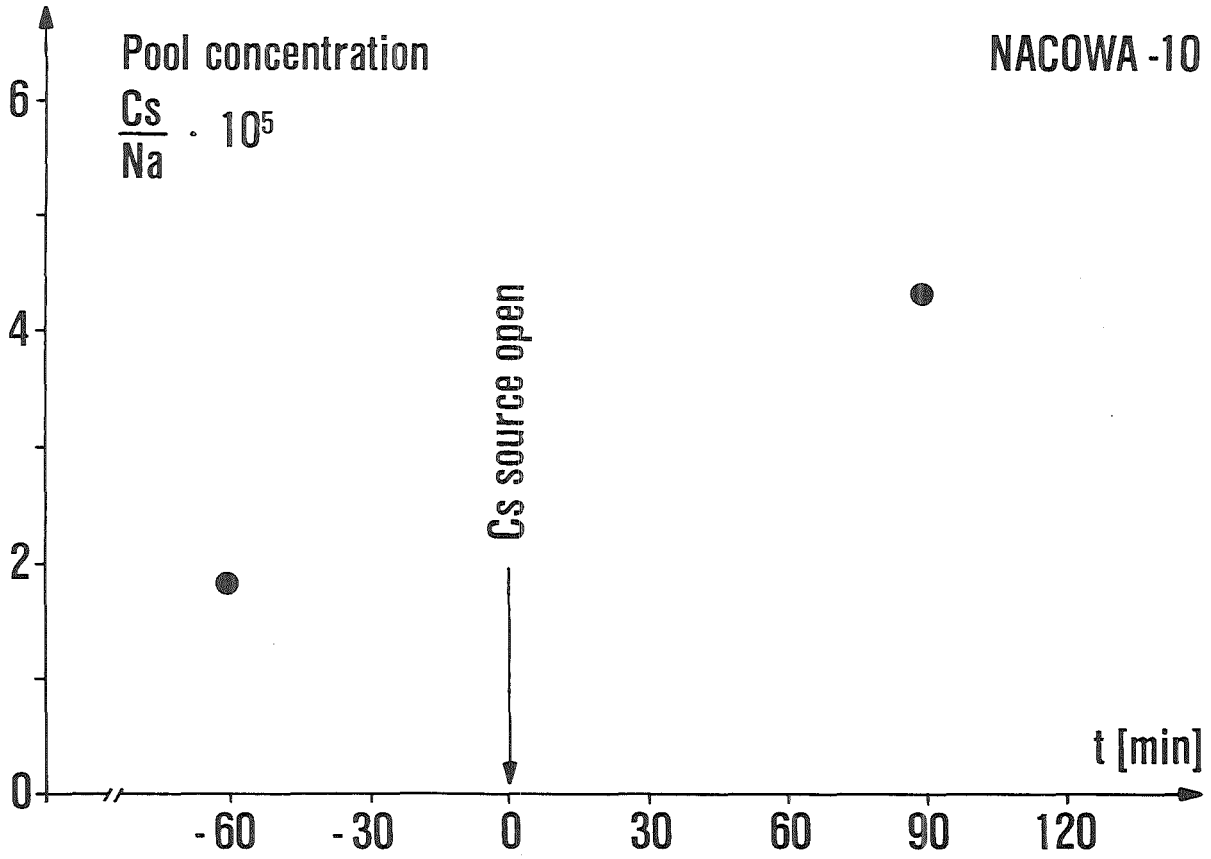

Fig. 11.8 Pool concentration near the surface before and after opening of the source.

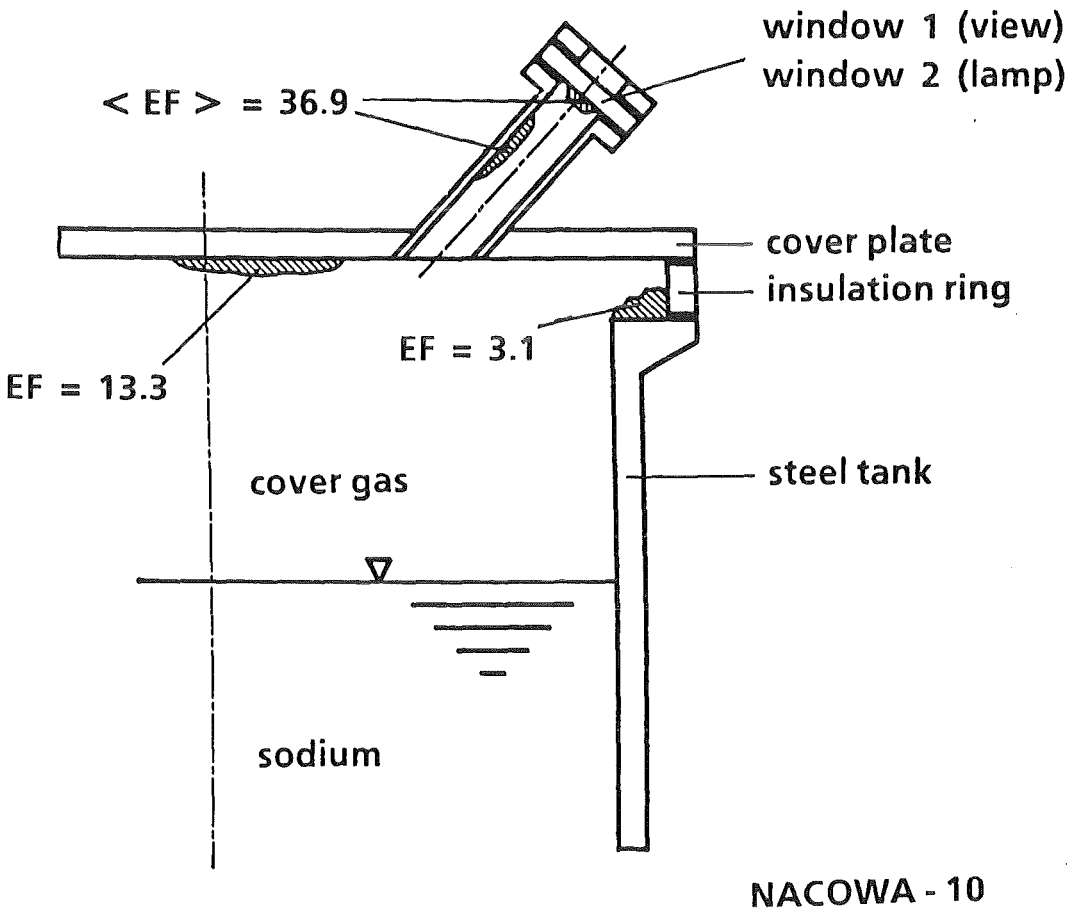

Fig. 11.9 Cesium enrichment factors from deposits on cover plate and upper rim of test vessel, NACOWA 10.

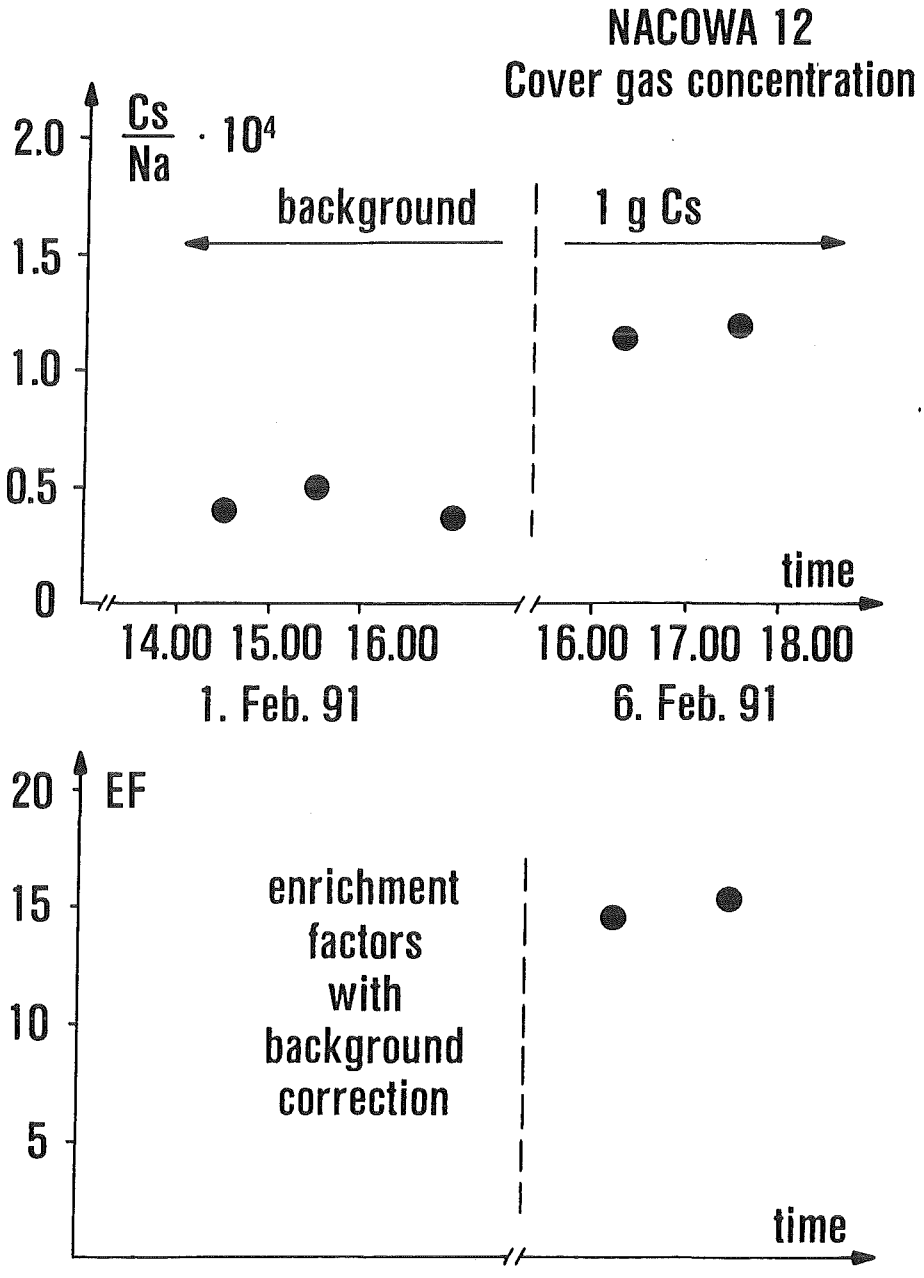

Fig. 11.10 Cesium cover gas concentration and enrichment factors before and after opening of the source, test NACOWA 12.

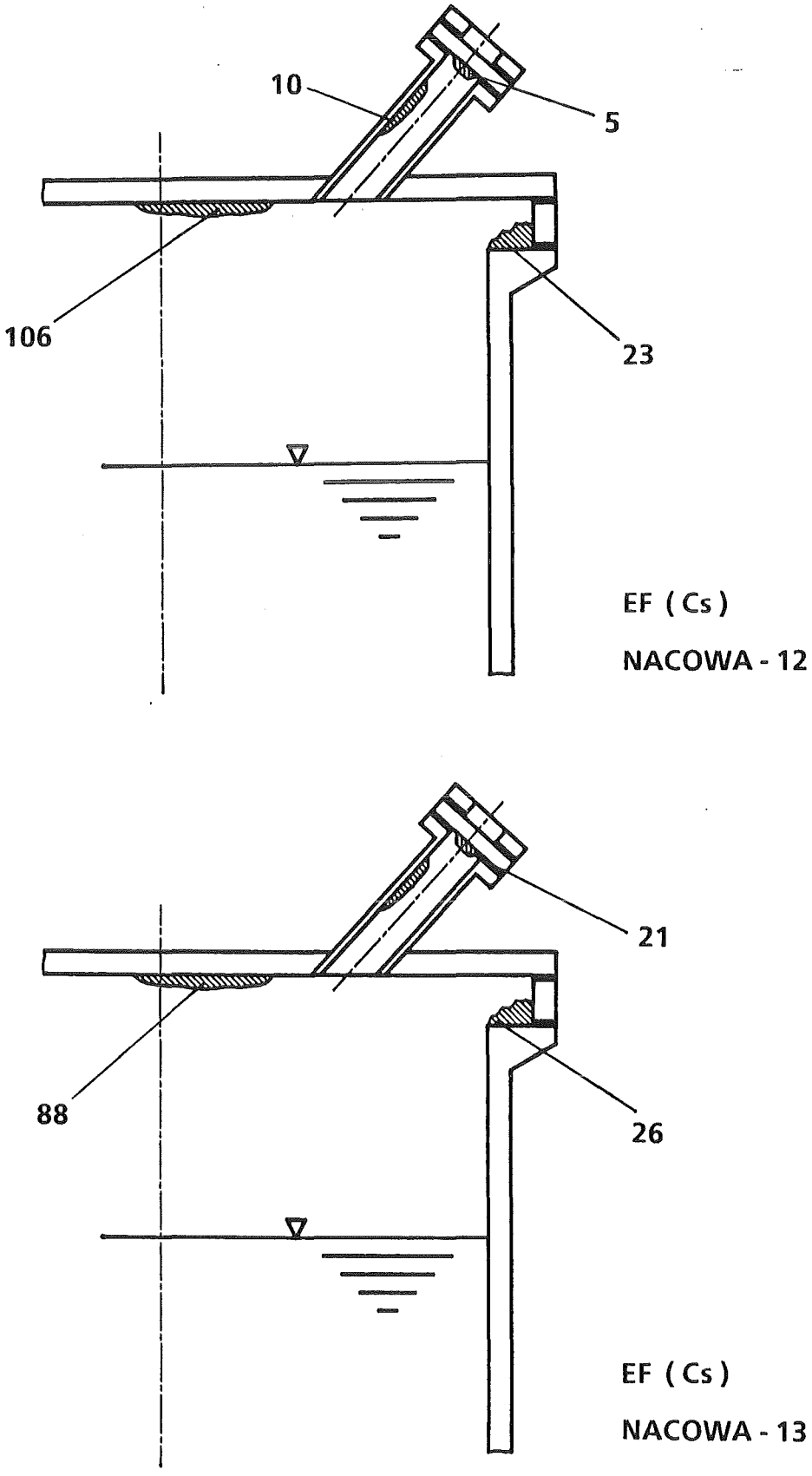

Fig. 11.11 Cesium enrichment factors from deposits on cover plate and upper rim of test vessel, tests NACOWA 12 and NACOWA 13 .

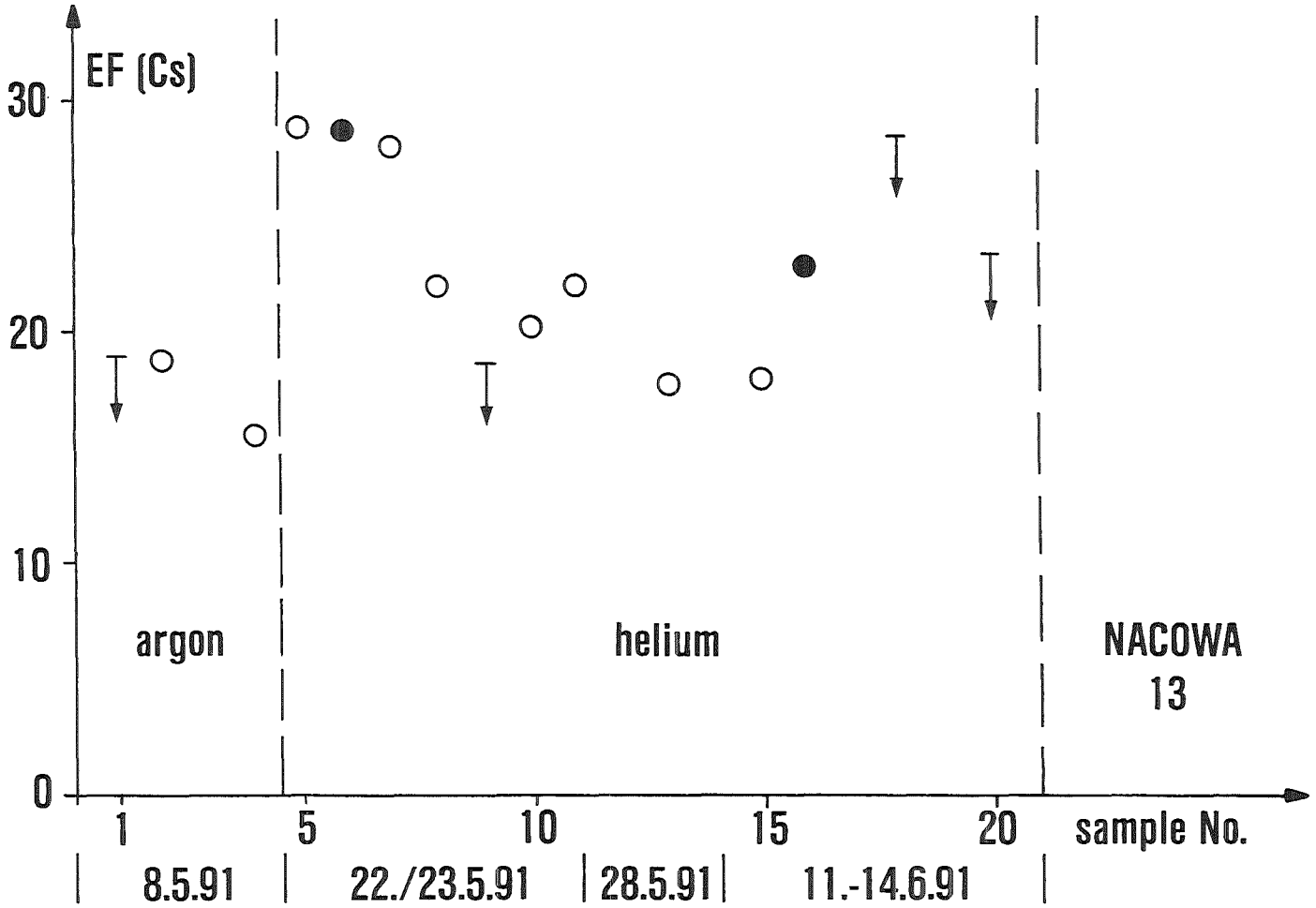

Fig. 11.12 Cesium enrichment factors from cover gas samples during test NACOWA 13, argon and helium atmosphere, wash-bubblers (open circles) and impactors (closed circles).

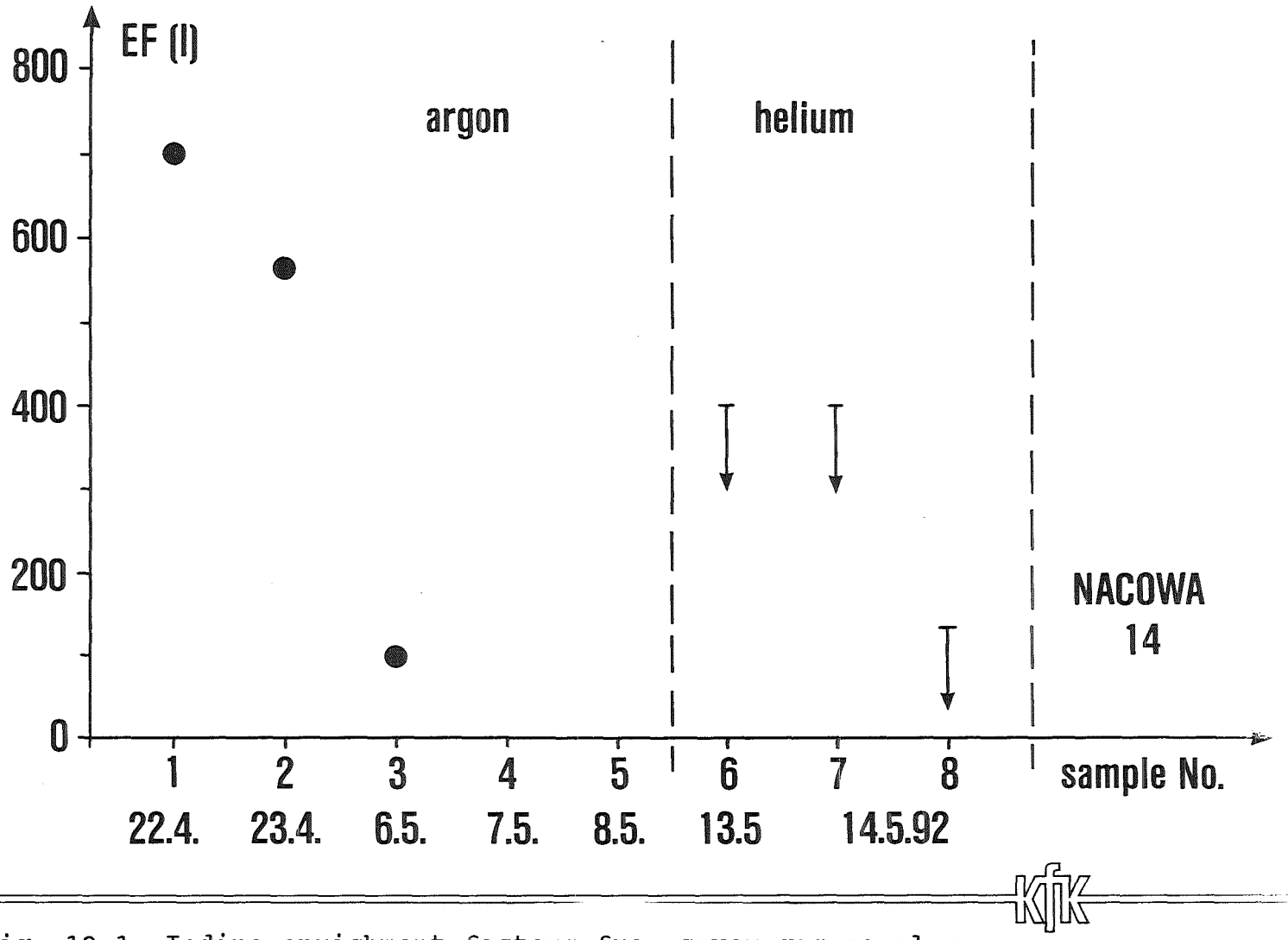

Fig. 12.1 Iodine enrichment factors from cover gas samples taken during test NACOWA-14.

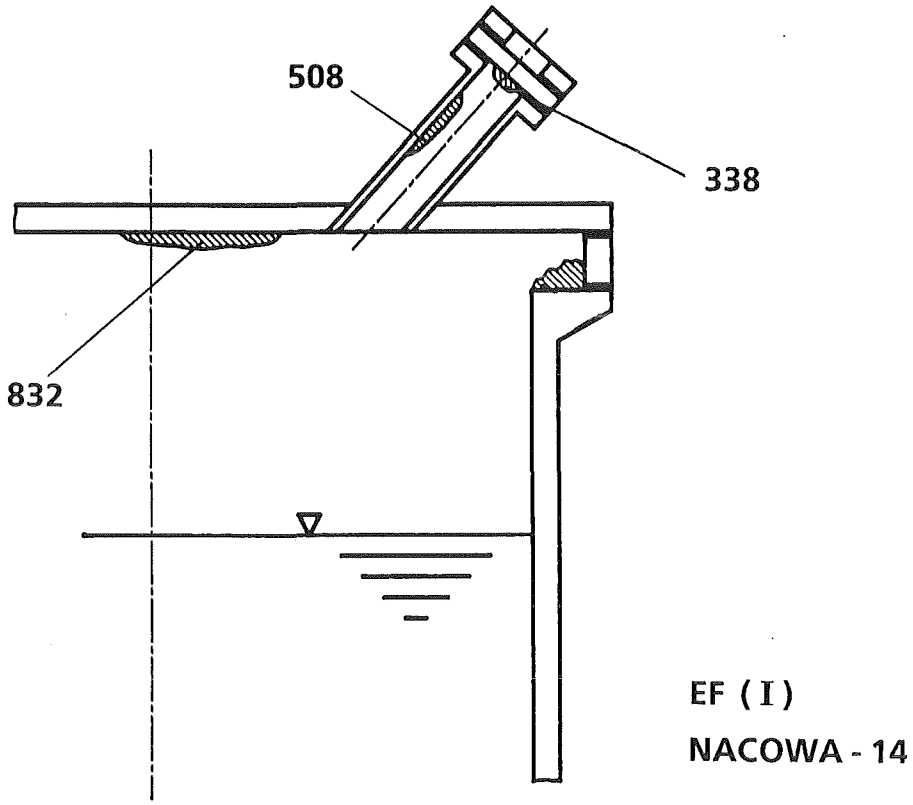

Fig. 12.2 Iodine enrichment factors from deposits on cover plate, test NACOWA-14.

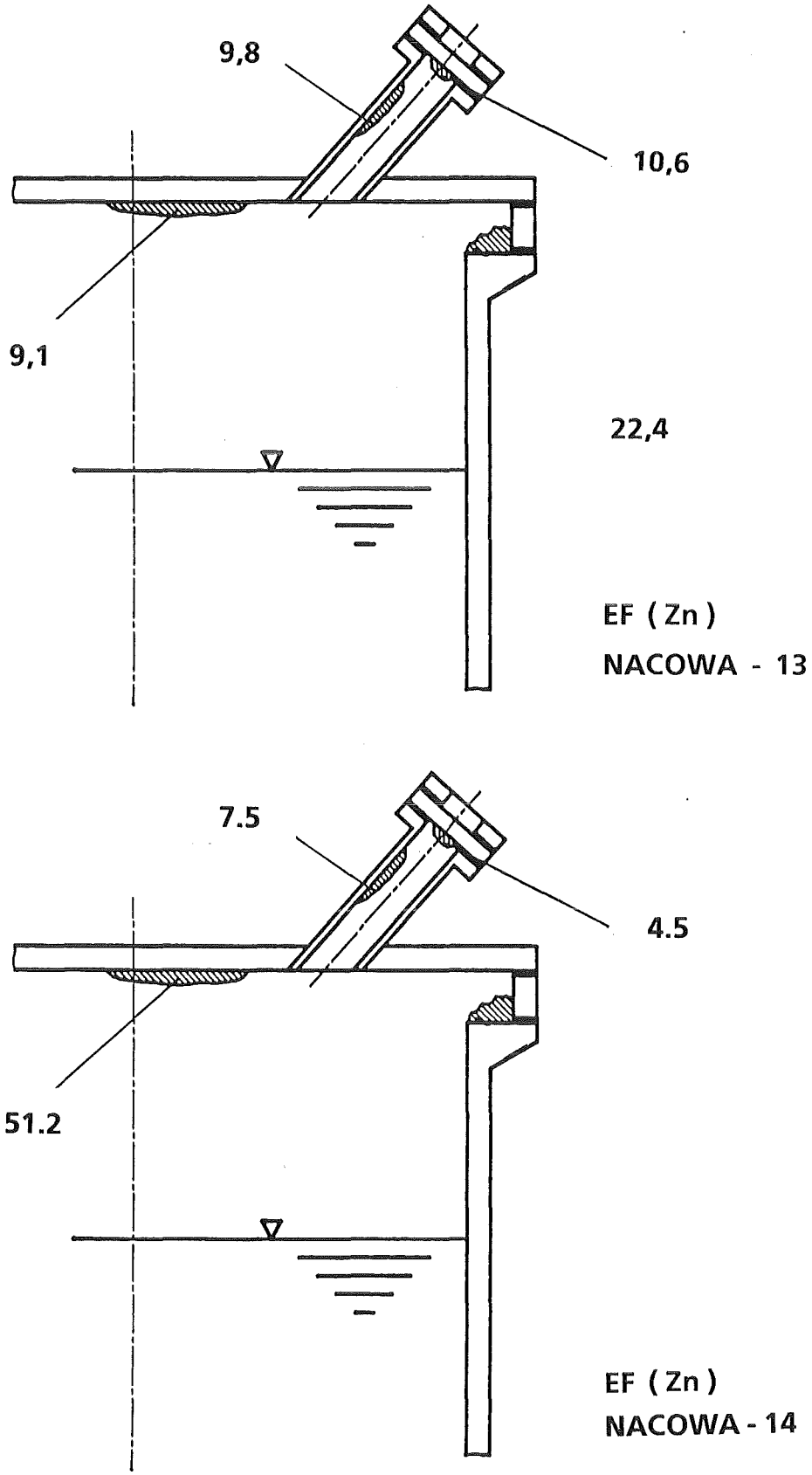

Fig. 13.1 Zinc enrichment factors from deposits on cover plate, tests NACOWA-13 and -14.